

รૂหนอนในทฤษฎีสัมพัทธภาพทั่วไปแบบปรับแต่ง



วิทยานิพนธ์นี้เป็นส่วนหนึ่งของการศึกษาตามหลักสูตรปริญญาวิทยาศาสตรดุษฎีบัณฑิต

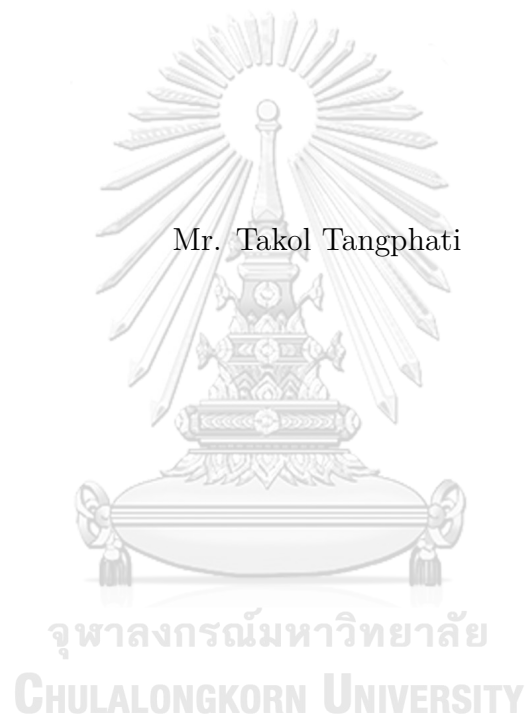
สาขาวิชาฟิสิกส์ ภาควิชาฟิสิกส์

คณะวิทยาศาสตร์ จุฬาลงกรณ์มหาวิทยาลัย

ปีการศึกษา 2563

ลิขสิทธิ์ของจุฬาลงกรณ์มหาวิทยาลัย

THE WORMHOLES IN THE MODIFICATION OF GENERAL RELATIVITY
THEORY



A Dissertation Submitted in Partial Fulfillment of the Requirements

for the Degree of Doctor of Science Program in Physics

Department of Physics

Faculty of Science

Chulalongkorn University

Academic Year 2020

Copyright of Chulalongkorn University

Thesis Title THE WORMHOLES IN THE MODIFICATION OF GENERAL
RELATIVITY THEORY
By Mr. Takol Tangphati
Field of Study Physics
Thesis Advisor Assistant Professor Auttakit Chatrabhuti, Ph.D.
Thesis Co-Advisor Associate Professor Phongpichit Channuie, Ph.D.

Accepted by the Faculty of Science, Chulalongkorn University in Partial Fulfillment
of the Requirements for the Doctoral Degree

..... Dean of the Faculty of Science
(Professor Polkit Sangvanich, Ph.D.)

THESIS COMMITTEE

..... Chairman
(Professor Parinya Karndumri, Ph.D.)

..... Thesis Advisor
(Assistant Professor Auttakit Chatrabhuti, Ph.D.)

..... Thesis Co-Advisor
(Associate Professor Phongpichit Channuie, Ph.D.)

..... Examiner
(Assistant Professor Pawin Ittisamai, Ph.D.)

..... Examiner
(Thiparat Chotibut, Ph.D.)

..... External Examiner
(Assistant Professor Pitayuth Wongjun, Ph.D.)

ถก ตั้ง ผาติ : รุหนอนในทฤษฎีสัมพัทธภาพทั่วไปแบบปรับแต่ง. (THE WORMHOLES IN THE MODIFICATION OF GENERAL RELATIVITY THEORY) อ.ที่ปรึกษาวิทยานิพนธ์หลัก : ผศ. ดร.อรรณกฤต ฉัตรภูติ, อ.ที่ปรึกษาวิทยานิพนธ์ร่วม : รศ. ดร.พงษ์พิชิต จันทร์นุ้ย, 133 หน้า.

รุหนอนแบบเดินทางได้เป็นหนึ่งในผลเฉลยของทฤษฎีสัมพัทธภาพซึ่งถูกเสนอครั้งแรกในปี คศ. 1988 โดยมอริสและทอร์น อย่างไรก็ตามการมีอยู่ของมันต้องการสสารแปลก (exotic matter) ซึ่งละเมิดเงื่อนไขพลังงาน (energy conditions) วิทยานิพนธ์ฉบับนี้ได้แสดงผลเฉลยรุหนอนในทฤษฎีความโน้มถ่วงแบบมีมวลที่ไม่เชิงเส้นและไม่มีอนุภาคผี (ghost) ถูกเสนอโดย de Rham, Gabadadze and Tolley (dRGT) เราจึงได้สร้างรุหนอนภายใต้ทฤษฎีสัมพัทธภาพปรับแต่ง วิเคราะห์หาเสถียรภาพ และเงื่อนไขของสสารแปลกต่อการสร้างรุหนอน ในการศึกษานี้ได้ใช้สองระเบียบวิธีในการสร้างรุหนอน คือ แบบ Lorentzian traversable และ แบบผนังบาง (thin-shell) มาศึกษาในทฤษฎีความโน้มถ่วงมีมวลแบบ dRGT เราได้พบว่ารุหนอนในทฤษฎีดังกล่าวนั้นต้องการสสารแปลกเพียงแค่ว่าบริเวณใกล้เคียงกับคอหอยรุหนอนเท่านั้น ไม่ได้ต้องการการกระจายตัวของสสารแปลกไปทั่วทั้งจักรวาลอย่างในทฤษฎีสัมพัทธภาพ

จุฬาลงกรณ์มหาวิทยาลัย
CHULALONGKORN UNIVERSITY

ภาควิชา ฟิสิกส์ ลายมือชื่อนิสิต

สาขาวิชา ฟิสิกส์ ลายมือชื่อ อ.ที่ปรึกษาหลัก

ปีการศึกษา 2563 ลายมือชื่อ อ.ที่ปรึกษาวิทยานิพนธ์ร่วม

6072805423 : MAJOR PHYSICS

KEYWORDS : MASSIVE GRAVITY, THIN-SHELL WORMHOLE, TRAVERSABLE
WORMHOLE

TAKOL TANGPHATI : THE WORMHOLES IN THE MODIFICATION
OF GENERAL RELATIVITY THEORY. ADVISOR : ASST. PROF.
AUTTAKIT CHATRABHUTI, Ph.D., CO-ADVISOR : ASSOC. PROF.
PHONGPICHIT CHANNUIE, Ph.D., 133 pp.

A traversable wormhole, which is a class of wormholes in general relativity (GR), was proposed by Morris and Thorne in 1988. However, its existence requires the exotic matter violating the energy conditions. This thesis examines the wormhole solutions in the theory of massive gravity, focusing only on the de Rham, Gabadadze and Tolley (dRGT) theory of massive gravity which is the nonlinear massive gravity without ghost and quantify the wormhole solutions. We construct the wormhole solutions in context of the modified GR, investigate their stability, and examine the conditions of the exotic matter. Two methods for wormhole constructions are applied i.e., the Lorentzian traversable and thin-shell wormholes. We found that the wormholes in dRGT massive gravity require the exotic matter only near their throats not spreading all the Universe like in GR.

Department : Physics Student's Signature

Field of Study : Physics Advisor's Signature

Academic Year : 2020 Co-Advisor's Signature

Acknowledgements

I am appreciated the academic support from my advisor; Asst. Prof. Dr. Auttakit Chatrabhuti, my coadvisor; Assoc. Prof. Dr. Phongpichit Channuie and my associate; Dr. Daris Samart. All enlight, aspire, and advise me in this thesis. Their visions and achievements in physics play the major roles for me to explore the wider picture of physics. Furthermore, I would like to thank them for the proof reading in this thesis.

I would like to thank Prof. Dr. Parinya Karndumri, Asst. Prof. Dr. Pawin Ittisamai, Asst. Prof. Dr. Pitayuth Wongjun, and Dr. Thiparat Chotibut for serving as my thesis committee and providing the beneficial suggestion for me in this thesis and the further plan after graduating. Without the useful advise from the post-doctors in CUniverse, this thesis would not finish very well.

I would like to thank Dr. Supakchai Ponglertsakul, Dr. Sirachak Panpanich and Mr. Chatchai Promsiri for introducing the massive gravity, black holes and wormholes which allow me to understand the bigger picture in the thesis. I would like to thank Dr. Kunanon Kittipute for the technical terms in the engineering signal process. The special thank to Mr. Kittisak Wetchprasarn and Mr. Likit Sittipun who have inspired and motivated me to this point. Last but not least I sincerely thank Mr. Chanthawit Anuntasethakul for the IT support.

Overall, this thesis would not be finished without an encouragement, helpfulness and mental support from my mother and my first-and-last girlfriend.

Contents

	Page
Abstract (Thai)	iv
Abstract (English)	v
Acknowledgements	vi
Contents	vii
List of Tables	xi
List of Figures	xii
Chapter	
I INTRODUCTION	1
1.1 Overview	1
1.2 The brief history of the wormhole development	3
1.3 Energy conditions	8
II Massive Gravity	11
2.1 Linearized general relativity	12
2.2 Fierz-Pauli (FP) action	16
2.3 vDVZ discontinuity	18

Chapter	Page
2.4 The Origin of vDVZ discontinuity: The Stueckelberg Trick	19
2.5 Nonlinear massive gravity	23
2.5.1 The extra degree of freedom in nonlinear Fierz-Pauli theory	24
2.5.2 The appearance of BD ghost: Stueckelberg trick	30
2.5.3 Elimination of the extra scalar mode by the Galileon theory	33
2.5.4 The ghost-free nonlinear massive gravity	34
III Wormholes in General Relativity	40
3.1 The Lorentzian traversable wormhole	40
3.1.1 Fundamental setup of traversable wormholes	41
3.1.2 Embedding diagram for traversable wormholes	42
3.1.3 The flaring-out condition for traversable wormhole	42
3.1.4 No-horizon conditions	43
3.1.5 The construction of the Lorentzian traversable wormhole .	43
3.2 Thin-shell wormhole	45
3.2.1 The fundamental setup for thin-shell wormhole	46
3.2.2 The embedding diagram for thin-shell wormhole	49
3.2.3 The flaring-out condition for thin-shell wormhole	49
3.2.4 Junction condition	50

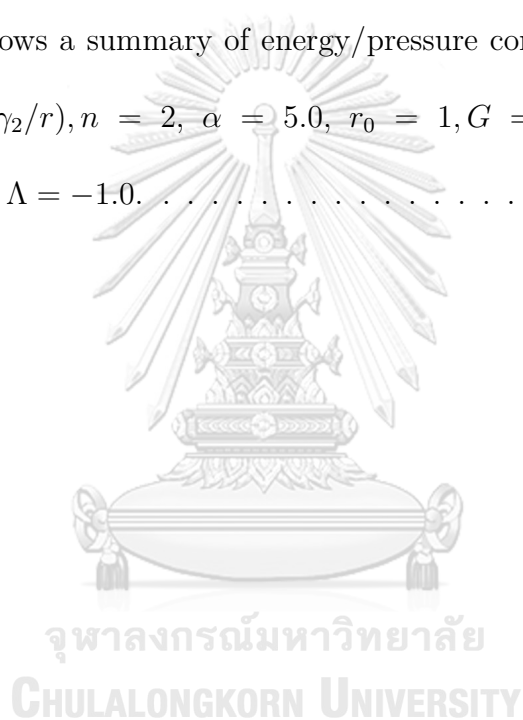
Chapter	Page
3.2.5 Stability of the thin-shell wormhole	54
IV Wormholes in Massive Gravity	57
4.1 Lorentzian Traversable Wormhole in dRGT massive gravity theory	59
4.1.1 Equation of motion for Lorentzian traversable wormhole .	60
4.1.2 Analyze the energy conditions for Lorentzian traversable wormholes	62
4.2 The thin-shell Wormhole in dRGT massive gravity theory	82
4.2.1 Linear model	91
4.2.2 Chaplygin gas model	93
4.2.3 Generalized Chaplygin gas model	98
4.2.4 Logarithm model	102
V Discussions and conclusions	107
Bibliography	111
References	121
Appendices	121
Appendix A The Vainshtein mechanism.....	122
Appendix B The higher order derivatives of the scalar field from BD ghost.....	125

Chapter	Page
B.1 The wrong sign of the kinetic terms from the scalar field	126
B.2 The instability from BD ghost	127
B.2.1 A bounded Hamiltonian	128
B.2.2 An unbounded Hamiltonian from the higher order derivative	129
Vitae	132



List of Tables

Table	Page
4.1 Table shows a summary of energy/pressure conditions for $\Phi(r) = p = 1.0, n = 2, \alpha = 5.0, r_0 = 1, G = 1, \gamma = 0.5,$ and $\Lambda = -1.0.$. . .	68
4.2 Table shows a summary of energy/pressure conditions for $\Phi(r) = \gamma_1/r, n = 2, \alpha = 5.0, r_0 = 1, G = 1, \gamma_1 = 1.0, \gamma = 0.5,$ and $\Lambda = -1.0.$ 74	74
4.3 Table shows a summary of energy/pressure conditions for $\Phi(r) = \log(1 + \gamma_2/r), n = 2, \alpha = 5.0, r_0 = 1, G = 1, \gamma_2 = 1.0, \gamma = 0.5,$ and $\Lambda = -1.0.$	81



List of Figures

Figure	Page
2.1 The proper length ds is calculated from the Pythagorean theorem in terms of ${}^{(3)}g_{ij}$, N and N^i . This figure is referenced from [32] . . .	25
4.1 Plots show embedding diagrams of the metric (3.4) for slices $t = \text{const}, \theta = \pi/2$. The left panel shows the 2-dimensional diagram of the traversable wormhole using $r_0 = 1.0$, and $\alpha = 1.0$ (a black dot-dashed line), $r_0 = 1.0$, and $\alpha = 3.0$ (a red dot line) and $r_0 = 1.0$, and $\alpha = 5.0$ and (a blue solid line). The right panel displays 3-dimensional diagram of the traversable wormholes using the same three sets of parameters.	63
4.2 We verify the properties of the shape function introduced in Eq. (4.11). The plots show behaviors of the proposed shape function against the requirements given by the embedding diagram and the flaring-out condition for traversable wormhole in Eqs. (3.6 - 3.9) using various values of $\alpha = 1.0, 3.0, 5.0$ and $r_0 = 1$. We find that the shape function of the wormhole is completely satisfied the requirements.	64
4.3 Figures demonstrate the variation of $\rho, \rho + P_r, \rho + P_t, \rho + P_r + 2P_t$ as a function of r with $\Phi(r) = p = 1, \alpha_1 = \pm 0.1$ and $n = 2$. We have used $\alpha = 5.0, r_0 = 1, G = 1$ and various values of γ and Λ . . .	66

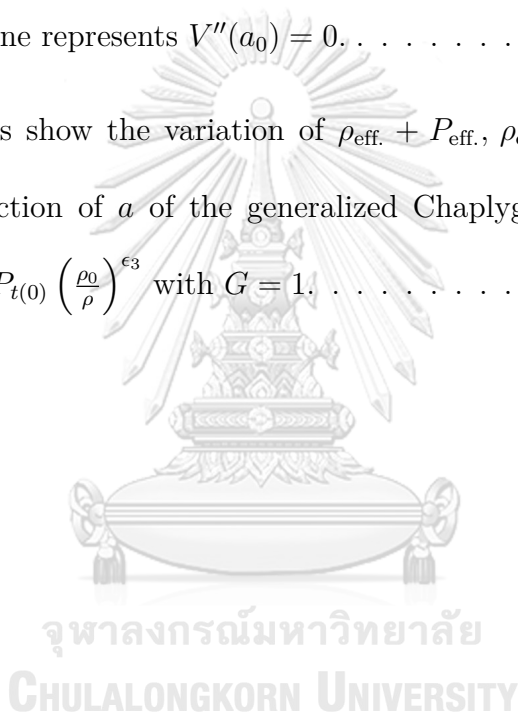
Figure	Page
4.4 Figures demonstrate the variation of $\rho, \rho + P_r, \rho + P_t, \rho + P_r + 2P_t$ as a function of r with $\Phi(r) = 1, \alpha_1 = \pm 0.01$ and $n = 2$. We have used $\alpha = 5.0, r_0 = 1, G = 1$ and various values of γ and Λ	67
4.5 Figures illustrate the variation of $\rho, \rho + P_r, \rho + P_t, \rho + P_r + 2P_t$ as a function of r with $\Phi(r) = \gamma_1/r$. Here we have used $\alpha_1 = \pm 0.1, n = 2, \alpha = 5.0, r_0 = 1, G = 1, \gamma_1 = 1.0$ and various values of γ and Λ	72
4.6 Figures illustrate the variation of $\rho, \rho + P_r, \rho + P_t, \rho + P_r + 2P_t$ as a function of r with $\Phi(r) = \gamma_1/r$. Here we have used $\alpha_1 = \pm 0.01, n = 2, \alpha = 5.0, r_0 = 1, G = 1, \gamma_1 = 1.0$ and various values of γ and Λ	73
4.7 Figures illustrate the variation of $\rho, \rho + P_r, \rho + P_t, \rho + P_r + 2P_t$ as a function of r with $\Phi(r) = \log(1 + \frac{\gamma_2}{r})$. Here we have used $\alpha_1 = \pm 0.1, n = 2, \alpha = 5.0, r_0 = 1, G = 1$ and $\gamma_2 = 1.0$ and various values of γ and Λ	79
4.8 Figures illustrate the variation of $\rho, \rho + P_r, \rho + P_t, \rho + P_r + 2P_t$ as a function of r with $\Phi(r) = \log(1 + \frac{\gamma_2}{r})$. Here we have used $\alpha_1 = \pm 0.01, n = 2, \alpha = 5.0, r_0 = 1, G = 1,$ and $\gamma_2 = 1.0$	80
4.9 This figure represents the characteristic of function $f(r)$ with parameters $G = 1, \Lambda = 0.0001, \gamma = 0.001, M = 1,$ and $\zeta = 0$. The red area represents the possible value of the static throat of thin-shell wormhole, $r_{EH} = 8.07 < a_0 \leq r_{FO} = 36.96$	89

Figure	Page
4.10 The plot shows the stable region of the linear model $P_t(\rho) = \epsilon_0\rho$ with $G = 1$. The contour shows that the constant ϵ_0 has negative values in the throat. The black shaded area is not possible for the thin-shell throat since this zone violates the flaring-out condition shown in cond. (4.67). The red dashed line represents $V''(a_0) = 0$.	92
4.11 The plots show the variation of $\rho_{\text{eff.}} + P_{\text{eff.}}$, $\rho_{\text{eff.}}$ and $\rho_{\text{eff.}} + 3P_{\text{eff.}}$ as a function of a of the linear model with $P_t(\rho) = \epsilon_0\rho$ with $G = 1$.	93
4.12 The plot shows the stable region of the Chaplygin gas model $p(\sigma) = \epsilon_1\left(\frac{1}{\rho} - \frac{1}{\rho_0}\right) + P_{t(0)}$ with $G = 1$ from the Vainshtein radius $r_V = 8.07$ to the upper limit of the flaring-out condition $r_{\text{FO}} = 36.96$. The red dashed line represents $V''(a_0) = 0$.	96
4.13 The plots show the variation of $\rho_{\text{eff.}} + P_{\text{eff.}}$, $\rho_{\text{eff.}}$ and $\rho_{\text{eff.}} + 3P_{\text{eff.}}$ as a function of a of the Chaplygin gas model with $P_t(\rho) = \epsilon_1\left(\frac{1}{\rho} - \frac{1}{\rho_0}\right) + P_{t(0)}$ with $G = 1$.	97
4.14 This plot illustrates the function of $P_{t(0)}$ against r with the set of parameters as $G = 1, \Lambda = 0.0001, \gamma = 0.001, M = 1$, and $\zeta = 0$. The value of $P_{t(0)}$ is positive for all range of r that satisfies the flaring-out condition ($r \in [2.00, 36.96]$).	99

4.15 The plot shows the stable region of the generalized Chaplygin gas model $P_{t(0)}(\rho) = P_{t(0)}(\frac{\rho_0}{\rho})^{\epsilon_2}$ with $G = 1$ from the Vainshtein radius $r_V = 8.07$ to the upper limit of the flaring-out condition $r_{FO} = 36.96$. The red dashed line represents $V''(a_0) = 0$ 100



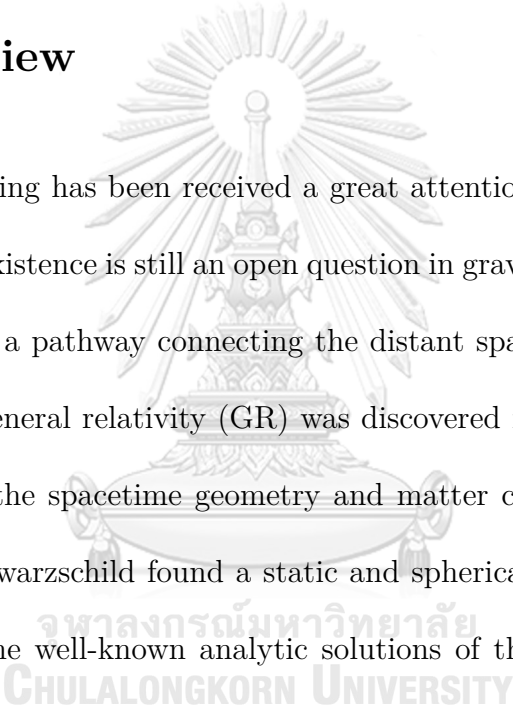
Figure	Page
4.16 The plots show the variation of $\rho_{\text{eff.}} + P_{\text{eff.}}$, $\rho_{\text{eff.}}$ and $\rho_{\text{eff.}} + 3P_{\text{eff.}}$ as a function of a of the generalized Chaplygin gas model with $P_t(\rho) = P_{t(0)} \left(\frac{\rho_0}{\rho}\right)^{\epsilon_2}$ with $G = 1$	101
4.17 The plot shows the stable region of the linear model $P_t(\rho) = \epsilon_3 \log\left(\frac{\rho}{\rho_0}\right) + P_{t(0)}$ with $G = 1$. The result shows that ϵ_3 can have both negative values and positive ones in the throat with radius a_0 . The red dashed line represents $V''(a_0) = 0$	105
4.18 The plots show the variation of $\rho_{\text{eff.}} + P_{\text{eff.}}$, $\rho_{\text{eff.}}$ and $\rho_{\text{eff.}} + 3P_{\text{eff.}}$ as a function of a of the generalized Chaplygin gas model with $P_t(\rho) = P_{t(0)} \left(\frac{\rho_0}{\rho}\right)^{\epsilon_3}$ with $G = 1$	106



CHAPTER I

INTRODUCTION

1.1 Overview



Interstellar travelling has been received a great attention and has a long history. Possibility of its existence is still an open question in gravitational physics research field. The idea of a pathway connecting the distant spacetimes had always been imaginary until general relativity (GR) was discovered in 1915. GR explains the relation between the spacetime geometry and matter constituting the Universe. In 1916, Karl Schwarzschild found a static and spherically symmetric black hole which is one of the well-known analytic solutions of the Einstein equations [1]. A black hole is the massive object that anything including light cannot escape when crossing its event horizon. In the same year of the Schwarzschild discovery, Ludwig Flamm discovered another solution of the Einstein's equation called white hole [2]. In contrary to a black hole, a white hole is supposed to eject matter and light from its event horizon. According to these two solutions, one can imagine that the spacetime in our Universe maybe connect by a conduit. In 1935, Einstein and Rosen successfully proposed the existence of the conduit named a bridge [3].

The term wormhole was first introduced by Misner and Wheeler [4]. The original version of the wormhole had been popular in the field before it was ruled out since the throat of wormhole is not stabilized and not possible to travel.

Nevertheless, in order to halt the wormhole's throat to shut, one could add a scalar field to couple to gravity for holding the throat long enough to send matter or light from one place to another. This concept initiated a new type of wormhole firstly proposed by Ellis [5] and independently by Bronnikov [6]. Unfortunately, it has a price to pay since the stable wormhole's requirement is the exotic matter which violates the energy conditions. Moreover, the exotic matter has never been discovered in our Universe. Some conditions to build the traversable wormholes were introduced by Morris and Throne in 1988, according to Ref.[7]. These solutions are obtained by considering an unusual type of exotic matter which can maintain the structure of the wormhole. Additionally, this exotic matter with negative energy density satisfies the flare-out condition but violates weak energy condition [7, 8].

The alternative theories of gravity play a major role in constructing traversable wormholes. In Ref. [9], the traversable wormholes in $f(R)$ gravity were investigated. Moreover, the factors responsible for the violation of energy conditions are discussed in the literature. The scalar tensor theory and $f(R)$ theory are applied to study the traversable wormholes in Ref. [10]. The influence of the shape and red shift functions on null and weak energy conditions has been conducted in Ref. [11]. Among various models of the modified gravity of theories, massive gravity theory is one of candidates to explain the accelerated expansion of the

Universe. In 1939, Fierz and Pauli proposed the linear theory of massive gravity as a mass of graviton [12]. Later in 1970, the theory was shown to suffer the van Dam, Veltman and Zakharov (vDVZ) discontinuity that the massless limit of FP theory does not converge to the standard GR [13, 14]. The nonlinear theory of massive gravity was first proposed by Vainshtein in Ref.[15] to solve the vDVZ discontinuity. The emergence of nonlinear massive gravity leads to a new problem called the Boulware-Deser (BD) ghost [16] which is eliminated by a new non-linear version of massive gravity proposed by de Rham, Gabadadze, and Tolley (dRGT) in 2010 [17].

In this thesis, we will provide a broad picture of the development in massive gravity from FP theory to dRGT massive gravity in section II. We introduce two types of wormholes; traversable and thin-shell wormholes in section III. Both wormholes in dRGT massive gravity will be explained in section IV. Our results are discussed and summarized in section V.

1.2 The brief history of the wormhole development

As it is well accepted, GR is an elegant theory describing the relation between the spacetime curvature and matter. Frankly speaking, this means that the spacetime can be curved by the mass and energy of the matter. GR has succeeded to predict the numerous events in nature, e.g., gravitational time dilation [18, 19], the precession of Mercury's orbit [20], and gravitational waves [21]. The detec-

tion of the gravitational waves, after 100 years of the GR predicted by Einstein, was first announced in 2016 by LIGO (Laser Interferometer Gravitational-Wave Observatory) [21].

According to GR, the Einstein field equations are given by the second order non-linear partial differential equations,

$$G_{\alpha\beta} = 8\pi GT_{\alpha\beta}, \quad (1.1)$$

where $G_{\alpha\beta}$ is the Einstein tensor containing the information of the spacetime's curvature, $T_{\alpha\beta}$ is the energy momentum tensor which has the energy density, momentum density, pressure and shear of matter, and G is the Newton's constant.

The Einstein tensor $G_{\alpha\beta}$ is defined as

$$G_{\alpha\beta} \equiv R_{\alpha\beta} - \frac{1}{2}g_{\alpha\beta}R, \quad (1.2)$$

where R is the Ricci scalar, which is the nontrivial contraction of a metric tensor and Ricci tensor defined as

$$R = g_{\alpha\beta}R^{\alpha\beta}, \quad (1.3)$$

$g_{\alpha\beta}$ is the metric tensor of the line element

$$ds^2 = g_{\alpha\beta}dx^\alpha dx^\beta, \quad (1.4)$$

x^α is the spacetime coordinates, $R_{\alpha\beta}$ is the Ricci tensor written in terms of Christoffel connection $\Gamma_{\alpha\beta}^\rho$ as follows:

$$R_{\alpha\beta} = \partial_\rho \Gamma_{\alpha\beta}^\rho - \partial_\beta \Gamma_{\rho\alpha}^\rho + \Gamma_{\rho\lambda}^\rho \Gamma_{\alpha\beta}^\lambda - \Gamma_{\beta\lambda}^\rho \Gamma_{\rho\alpha}^\lambda, \quad (1.5)$$

We recall the Bianchi identity, i.e.,

$$\nabla^\alpha R_{\alpha\beta} = \frac{1}{2}\nabla_\beta R. \quad (1.6)$$

This leads to $\nabla^\alpha G_{\alpha\beta} = 0$. In this thesis, we consider only the four-dimensional spacetime in spherical coordinates $x^\alpha = (t, r, \theta, \phi)$.

The metric $g_{\mu\nu}$ plays the major role of the dynamical variable of the theory. The Einstein-Hilbert action providing the Einstein field equation by the variational principle is given by

$$S_{\text{EH}} = \int d^4x \sqrt{-g} R. \quad (1.7)$$

Applying the principle of variation, we obtain

$$\delta S_{\text{EH}} = \int d^4x \sqrt{-g} R_{\alpha\beta} \delta g^{\alpha\beta} + \int d^4x R \delta \sqrt{-g} + \int d^4x \sqrt{-g} g_{\alpha\beta} \delta R^{\alpha\beta}. \quad (1.8)$$

In order to obtain the equations of motion, we apply the identity

$$\ln(\det M) = \text{Tr}(\ln M), \quad (1.9)$$

where M is a square matrix with nonvanishing determinant. By varying Eq. (1.9), we obtain

$$\frac{1}{\det M} \delta(\det M) = \text{Tr}(M^{-1} \delta M). \quad (1.10)$$

Taking $M = g$, we get

$$\delta g = g(g^{\alpha\beta} \delta g_{\alpha\beta}) = -g(g_{\alpha\beta} \delta g^{\alpha\beta}). \quad (1.11)$$

Then the second term of Eq. (1.8) becomes

$$\int d^4x R \delta \sqrt{-g} = - \int d^4x \frac{1}{2} R g_{\alpha\beta} \delta g^{\alpha\beta}. \quad (1.12)$$

It is straightforward to show that the variation of the Riemann tensor can be written in the following form

$$\delta R_{\alpha\lambda\beta}^{\rho} = \nabla_{\lambda} (\delta\Gamma_{\alpha\beta}^{\rho}) - \nabla_{\beta} (\delta\Gamma_{\lambda\alpha}^{\rho}). \quad (1.13)$$

With the variation of Riemann tensor in Eq. (1.13), metric compatibility ($\nabla^{\rho}g_{\alpha\beta}$) and the expansion of $\delta\Gamma_{\alpha\beta}^{\rho}$ in terms of $\delta g^{\alpha\beta}$, the last term in Eq. (1.8) yields

$$\int d^4x \sqrt{-g} g_{\alpha\beta} \delta R^{\alpha\beta} = \int d^4x \sqrt{-g} \nabla_{\rho} [g_{\alpha\beta} \nabla^{\rho} (\delta g^{\alpha\beta}) - \nabla_{\lambda} (\delta g^{\rho\lambda})]. \quad (1.14)$$

Using the Stokes's theorem, these terms are the boundary contribution at infinity. Normally we could set them to zero by vanishing the variation at infinity. However, the boundary term does not only consist of the metric variation, but also the variation of the first derivative of $g^{\alpha\beta}$ which is not conventionally zero. One might intentionally neglect the boundary terms when considering what happens in the bulk of the spacetime (inside the spacetime volume) not on the boundary. Nevertheless, the boundary term is crucial to our work since it plays the important role in testing the stability of a wormhole which will be presented in thin-shell method.

For now, we consider some solutions of the Einstein equation in Eq. (1.1). Firstly, the Schwarzschild solution from the reference [1] is the unique spherically symmetric vacuum solution ($T^{\mu}_{\nu} = 0$), according to Birkhoff's theorem, in which the Schwarzschild metric is given by

$$ds^2 = - \left(1 - \frac{2GM}{c^2 r} \right) dt^2 + \frac{dr^2}{\left(1 - \frac{2GM}{c^2 r} \right)} + r^2 d\theta^2 + r^2 \sin^2 \theta d\phi^2, \quad (1.15)$$

where M is the black hole's mass. The event horizon is at $r_S = 2GM/c^2$ which is the coordinate singularity. While the real singularity is at the center of the black

hole $r = 0$.

Another interesting solution to the Einstein equation is a wormhole. The Schwarzschild metric can describe a wormhole; however, the Schwarzschild wormhole's horizon does not allow the two-way travel. Moreover, the throat of the Schwarzschild wormhole collapse so fast that one-way travel is not even possible. A well-known wormhole that allows space adventures to travel from two directions are called a traversable wormhole. It was firstly proposed by Morris and Throne [7] where its metric tensor is given by

$$ds^2 = -e^{2\Phi(r)} dt^2 + \frac{dr^2}{1 - \frac{b(r)}{r}} + r^2 d\theta^2 + r^2 \sin^2 \theta d\phi^2, \quad (1.16)$$

where $\Phi(r)$ is the red shift function and $b(r)$ is the shape function of the wormhole. Unlike the Schwarzschild black hole solution, the wormhole solution is not a vacuum solution because it needs material ($T^\mu_\nu \neq 0$) to distort the spacetime for forming the stable shortcut between two distance points in the Universe.

However, there are some open questions that GR still cannot explain. For instance, the acceleration of the Universe expansion in the extragalactic scale [22, 23] and the asymptotically flat rotation curves of the galaxies [24].

There still remains a question that how much similarity of the solutions between GR and the modified one? A black hole in the massive gravity has been studied widely [25, 26, 27]. However, there are few work on the solution of the wormholes in massive gravity theory [28]. Thus, in this thesis, the two methods for the wormhole construction; the Lorentzian traversable wormhole and the thin-shell wormholes, are studied in the modified GR approach.

1.3 Energy conditions

We need some tools in GR to analyze whether the wormhole solutions can be constructed or not. Due to the principle of GR, it does not compel the type of matter in the solutions which leads to many possibilities in GR solutions, including exotic phenomena. The energy conditions are the criteria describing the physical behavior of matter and rule out the nonphysical one. To generate the energy conditions, the energy-momentum tensor $T_{\mu\nu}$ must contract to the four-vectors. Each type of the four-vectors, for instance, null vector l^μ or timelike vector t^μ , provide different energy conditions. The energy-momentum tensor of the isotropic fluid is given by

$$T_{\mu\nu} = (\rho + P) u_\mu u_\nu + P g_{\mu\nu}, \quad (1.17)$$

where ρ is the energy density, P is the pressure, and u_μ is a four velocity ($u_\mu u^\mu = -1$). In this thesis, we consider the three types of energy conditions to study wormholes [29].

- Null energy condition (NEC) determines the non-negative value of energy momentum tensor contracting with null vector l_μ where $l^\mu l_\mu = 0$.

$$\begin{aligned} 0 \leq T_{\mu\nu} l^\mu l^\nu &= ((\rho + P) u_\mu u_\nu + P g_{\mu\nu}) l^\mu l^\nu \\ &= (\rho + P) (u_\mu l^\mu)^2 + P l_\mu l^\mu \\ &= (\rho + P) (u_\mu l^\mu)^2. \end{aligned} \quad (1.18)$$

Then the NEC for isotropic fluid reads

$$\rho + P \geq 0. \quad (1.19)$$

Null energy condition can be interpreted as the energy of particles traveling along a null geodesic, such as photon and massless particles, which must be non-negative. The energy density or pressure can be negative as long as their summation is still equal or greater than zero.

- Weak energy condition (WEC) determines the non-negative value of energy momentum tensor contracting with timelike vector t_μ where $t_\mu t^\mu < 0$

$$\begin{aligned} 0 \leq T_{\mu\nu} t^\mu t^\nu &= ((\rho + P) u_\mu u_\nu + P g_{\mu\nu}) t^\mu t^\nu \\ &= (\rho + P)(u_\mu t^\mu)^2 + P t_\mu t^\mu. \end{aligned} \quad (1.20)$$

Assume $t_\mu = \| t \| v_\mu$, where $\| t \| = \sqrt{-t_\mu t^\mu} \geq 0$ and $v^2 = -1$ and apply Cauchy-Schwartz inequality, $|x_\mu y^\mu| \leq \| x_\mu \| \| y_\mu \|$ where x and y are null or timelike vector into the WEC, then we find

$$\frac{P}{(u_\mu v^\mu)^2} \leq \frac{P}{\| u_\mu \| \| v_\mu \|} = P \leq \rho + P \iff \rho \geq 0. \quad (1.21)$$

Then WEC is decomposed into two conditions as follows

$$\rho + P \geq 0 \text{ and } \rho \geq 0. \quad (1.22)$$

This condition is stronger than NEC since the energy density must be non-negative and so does the summation of the energy density and pressure.

- Strong energy condition (SEC) reads

$$T_{\mu\nu} t^\mu t^\nu \geq \frac{1}{2} T_\alpha^\alpha t^\beta t_\beta, \quad (1.23)$$

where t_μ is a timelike vector.

$$\begin{aligned}
\left(T_{\mu\nu} - \frac{1}{2}Tg_{\mu\nu}\right)t^\mu t^\nu &\geq 0 \\
\left((\rho + P)u_\mu u_\nu + Pg_{\mu\nu} - \frac{1}{2}(-\rho + 3P)g_{\mu\nu}\right)t^\mu t^\nu &\geq 0 \\
(\rho + P)(u_\mu t^\mu)^2 + \frac{1}{2}(\rho - P)t_\mu t^\mu &\geq 0 \\
\rho + P &\geq \frac{1}{2}(\rho - P) \geq \frac{\rho - P}{2 \|u_\mu\| \|v_\mu\|} \\
\rho + 3P &\geq 0.
\end{aligned} \tag{1.24}$$

Then SEC is decomposed into the following conditions

$$\rho + P \geq 0 \text{ and } \rho + 3P \geq 0. \tag{1.25}$$

SEC covers NEC and avoids excessively large negative pressure. However, SEC still allows the negative value of energy density such that SEC does not imply WEC.

Unfortunately, the traversable wormholes in some particular models [7] need the exotic matter which violates the energy conditions. Even though a wormhole is a solution to the Einstein's equation, it exists only in a theoretical concept. In this thesis, we will use NEC, WEC and SEC to examine the possibility of the wormhole solutions in the massive gravity theory.

CHAPTER II

Massive Gravity

Massive gravity has gained a monumental interest among gravitational and cosmological communities during the past decade due to recent progress which has overcome its traditional problems, yielding an avenue for addressing some important open questions such as the dark energy problem.

Theories with massive graviton have been studied on and off for more than 70 years. During this long development, it has been shown that massive gravity suffers from some crucial inconsistencies such as the van Dam-Veltman-Zakharov (vDVZ) discontinuity and the Boulware-Deser ghost. In this chapter, we re-examine these problems in a pedagogical manner. We first discuss the linearized General relativity and derive the equation of motion for a spin-2 “massless” graviton. Then we move on to the linear Fierz-Pauli (FP) theory and explain the mass term to the graviton along with the general solutions of the spin-5 massive graviton. The discrepancy between GR and massless limit in FP theory is known as vDVZ discontinuity. We apply the Stückelberg formalism to reveal the origin of this discontinuity from the modern effective field theory viewpoint. The linear FP theory can be generalized to the nonlinear massive gravity (NLMG). How-

ever, NLMG also experiences the ghost problem causing the instability of massive graviton. Here, we review the de Rham, Gabadadze and Tolley (dRGT) massive gravity which offer the mechanism to eliminate all the problems we mentioned above.

2.1 Linearized general relativity

Before revisiting the FP theory, we firstly study the linearized action of GR. For convenience, we use the unit $c = 1$. We start with the Einstein-Hilbert action in 4D spacetime described by the following equation

$$S_{\text{EH+matter}} = \int d^4x \sqrt{-g} \left(\frac{R}{16\pi G} + \mathcal{L}_{\text{matter}} \right), \quad (2.1)$$

where $\mathcal{L}_{\text{matter}}$ is the Lagrangian density of matter on the curved spacetime. The term “matter” refers to any matter in the Universe except the massive graviton. At this point, we are still in Einstein’s theory of GR. Applying the Euler-Lagrange method provides the equations of motion,

$$G_{\mu\nu} = R_{\mu\nu} - \frac{1}{2}g_{\mu\nu}R = 8\pi GT_{\mu\nu}, \quad (2.2)$$

where $T_{\mu\nu} = -\frac{2}{\sqrt{-g}} \frac{\delta(\sqrt{-g}\mathcal{L}_{\text{matter}})}{\delta g^{\mu\nu}}$ is the energy-momentum tensor of the matter. To linearize GR, we expand the metric $g_{\mu\nu}$ around the flat space as

$$g_{\mu\nu} = \eta_{\mu\nu} + h_{\mu\nu}, \quad (2.3)$$

where $h_{\mu\nu}$ is called the metric perturbation which transforms as a tensor under Lorentz transformations. The lowest order of the linearized GR action becomes

$$S_{\text{EH+matter}} \approx \int d^4x \left(-\frac{1}{2} \partial_\lambda h_{\mu\nu} \partial^\lambda h^{\mu\nu} + \partial_\mu h_{\nu\lambda} \partial^\nu h^{\mu\lambda} - \partial_\mu h^{\mu\nu} \partial_\nu h + \frac{1}{2} \partial_\lambda h \partial^\lambda h + 8\pi G h_{\mu\nu} T^{\mu\nu} \right), \quad (2.4)$$

where $T^{\mu\nu}(x)$ is a fixed external symmetric source. Using the integration by part technique, the linearized Einstein-Hilbert action can be written in term of a propagator

$$S_{\text{EH+matter}} = \int d^4x \left(\frac{1}{2} h_{\mu\nu} \Sigma^{\mu\nu, \alpha\beta} h_{\alpha\beta} + 8\pi G h_{\mu\nu} T^{\mu\nu} \right), \quad (2.5)$$

where the kinetic operator is defined as follows:

$$\Sigma_{\alpha\beta}^{\mu\nu} \equiv \left(\eta_\alpha^{(\mu} \eta_\beta^{\nu)} - \eta^{\mu\nu} \eta_{\alpha\beta} \right) \square - 2\eta_{(\alpha}^{(\mu} \partial^{\nu)} \partial_\beta) + \eta_{\alpha\beta} \partial^\mu \partial^\nu + \eta^{\mu\nu} \partial_\alpha \partial_\beta, \quad (2.6)$$

where $\square = \partial^\alpha \partial_\alpha$. The diffeomorphism invariance of GR implies a gauge symmetry for the metric perturbation as follow

$$h_{\mu\nu} \rightarrow h_{\mu\nu} + \partial_\mu \xi_\nu + \partial_\nu \xi_\mu. \quad (2.7)$$

Varying the action in Eq. (2.5) with respect to the metric perturbation $h_{\mu\nu}$, we obtain the equation of motion of the linearized GR

$$\frac{1}{2} \Sigma_{\mu\nu}^{\alpha\beta} h_{\alpha\beta} = \partial^\lambda \partial_{(\mu} h_{\nu)\lambda} - \frac{1}{2} \square h_{\mu\nu} - \frac{1}{2} \partial_\mu \partial_\nu h - \frac{1}{2} \eta_{\mu\nu} (\partial^\rho \partial^\sigma h_{\rho\sigma} - \square h) = 8\pi G T_{\mu\nu}. \quad (2.8)$$

To solve $h_{\mu\nu}$, we choose the Lorentz gauge,

$$\partial^\mu \bar{h}_{\mu\nu} = 0, \quad (2.9)$$

where $\bar{h}_{\mu\nu} = h_{\mu\nu} - \frac{1}{2} \eta_{\mu\nu} h$. The linearized GR equation, Eq. (2.8), reduces to

$$\square \bar{h}_{\mu\nu} = \square h_{\mu\nu} - \frac{1}{2} \eta_{\mu\nu} \square h = -8\pi G T_{\mu\nu}. \quad (2.10)$$

Its trace reads

$$\square h = 8\pi GT. \quad (2.11)$$

We substitute the trace in Eq. (2.11) into Eq. (2.10) to yield

$$\square h_{\mu\nu} = -8\pi G \left(T_{\mu\nu} - \frac{\eta_{\mu\nu}}{2} T \right). \quad (2.12)$$

We note here that we have 10 components of the four-dimensional symmetric tensor of $h_{\mu\nu}$. There are four constraints from the diffeomorphism invariance in Eq. (2.7), and four more constraints from the Lorentz gauge in Eq. (2.9). The total degrees of freedom of $h_{\mu\nu}$ is $10 - 4 - 4 = 2$.

According to Green's function method, the solution of $h_{\mu\nu}$ is

$$h_{\mu\nu} = 8\pi G \int \frac{d^4 p}{(2\pi)^4} \frac{e^{ip^\beta x_\beta}}{p^\alpha p_\alpha} \left(\tilde{T}_{\mu\nu}(p) - \frac{\eta_{\mu\nu}}{2} \tilde{T}(p) \right), \quad (2.13)$$

where $\tilde{T}_{\mu\nu}(p) = \int d^4 x e^{-ip^\beta x_\beta} T_{\mu\nu}(x)$ is the function by Fourier transform of the source $T_{\mu\nu}$ and $p^\beta x_\beta = -p_t t + p_x x + p_y y + p_z z$ is the scalar product of 4-dimensional vectors (p and x). We consider the conserved source as the point mass,

$$T_{\mu\nu}(x) = M g_{\mu 0} g_{\nu 0} \delta^3(x),$$

$$\tilde{T}_{\mu\nu}(p) = 2\pi M g_{\mu 0} g_{\nu 0} \delta(p^0). \quad (2.14)$$

Then the components of h_{ij} vanish. Now we consider

$$\begin{aligned} h_{00} &= 8\pi G \int \frac{d^4 p}{(2\pi)^4} \frac{e^{ip^\beta x_\beta}}{p^\alpha p_\alpha} \left(\tilde{T}_{00}(p) - \frac{\eta_{00}}{2} \tilde{T}(p) \right) \\ &= 8\pi G \int \frac{d^4 p}{(2\pi)^4} \frac{e^{ip^\beta x_\beta}}{p^\alpha p_\alpha} \pi M \delta(p^0) \\ &= 4\pi G \int \frac{d^3 p}{(2\pi)^3} \frac{e^{i\vec{p}\vec{x}} M}{\vec{p}^2}, \end{aligned} \quad (2.15)$$

where $\tilde{T}(p) = \tilde{T}_\mu^\mu = g^{\mu\nu}\tilde{T}_{\mu\nu} = 2\pi M\delta_0^\mu g_{\mu 0}\delta(p^0) = -2\pi M\delta(p^0)$ and $\vec{p}\vec{x} = p_x x + p_y y + p_z z = pr \cos(\theta)$ is the scalar product of 3-dimensional vectors (\vec{p} and \vec{x}).

According to the complex analysis, we move the pole of the complex integral by adding an infinitesimal value ϵ :

$$\begin{aligned}
h_{00} &= 4\pi GM \int \frac{d^3 p}{(2\pi)^3} \frac{e^{i\vec{p}\vec{x}}}{p^2 + \epsilon^2} \\
&= 4\pi GM \int \frac{p^2 dp \sin\theta d\theta d\phi}{(2\pi)^3} \frac{e^{ipr \cos\theta}}{(p+i\epsilon)(p-i\epsilon)} \\
&= 4\pi GM \int_0^\infty \frac{dp}{(2\pi)^2} \frac{p(e^{ipr} - e^{-ipr})}{ir(p+i\epsilon)(p-i\epsilon)} \\
&= 4\pi GM \int_{-\infty}^\infty \frac{dp}{(2\pi)^2} \frac{pe^{ipr}}{ir} \left(\frac{1}{2(p+i\epsilon)} + \frac{1}{2(p-i\epsilon)} \right) \\
&= 4\pi GM \left(\frac{1}{(2\pi)^2 ir} \left[2\pi i \lim_{p \rightarrow i\epsilon} (p-i\epsilon) \frac{e^{ipr}}{2(p-i\epsilon)} \right] \right) = \frac{GM}{r}. \quad (2.16)
\end{aligned}$$

In the last line, we have chosen the upper contour integral that covers $k = i\epsilon$ and applied the residue theorem. Next, we consider h_{ij} such that

$$\begin{aligned}
h_{ij} &= 8\pi G \int \frac{d^4 p}{(2\pi)^4} \frac{e^{ipx}}{p^2} \left(-\frac{\eta_{ij}}{2} \tilde{T}(p) \right) \\
&= 8\pi G \int \frac{d^4 p}{(2\pi)^4} \frac{e^{ipx}}{p^2} \pi M \delta(p^0) \eta_{ij} \\
&= 4\pi G \int \frac{d^3 p}{(2\pi)^3} \frac{e^{i\vec{p}\vec{x}}}{p^2} M \delta_{ij}, \quad (2.17)
\end{aligned}$$

where $\eta_{ij} = \delta_{ij}$. With the same technique for calculating h_{00} , we finally get

$$h_{ij} = \frac{GM}{r} \delta_{ij}. \quad (2.18)$$

In conclusion, the non-trivial solutions of the perturbation tensor $h_{\mu\nu}$ in GR in four dimensions take the form:

$$h_{tt} = h_{rr} = h_{\theta\theta} = h_{\phi\phi} = \frac{GM}{r}. \quad (2.19)$$

2.2 Fierz-Pauli (FP) action

Now we consider the FP linear theory where its action is the linearized GR with the massive terms of metric perturbation (up to second order) [12, 16],

$$S_{\text{FP+matter}} = \int d^4x \left(\frac{1}{2} h_{\mu\nu} \Sigma^{\mu\nu, \alpha\beta} h_{\alpha\beta} - \frac{1}{2} m^2 (h_{\mu\nu} h^{\mu\nu} - h^2) + 8\pi G h_{\mu\nu} T^{\mu\nu} \right), \quad (2.20)$$

where m is the mass of graviton, and $T^{\mu\nu}$ is an external symmetric source. The mass term, $\frac{1}{2} m^2 (h_{\mu\nu} h^{\mu\nu} - h^2)$, is the modification by massive gravity. The equation of motion of the FP theory in Eq. (2.20) is given by [16]

$$\frac{1}{2} \Sigma_{\mu\nu}^{\alpha\beta} h_{\alpha\beta} + m^2 (h_{\mu\nu} - \eta_{\mu\nu} h) = 8\pi G T_{\mu\nu} \quad (2.21)$$

To find the solution of the massive graviton in FP action, we first take ∂^μ to the Eq. (2.21) to obtain

$$\partial^\mu h_{\mu\nu} - \partial_\nu h = \frac{8\pi G}{m^2} \partial^\mu T_{\mu\nu} = 0, \quad (2.22)$$

where we have applied a conserved source, $\partial^\mu T_{\mu\nu} = 0$. Substituting Eq. (2.22) into Eq. (2.21) and taking trace, we have

$$h = -\frac{8\pi G}{3} \left(\frac{T}{m^2} - \frac{2}{m^4} \partial_\mu \partial^\mu T \right) = -\frac{8\pi G T}{3m^2}. \quad (2.23)$$

Plugging Eq. (2.23) into Eq. (2.21), we obtain

$$\partial^\mu h_{\mu\nu} = -\frac{8\pi G}{3m^2} \partial_\nu T. \quad (2.24)$$

We use Eq. (2.21, 2.23, 2.24) to obtain [16]

$$(\square - m^2) h_{\mu\nu} = -8\pi G \left(T_{\mu\nu} - \frac{1}{3} \left(\eta_{\mu\nu} - \frac{\partial_\mu \partial_\nu}{m^2} \right) T \right). \quad (2.25)$$

In FP theory, there is no gauge symmetry like in GR. However, there are 4 constraints from Eq. (2.24) and one more constraint from Eq. (2.23). The total degrees of freedom of $h_{\mu\nu}$ for FP theory is just $10 - 4 - 1 = 5$.

According to the Green's function method, we use the frequency domain to investigate the solution of $h_{\mu\nu}$ from Eq. (2.25)

$$h_{\mu\nu}(x) = 8\pi G \int \frac{d^4 p}{(2\pi)^4} \frac{e^{ip^\beta x_\beta}}{p^\alpha p_\alpha + m^2} \left(\tilde{T}_{\mu\nu}(p) - \frac{1}{3} \left(\eta_{\mu\nu} + \frac{p_\mu p_\nu}{m^2} \right) \tilde{T}(p) \right), \quad (2.26)$$

where $\tilde{T}_{\mu\nu}(p) = \int d^4 x e^{-ip^\alpha x_\alpha} T_{\mu\nu}(x)$. We apply the point mass as the conserved source as Eq. (2.14), and consider the general solutions for Eq. (2.26). Here we have

$$\begin{aligned} h_{tt} &= \frac{16\pi GM}{3} \int \frac{d^3 p}{(2\pi)^3} \frac{e^{i\vec{p}\vec{x}}}{\vec{p}^2 + m^2} \\ &= \frac{16\pi GM}{3ir} \int_{-\infty}^{\infty} \frac{dp}{2\pi} e^{ipr} \left(\frac{1}{2(p+im)} + \frac{1}{2(p-im)} \right) \\ &= \frac{4GM}{3r} e^{-mr}, \\ h_{ti} &= h_{it} = 0, \\ h_{rr} &= \frac{2GM}{3r} e^{-mr} \left(\frac{1+mr}{m^2 r^2} \right), \\ h_{\theta\theta} &= \frac{2GM}{3r} e^{-mr} \left(\frac{1+mr+m^2 r^2}{m^2 r^2} \right), \\ h_{\phi\phi} &= \frac{2GM \sin^2 \theta}{3r} e^{-mr} \left(\frac{1+mr+m^2 r^2}{m^2 r^2} \right). \end{aligned} \quad (2.27)$$

With the massless limit ($r \ll 1/m$), the non-zero terms of the general solutions

reduce to

$$\begin{aligned}
 h_{tt} &= \frac{4GM}{3r}, \\
 h_{rr} &= \frac{4GM}{3m^2r^3}, \\
 h_{\theta\theta} &= \frac{2GM}{3m^2r^3}, \\
 h_{\phi\phi} &= \frac{2GM \sin^2 \theta}{3m^2r^3}.
 \end{aligned} \tag{2.28}$$

2.3 vDVZ discontinuity

The prediction in FP theory should reduce to GR when taking limit $m \rightarrow 0$. However, the solutions of FP theory in Eq. (2.28) do not converge to those in linearized GR in Eq. (2.19) as the graviton mass converge to zero. In this section, the limitation of the FP massive gravity theory will be discussed via the gravitational lensing. We follow the procedure and analyze of the light bending in the weak field limit in Ref. [29]. The components of metric tensor read

$$\begin{aligned}
 g_{tt}(r \rightarrow \infty) &= -(1 + \Phi(r)), \\
 g_{rr}(r \rightarrow \infty) &= (1 - \Psi(r)),
 \end{aligned} \tag{2.29}$$

where $\Phi(r)$ and $\Psi(r)$ are the arbitrary functions of r . For the case that $\Phi(r)$ is proportional to $\Psi(r)$, we consider $\Psi(r) = \gamma\Phi(r)$ where γ is called the Parameterized-Post-Newtonian (PPN) parameter. The light is bent with the angle given by

$$\alpha = \frac{2GM(1 + \gamma)}{b}, \tag{2.30}$$

where b is the impact parameter from a massive source.

We first consider the solution in the linearized GR from Eq. (2.3) and their solutions from Eqs. (2.13). The arbitrary functions for massless case are given by

$$\Phi_{\text{GR}}(r) = \Psi_{\text{GR}}(r) = -\frac{GM}{r}. \quad (2.31)$$

In this case, the PPN parameter $\gamma = 1$ and the light bending angle is

$$\alpha = \frac{4GM}{b}. \quad (2.32)$$

Then we consider the solution in the FP theory in Eqs. (2.26). The arbitrary functions for massless limit of FP theory are given by

$$\begin{aligned} \Phi_{\text{FP}}(r) &= -\frac{4GM}{3r} \\ \Psi_{\text{FP}}(r) &= -\frac{2GM}{3r} \end{aligned} \quad (2.33)$$

The PPN parameter $\gamma = \frac{1}{2}$, then the light bending angle is

$$\alpha = \frac{3GM}{b}. \quad (2.34)$$

There is 25 percent difference of light bending angle of FP theory, comparing to GR. Even if the limit of the graviton mass is zero, this discrepancy does not disappear. This is called van Dam-Veltman-Zakharov (vDVZ) discontinuity [13, 14].

2.4 The Origin of vDVZ discontinuity: The Stueckelberg Trick

We presented in the section (2.3) that the FP massive gravity in the massless limit cannot reduce to GR, according to vDVZ discontinuity. In this section, we will

apply the Stueckelberg trick to show the origin of the vDVZ discontinuity.

Let consider the FP massive gravity from Eq. (2.20)

$$S_{\text{FP+matter}} = \int d^4x \left(\frac{1}{2} h_{\mu\nu} \Sigma^{\mu\nu, \alpha\beta} h_{\alpha\beta} - \frac{1}{2} m^2 (h_{\mu\nu} h^{\mu\nu} - h^2) + 8\pi G h_{\mu\nu} T^{\mu\nu} \right),$$

where $\frac{1}{2} h_{\mu\nu} \Sigma^{\mu\nu, \alpha\beta} h_{\alpha\beta}$ is the massless term of the linear theory. We introduce a Stueckelberg vector field A_μ such that

$$h_{\mu\nu} \rightarrow h_{\mu\nu} + \partial_\mu A_\nu + \partial_\nu A_\mu. \quad (2.35)$$

Let consider the change of each term via the transformation in Eq. (2.35),

$$\frac{1}{2} h_{\mu\nu} \Sigma^{\mu\nu, \alpha\beta} h_{\alpha\beta} \rightarrow \frac{1}{2} h_{\mu\nu} \Sigma^{\mu\nu, \alpha\beta} h_{\alpha\beta} \text{ (invariant)}, \quad (2.36)$$

$$h_{\mu\nu} h^{\mu\nu} - h^2 \rightarrow h_{\mu\nu} h^{\mu\nu} - h^2 + 4(h_{\mu\nu} \partial^\mu A^\nu - h \partial^\mu A_\mu) + F_{\mu\nu} F^{\mu\nu}, \quad (2.37)$$

$$h_{\mu\nu} T^{\mu\nu} \rightarrow h_{\mu\nu} T^{\mu\nu} - 2A_\nu \partial_\mu T^{\mu\nu}, \quad (2.38)$$

where $F_{\mu\nu} \equiv \partial_\mu A_\nu - \partial_\nu A_\mu$ and the last term is integrated by part to yield $T^{\mu\nu} \partial_\mu A_\nu = \partial_\mu (A_\nu T^{\mu\nu}) - A_\nu \partial_\mu T^{\mu\nu}$. The total derivative is negligible. Then the FP action becomes

$$S_{\text{FP+matter}} \rightarrow \int d^4x \left(\frac{1}{2} h_{\mu\nu} \Sigma^{\mu\nu, \alpha\beta} h_{\alpha\beta} - \frac{1}{2} m^2 (h_{\mu\nu} h^{\mu\nu} - h^2) + 8\pi G h_{\mu\nu} T^{\mu\nu} - \frac{m^2}{2} F_{\mu\nu} F^{\mu\nu} - 2m^2 (h_{\mu\nu} \partial^\mu A^\nu - h \partial^\mu A_\mu) - 16\pi G A_\nu \partial_\mu T^{\mu\nu} \right). \quad (2.39)$$

The gauge symmetry is given by

$$\delta h_{\mu\nu} = \partial_\mu \xi_\nu + \partial_\nu \xi_\mu, \quad \delta A_\mu = -\xi_\mu. \quad (2.40)$$

So at this point, the massless limit is still not smooth, since we lose one of the original 5 degrees of freedom [16].

In the next step, we introduce a scalar gauge symmetry by another Stueckelberg field ϕ . So that

$$A_\mu \rightarrow A_\mu + \partial_\mu \phi. \quad (2.41)$$

Any term with A_μ changes under the transformation in Eq. (2.41) as follows

$$F_{\mu\nu}F^{\mu\nu} \rightarrow F_{\mu\nu}F^{\mu\nu} (\text{invariant}), \quad (2.42)$$

$$h_{\mu\nu}\partial^\mu A^\nu - h\partial^\mu A_\mu \rightarrow h_{\mu\nu}\partial^\mu A^\nu - h\partial^\mu A_\mu + h_{\mu\nu}\partial^\mu\partial^\nu\phi - h\partial_\mu\partial^\mu\phi, \quad (2.43)$$

$$A_\mu\partial_\nu T^{\mu\nu} \rightarrow A_\mu\partial_\nu T^{\mu\nu} - \phi\partial_\mu\partial_\nu T^{\mu\nu}, \quad (2.44)$$

where we have applied the integration by parts for the last line. The FP action reads

$$\begin{aligned} S_{\text{FP+matter}} \rightarrow & \int d^4x \left(\frac{1}{2}h_{\mu\nu}\Sigma^{\mu\nu,\alpha\beta}h_{\alpha\beta} - \frac{1}{2}m^2(h_{\mu\nu}h^{\mu\nu} - h^2) + 8\pi Gh_{\mu\nu}T^{\mu\nu} \right. \\ & - \frac{m^2}{2}F_{\mu\nu}F^{\mu\nu} - 2m^2(h_{\mu\nu}\partial^\mu A^\nu - h\partial^\mu A_\mu) - 2m^2(h_{\mu\nu}\partial^\mu\partial^\nu\phi - h\partial_\mu\partial^\mu\phi) \\ & \left. - 16\pi G(A_\nu\partial_\mu T^{\mu\nu} - \phi\partial_\mu\partial_\nu T^{\mu\nu}) \right). \end{aligned} \quad (2.45)$$

To investigate the linear massive gravity, we take $m \rightarrow 0$ limit to the action. However, the degrees of freedom will be lost. To avoid so, we rescale the Stueckelberg fields using

$$A_\mu \rightarrow \frac{A_\mu}{m}, \quad \phi \rightarrow \frac{\phi}{m^2}. \quad (2.46)$$

The FP action becomes

$$\begin{aligned} S_{\text{FP+matter}} = & \int d^4x \left(\frac{1}{2}h_{\mu\nu}\Sigma^{\mu\nu,\alpha\beta}h_{\alpha\beta} - \frac{1}{2}m^2(h_{\mu\nu}h^{\mu\nu} - h^2) + 8\pi Gh_{\mu\nu}T^{\mu\nu} \right. \\ & - \frac{1}{2}F_{\mu\nu}F^{\mu\nu} - 2m(h_{\mu\nu}\partial^\mu A^\nu - h\partial^\mu A_\mu) - 2(h_{\mu\nu}\partial^\mu\partial^\nu\phi - h\partial_\mu\partial^\mu\phi) \\ & \left. - 16\pi G \left(\frac{A_\nu}{m}\partial_\mu T^{\mu\nu} - \frac{\phi}{m^2}\partial_\mu\partial_\nu T^{\mu\nu} \right) \right). \end{aligned} \quad (2.47)$$

Gauge transformations of functions are given by

$$\begin{aligned}\delta h_{\mu\nu} &= \partial_\mu \xi_\nu + \partial_\nu \xi_\mu, & \delta A_\mu &= -m\xi_\mu, \\ \delta A_\mu &= \partial_\mu \Lambda, & \delta \phi &= -m\Lambda.\end{aligned}\quad (2.48)$$

To consider the massless limit, we have to assume the conserved source ($\partial_\mu T^{\mu\nu} = 0$) to prevent the divergence from the coupled terms $\frac{A_\nu}{m} \partial_\mu T^{\mu\nu}$ and $\frac{\phi}{m^2} \partial_\mu \partial_\nu T^{\mu\nu}$.

The rescaled FP action reads

$$\begin{aligned}S_{\text{FP+matter}} &= \int d^4x \left(\frac{1}{2} h_{\mu\nu} \Sigma^{\mu\nu, \alpha\beta} h_{\alpha\beta} + 8\pi G h_{\mu\nu} T^{\mu\nu} - \frac{1}{2} F_{\mu\nu} F^{\mu\nu} \right. \\ &\quad \left. - 2(h_{\mu\nu} \partial^\mu \partial^\nu \phi - h \partial_\mu \partial^\mu \phi) \right).\end{aligned}\quad (2.49)$$

To see the reason behind the vDVZ discontinuity, we will decouple the tensor $h_{\mu\nu}$ from the scalar field ϕ by considering [16]

$$h_{\mu\nu} = h'_{\mu\nu} + \phi \eta_{\mu\nu}.\quad (2.50)$$

It is straightforward to show that

$$\begin{aligned}\frac{1}{2} h_{\mu\nu} \Sigma^{\mu\nu, \alpha\beta} h_{\alpha\beta} &= \frac{1}{2} h'_{\mu\nu} \Sigma^{\mu\nu, \alpha\beta} h'_{\alpha\beta} \\ &\quad + 2 \left(\partial_\mu \phi \partial^\mu h' - \partial_\mu \phi \partial_\nu h'^{\mu\nu} + \frac{3}{2} \partial_\mu \phi \partial^\mu \phi \right)\end{aligned}\quad (2.51)$$

$$8\pi G h_{\mu\nu} T^{\mu\nu} = 8\pi G (h'_{\mu\nu} T^{\mu\nu} + \phi T)\quad (2.52)$$

$$-2(h_{\mu\nu} \partial^\mu \partial^\nu \phi - h \partial_\mu \partial^\mu \phi) = -2h'_{\mu\nu} \partial^\mu \partial^\nu \phi + 2h' \partial_\mu \partial^\mu \phi + 6\phi \partial_\mu \partial^\mu \phi.\quad (2.53)$$

Using the integration by parts for Eq. (2.53) and neglecting the total derivative terms, so the massless limit FP action eventually becomes

$$\begin{aligned}S_{\text{FP+matter}} &= \int d^4x \left(\frac{1}{2} h'_{\mu\nu} \Sigma^{\mu\nu, \alpha\beta} h'_{\alpha\beta} + 8\pi G h'_{\mu\nu} T^{\mu\nu} + 8\pi G \phi T \right. \\ &\quad \left. - \frac{1}{2} F_{\mu\nu} F^{\mu\nu} - 3\partial_\mu \phi \partial^\mu \phi \right).\end{aligned}\quad (2.54)$$

In the massless limit, the total degrees of freedom is still 5; one from the scalar field ϕ , two from massless photon A_μ , and another two from massless graviton $h_{\mu\nu}$. Note that there is the coupling term between the scalar field ϕ and the trace of the energy momentum tensor T as $8\pi G\phi T$, thanks to the Stueckelberg trick. Moreover the term also has the same strength as the massless tensor $h_{\mu\nu}$ couples to the energy momentum tensor $T^{\mu\nu}$. So it causes the vDVZ discontinuity in massless limit FP theory since there is no such term in GR. It shows that the FP theory does not recover GR in the massless limit.

2.5 Nonlinear massive gravity

According to the study of the FP theory, the mechanism of the vDVZ discontinuity is revealed by the Stueckelberg trick. The linear theory of massive gravity is the first step for the full nonlinear theory in massive theory. There was a study showing that the length of nonlinearity dominates over the linear theory when the distance is smaller than a length scale called Vainshtein radius, $r_V = \left(\frac{GM}{m^4}\right)^{1/5}$ [15]. The proof of the Vainshtein radius is shown in the Appendix A (see Eq. (A.13)). The result from the FP theory works well with the large distance $r > r_V$. However, the nonlinear massive gravity theory dominates in the range $r < r_V$. With a limit of $m \rightarrow 0$, the Vainshtein radius increases to infinity. In this section, we will begin to construct the simplest case of nonlinear massive gravity. The action consists of the kinetic terms from Ricci scalar like GR, $L_{\text{kinetic}} = \frac{R}{16\pi G}$ and the FP mass term $L_{\text{mass}} = -\frac{1}{2}m^2(h_{\mu\nu}h^{\mu\nu} - h^2)$. Unfortunately, it leads to the

BD ghost in the system [34]. The BD ghost does not only cause the negative energy when interacting with matter but also causes the unphysical extra degree of freedom (dof). Then there are 6 degrees of freedom in this case. To eliminate the extra scalar mode from BD ghost, one could apply the same technique in the Galileon theory that provides non-extra scalar mode. The nonlinear massive gravity without ghost was successfully discovered by de Rham, Gabadadze and Tolley (dRGT). The dRGT action and the static solution is presented in this section.

2.5.1 The extra degree of freedom in nonlinear Fierz-Pauli theory

Before continuing the study about the full nonlinear massive gravity, we investigate another problem emerging from the nonlinear extension. The first sign of the ghost is the extra degree of freedom appearing in the nonlinear massive gravity. The metric tensor $g_{\mu\nu}$ can be split into two terms; the reference metric (or fiducial metric) $f_{\mu\nu}$ and the metric perturbation $h_{\mu\nu}$,

$$g_{\mu\nu} = f_{\mu\nu} + h_{\mu\nu}. \quad (2.55)$$

The reference metric describes the propagation of the linear massive graviton which can be seen further in the appendix A. We use the nonlinearity from Einstein-Hilbert action and consider the nonlinear GR with the flat reference metric $f^{\mu\nu} =$

$\eta^{\mu\nu}$,

$$\begin{aligned} S &= \frac{1}{16\pi G} \int d^4x \left[\sqrt{-g}R - \frac{1}{2}m^2 (h_{\mu\nu}h^{\mu\nu} - h^2) \right] \\ &= \frac{1}{16\pi G} \int d^4x \left[\sqrt{-g}R - \frac{1}{2}m^2 \eta^{\mu\alpha} \eta^{\nu\beta} (h_{\mu\nu}h_{\alpha\beta} - h_{\mu\alpha}h_{\nu\beta}) \right], \end{aligned} \quad (2.56)$$

where the Ricci scalar is the kinetic term of the field $g_{\mu\nu}$ and also responsible for nonlinearity. While the massive terms are borrowed from FP theory.

The ADM formalism is applied to study the ghost in nonlinear massive gravity [30, 31]. We begin with describing the four-dimensional spacetime by the series of spacelike hypersurfaces Σ_t where t is time on the hypersurface. We introduce the normal vector n_i on the hypersurfaces where $n_i n^i = -1$ is a time-like condition. A spatial three-dimensional metric ${}^{(3)}g_{ij}$ is defined as follows [32]:

$${}^{(3)}g_{ij} = g_{ij} + n_i n_j, \quad (2.57)$$

where g_{ij} is the spatial component of $g_{\mu\nu}$. Since ${}^{(3)}g_{ij}$ is a tangent on hypersurface Σ_t , then ${}^{(3)}g_{ij}$ is perpendicular to the normal vector n_i , i.e. ${}^{(3)}g_{ij} n^i = 0$.

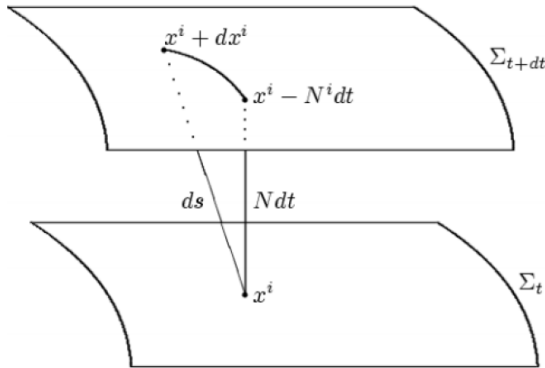


Figure 2.1: The proper length ds is calculated from the Pythagorean theorem in terms of ${}^{(3)}g_{ij}$, N and N^i . This figure is referenced from [32]

To define the proper length ds between two arbitrary points on hypersurfaces, we demonstrate the geometry in the figure 2.1. We consider the path that start from the point x^i on the hypersurface Σ_t and terminates at the point $x^i + dx^i$ on the hypersurface Σ_{t+dt} . It takes two steps to move from x^i on Σ_t to $x^i + dx^i$ on Σ_{t+dt} . The first step is to follow the proper time distance from Σ_t to Σ_{t+dt} along the normal vector n and it is equal to Ndt where N is called the lapse function. In the second step, the point is shifted on hypersurface Σ_{t+dt} from $x^i - N^i dt$ to $x^i + dx^i$ where N^i is the shift vector on the hypersurface.

We rewrite the metric components in terms of the spatial metric g_{ij} , the shift N_i and the lapse N ,

$$\begin{aligned} ds^2 &= -(\text{proper time})^2 + (\text{coordinate distance})^2 \\ &= -(Ndt)^2 + g_{ij}(dx^i + N^i dt)(dx^j + N^j dt), \end{aligned} \quad (2.58)$$

where g^{ij} is the inverse of the spatial metric g_{ij} . Using ADM formalism, the total degrees of freedom are still 10; 6 from the symmetric spatial three-metric g_{ij} , 3 from the shift vector N^i and 1 from the lapse function N . The four-dimensional metric components $g_{\mu\nu}$ can be written in terms of the ADM variables as follows:

$$\begin{aligned} g_{\mu\nu} &= \begin{pmatrix} g_{00} & g_{0j} \\ g_{i0} & g_{ij} \end{pmatrix} \\ &= \begin{pmatrix} -N^2 + {}^{(3)}g^{ij}N_iN_j & N_j \\ N_i & {}^{(3)}g_{ij} \end{pmatrix}. \end{aligned} \quad (2.59)$$

Now we consider the massless case or GR. The action becomes [33]

$$\begin{aligned} S_{\text{EH}} &= \frac{1}{16\pi G} \int d^4x \sqrt{-g} R \\ &= \frac{1}{16\pi G} \int d^4x \sqrt{{}^{(3)}g} N [R^{(3)} - K^2 + K^{ij} K_{ij}], \end{aligned} \quad (2.60)$$

where ${}^{(3)}g$ is the determinant of spatial metric g_{ij} , $R^{(3)}$ is the Ricci scalar in spatial metric g_{ij} and K_{ij} is the extrinsic curvature of the spatial hypersurfaces Σ_t which is a quantity that measures the rate of change of unit normal vector on hypersurface and is given by

$$K_{ij} = {}^{(3)}g_{ik} \nabla^k n_j, \quad (2.61)$$

where K_{ij} is symmetric and tangent to hypersurface Σ_t . $\nabla_k n_j$ collects the information of the curvature on the hypersurface where ${}^{(3)}g_i^k$ projects the information on the three-dimensional hypersurface. In addition, the extrinsic curvature can be written in terms of the ADM variables as shown below

$$K_{ij} = \frac{1}{2N} ({}^{(3)}\dot{g}_{ij} - {}^{(3)}\nabla_i N_j - {}^{(3)}\nabla_j N_i), \quad (2.62)$$

The Ricci scalar is also written in terms of ADM variables as

$$R = {}^{(3)}R + K_{ij} K^{ij} - K^2, \quad (2.63)$$

where ${}^{(3)}R$ is the Ricci scalar of the spatial metric ${}^{(3)}g_{ij}$.

Before investigating the ghost in massive gravity, we will study the ADM formalism in GR. Then we start from the Einstein-Hilbert action written in terms of ADM variables given by Eq. (2.60). The canonical momenta is given by

$${}^{(3)}p^{ij} = \frac{\delta L}{\delta {}^{(3)}\dot{g}_{ij}} = \sqrt{{}^{(3)}g} (K^{ij} - K^{(3)} g^{ij}). \quad (2.64)$$

The Einstein-Hilbert action can be written in terms of Hamiltonian H :

$$S_{\text{EH}} = \int dt L = \frac{1}{16\pi G} \int dt \left(\int_{\Sigma_t} d^3x [p^{ij} \dot{g}_{ij}] - H \right). \quad (2.65)$$

In this case, Hamiltonian H is given by [33]

$$H = \int_{\Sigma_t} d^3x (NC + N_i C^i), \quad (2.66)$$

where there are 12 phase space metric components; 6 from g_{ij} and another 6 from

p_{ij} ,

$$C = \sqrt{{}^{(3)}g} ({}^{(3)}R - K^2 + K^{ij} K_{ij}), \quad (2.67)$$

$$C^i = \sqrt{{}^{(3)}g} {}^{(3)}\nabla_j (K^{ij} - {}^{(3)}g^{ij} K), \quad (2.68)$$

$$N_j = g_{0j}, \quad (2.69)$$

$$N = (g_{00} - g^{ij} g_{0i} g_{0j})^{1/2}. \quad (2.70)$$

We apply the Hamiltonian H from Eq. (2.66) into Eq. (2.65) to obtain

$$S_{\text{EH}} = \frac{1}{16\pi G} \int d^4x [{}^{(3)}p^{ij} {}^{(3)}\dot{g}_{ij} - NC - N_i C^i]. \quad (2.71)$$

The shift N_i and the lapse N become the Lagrange multipliers for Eq. (2.66) and Eq. (2.71) then we have 4 constraints; $C = 0$ and $C^i = 0$. There are 4 more constraints from the gauge symmetry in GR from Eq. (2.7). The total phase space degrees of freedom is $12 - 4 - 4 = 4$ which are 2 polarizations of massless graviton and another 2 polarizations of massless graviton's conjugate momenta. It can be interpreted that there are only 2 real degrees of freedom for GR case.

We turn to massive gravity where the kinetic part is exactly the same as the GR case, so we consider the mass term from FP theory only. The mass term in

FP theory can be written in terms of ADM variables given by

$$\begin{aligned} \eta^{\mu\alpha}\eta^{\nu\beta} (h_{\mu\nu}h_{\alpha\beta} - h_{\mu\alpha}h_{\nu\beta}) &= \eta^{ik}\eta^{jl} (h_{ij}h_{kl} - h_{ik}h_{jl}) + 2\eta^{ij}h_{ij} \\ &\quad - 2N^2\eta^{ij}h_{ij} + 2N_i \left({}^{(3)}g^{ij} - \eta^{ij} \right) N_j. \end{aligned} \quad (2.72)$$

The total action of FP theory in Eq. (2.56) in terms of ADM variables is given by

$$\begin{aligned} S &= \frac{1}{16\pi G} \int d^4x \left[{}^{(3)}p^{ij}{}^{(3)}\dot{g}_{ij} - NC - N_i C^i \right. \\ &\quad \left. - \frac{m^2}{2} (h_{ij}h^{ij} - h^2 + 2(1 - N^2)h + 2h^{ij}N_i N_j) \right]. \end{aligned} \quad (2.73)$$

In this case, the lapse and the shift functions cannot be the Lagrange multipliers due to their quadratic terms (N^2 and $N_i N_j$) as shown in Eq. (2.73). Both functions are still auxiliary fields which are analytically solved by the variational principle as follows

$$N = \frac{C}{m^2\eta^{ij}h_{ij}}, \quad N_i = \frac{C_i}{m^2({}^{(3)}g^{ij} - \eta^{ij})}. \quad (2.74)$$

By substituting the shift and lapse functions into the FP action in Eq. (2.73), we obtain the action with no constraints or gauge symmetries at all,

$$S = \frac{1}{16\pi G} \int d^4x \left({}^{(3)}p^{ij}{}^{(3)}\dot{g}_{ij} - H \right), \quad (2.75)$$

where the Hamiltonian H takes the form

$$\begin{aligned} H &= \int d^3x \left(\frac{1}{2m^2} \frac{C^2}{\eta^{ij}h_{ij}} + \frac{1}{2m^2} \frac{C^i C^j}{{}^{(3)}g^{ij} - \eta^{ij}} \right. \\ &\quad \left. + \frac{1}{4} m^2 [\eta^{ij}\eta^{kl} (h_{ij}h_{kl} - h_{ik}h_{jl} + 2\eta^{ij}h_{ij})] \right), \end{aligned} \quad (2.76)$$

We totally have 12 phase space degrees of freedom or 6 real degrees of freedom in the FP massive gravity which is different from GR that has 2 real degrees

of freedom left since it has constraints and gauge symmetries. The linearized massive gravity has 5 real degrees of freedom while the nonlinear massive gravity with FP mass term in Eq. (2.56) has 6 real degrees of freedom. The extra degree of freedom from the nonlinear massive gravity is called the Boulware-Deser (BD) ghost [34, 35].

2.5.2 The appearance of BD ghost: Stueckelberg trick

By the ADM formalism, we now see the extra degree of freedom from the nonlinear massive gravity but it is not enough to quantify the ghost terms. To reveal the ghost terms in the nonlinear massive gravity action, we apply the Stueckelberg trick to formally restore the diffeomorphism invariance by including four Stueckelberg field ϕ^a and the reference metric transforms as follows: [36]

$$f_{\mu\nu} \rightarrow \hat{f}_{\mu\nu} = \partial_\mu \phi^a \partial_\nu \phi^b f_{ab}, \quad (2.77)$$

where $\hat{f}_{\mu\nu}$ transforms as a tensor under coordinate transformations with the four Stueckelberg fields ϕ^a transforming as scalars. In the unitary gauge, where the Stueckelberg fields are $\phi^a = x^a$, we recover $\hat{f}_{\mu\nu} = f_{\mu\nu}$. It is convenient to define the following tensor quantity,

$$\mathbb{X}_\nu^\mu \equiv g^{\mu\rho} f_{\rho\nu} = \delta_\nu^\mu - h_\nu^\mu, \quad (2.78)$$

where its transformation is given by

$$\begin{aligned} \mathbb{X}_\nu^\mu &\rightarrow \hat{\mathbb{X}}_\nu^\mu = g^{\mu\rho} \hat{f}_{\rho\nu} \\ &= g^{\mu\rho} \partial_\rho \phi^a \partial_\nu \phi^b f_{ab} \\ &= \partial^\mu \phi^a \partial_\nu \phi^b f_{ab} \equiv \delta_\nu^\mu - H_\nu^\mu. \end{aligned} \quad (2.79)$$

For simplicity, we can choose $f_{ab} = \eta_{ab}$ and split the Stueckelberg fields as $\phi^a = x^a - \chi^a$ where χ^a can be decomposed into traversable vector field A^a and the longitudinal mode π as $\chi^a = \frac{1}{m}A^a + \frac{1}{m^2}\eta^{ab}\partial_b\pi$. The flat reference metric $f_{\mu\nu} = \eta_{\mu\nu}$ transforms as

$$\begin{aligned}
f_{\mu\nu} = \eta_{\mu\nu} \rightarrow \hat{f}_{\mu\nu} &= \partial_\mu\phi^a\partial_\nu\phi^b f_{ab} \\
&= \eta_{\mu\nu} - (\partial_\mu\chi_\nu + \partial_\nu\chi_\mu) + \partial_\mu\chi^a\partial_\nu\chi^b\eta_{ab} \\
&= \eta_{\mu\nu} - \frac{1}{m}(\partial_\mu A_\nu + \partial_\nu A_\mu) - \frac{2}{m^2}\Pi_{\mu\nu} \\
&\quad + \frac{1}{m^2}\partial_\mu A^\alpha\partial_\nu A_\alpha + \frac{2}{m^3}\partial_\mu A^\alpha\Pi_{\nu\alpha} + \frac{1}{m^4}\Pi_\mu^\alpha\Pi_{\alpha\nu},
\end{aligned} \tag{2.80}$$

where $\Pi_{\mu\nu} \equiv \partial_\mu\partial_\nu\pi$.

The fluctuations $h_{\mu\nu}$ about the flat spacetime are promoted to the tensor $H_{\mu\nu}$:

$$\begin{aligned}
h_{\mu\nu} = g_{\mu\nu} - f_{\mu\nu} \rightarrow H_{\mu\nu} &= g_{\mu\nu} - \hat{f}_{\mu\nu} \\
&= h_{\mu\nu} + \partial_\mu\chi_\nu + \partial_\nu\chi_\mu - \partial_\mu\chi^a\partial_\nu\chi^b\eta_{ab} \\
&= h_{\mu\nu} + \frac{1}{m}(\partial_\mu A_\nu + \partial_\nu A_\mu) + \frac{2}{m^2}\Pi_{\mu\nu} \\
&\quad - \frac{1}{m^2}\partial_\mu A^\alpha\partial_\nu A_\alpha - \frac{2}{m^3}\partial_\mu A^\alpha\Pi_{\nu\alpha} - \frac{1}{m^4}\Pi_\mu^\alpha\Pi_{\alpha\nu}.
\end{aligned} \tag{2.81}$$

Then the tensor $\hat{\mathbb{X}}_\nu^\mu$ becomes

$$\begin{aligned}
\hat{\mathbb{X}}_\nu^\mu = \delta_\nu^\mu - H_\nu^\mu &= \delta_\nu^\mu - h_\nu^\mu - \partial^\mu\chi_\nu - \partial_\nu\chi^\mu + \partial^\mu\chi^a\partial_\nu\chi^b\eta_{ab} \\
&= \mathbb{X}_\nu^\mu - \frac{1}{m}(\partial^\mu A_\nu + \partial_\nu A^\mu) - \frac{2}{m^2}\Pi_\nu^\mu \\
&\quad + \frac{1}{m^2}\partial^\mu A^\alpha\partial_\nu A_\alpha + \frac{2}{m^3}\partial^\mu A^\alpha\Pi_{\nu\alpha} + \frac{1}{m^4}\Pi^{\mu\alpha}\Pi_{\alpha\nu}.
\end{aligned} \tag{2.82}$$

Since we have shown in the previous subsection that the extra scalar mode takes responsibility on the BD ghost. We will focus only on the helicity-0 mode, π ,

and omit the part of tensor and vector modes in the mass term of the FP theory.

The mass term, which is borrowed from the FP theory in Eq. (2.56), transforms as follow [16]

$$\begin{aligned}
L_{\text{mass}} &\rightarrow -\frac{1}{2}m^2 (H_{\mu\nu}H^{\mu\nu} - H^2) \\
&= -\frac{1}{2}m^2 \left([(\mathbb{I} - \hat{\mathbb{X}})^2] - [\mathbb{I} - \hat{\mathbb{X}}]^2 \right) \\
&= -\frac{2}{m^2} ([\Pi^2] - [\mathbb{I}]^2) + \frac{2}{m^4} ([\Pi^3] - [\mathbb{I}] [\Pi^2]) \\
&\quad + \frac{1}{2m^6} ([\Pi^4] - [\Pi^2]^2) + \dots, \tag{2.83}
\end{aligned}$$

where the bracket is the trace of the tensor. With the integration by parts, the quadratic terms of the scalar mode in Eq. (2.83) is the total derivative as follow

$$\begin{aligned}
[\Pi^2] - [\mathbb{I}]^2 &= \{ \partial_\rho (\partial^\mu \pi \partial^\rho \partial_\mu \pi) - \partial^\mu (\pi \partial_\rho \partial^\rho \partial_\mu \pi) + \pi \partial_\rho \partial^\rho \partial_\mu \partial^\mu \pi \} \\
&\quad - \{ \partial_\rho (\partial^\rho \pi \partial^\mu \partial_\mu \pi) - \partial^\rho (\pi \partial_\rho \partial^\mu \partial_\mu \pi) + \pi \partial_\rho \partial^\rho \partial_\mu \partial^\mu \pi \} \\
&= \partial_\rho (\partial^\mu \pi \partial^\rho \partial_\mu \pi) - \partial_\rho (\partial^\rho \pi \partial^\mu \partial_\mu \pi). \tag{2.84}
\end{aligned}$$

However, the cubic and quartic interactions in Eq. (2.83) cannot be solely written in terms of total derivative. At this point, we see that these higher order derivatives terms, i.e. $([\Pi^3] - [\mathbb{I}] [\Pi^2])$ and $([\Pi^4] - [\Pi^2]^2)$ lead to the extra degree of freedom from the BD ghost [36]. As shown in the appendix B, the higher order derivatives of the scalar field are the major problem in nonlinear massive gravity because there is a negative the kinetic term of the scalar field leading to unbounded Hamiltonian [34, 35]. When the wrong sign kinetic term of scalar field couples with ordinary matter, it cause the instability to the system. This is the reason why the nonlinear massive gravity with FP mass terms is ruled out by the appearance of BD ghost.

2.5.3 Elimination of the extra scalar mode by the Galileon theory

As mentioned using the Stueckelberg trick, the scalar field in nonlinear massive gravity plays a major role for the appearance of the ghost. Even though the scalar field of FP theory causes the extra degree of freedom from the BD ghost, we find that the ghost term does not come from the quadratic terms since they all can be written in terms of total derivatives. Upon this fact, we are able to choose the contractions of $\Pi_{\mu\nu}$ in higher order that reduces to total derivatives. In this subsection, we will consider solely the form of scalar field that eliminates the BD ghost before combining the vector and tensor mode for the full nonlinear massive gravity.

In Refs. [35, 37, 38], there is the unique combination of $\Pi_{\mu\nu}$ from the Galileon theory leading to the total derivative as follows:

$$L_2^{\text{TD}} = [\Pi]^2 - [\Pi^2], \quad (2.85)$$

$$L_3^{\text{TD}} = [\Pi]^3 - 3[\Pi][\Pi^2] + 2[\Pi^3], \quad (2.86)$$

$$L_4^{\text{TD}} = [\Pi]^4 - 6[\Pi^2][\Pi]^2 + 8[\Pi^3][\Pi] + 3[\Pi^2]^2 - 6[\Pi^4], \quad (2.87)$$

⋮

where L_2^{TD} is the same as FP term. One could apply the integration by parts on L_n^{TD} to obtain the total derivatives for all n . The term L_n^{TD} vanishes identically when $n > 4$ since we consider the 4D spacetime. To avoid the BD ghost, the scalar mode in the mass terms must be written in the combination of Eq. (2.85),

Eq. (2.86) and Eq. (2.87) as follow:

$$L^{\text{TD}} = ([\Pi]^2 - [\Pi^2]) + \alpha_3 ([\Pi]^3 - 3 [\Pi] [\Pi]^2 + 2 [\Pi^3]) \\ + \alpha_4 ([\Pi]^4 - 6 [\Pi^2] [\Pi]^2 + 8 [\Pi^3] [\Pi] + 3 [\Pi^2]^2 - 6 [\Pi^4]), \quad (2.88)$$

where α_3 and α_4 are constants.

With this Lagrangian of the scalar field in Eq. (2.88), the quadratic, cubic, and quartic interactions can be written in terms of total derivatives, so there is no higher derivatives. For this case, the scalar field is not dynamical (the total degree of freedom is zero), so ghost is eliminated from the system.

2.5.4 The ghost-free nonlinear massive gravity

In the nonlinear massive gravity, there are three modes; tensor $h_{\mu\nu}$, vector A_μ and scalar ϕ modes. One can make use of the ghost-free Lagrangian of scalar mode in Eq. (2.88) to have all three modes and there is still no the BD ghost. To do so, we first recall the tensor $\hat{\mathbb{X}}_\nu^\mu$ and split into two main terms as follow

$$\hat{\mathbb{X}}_\nu^\mu = \hat{\mathbb{Y}}_\nu^\mu + \hat{\mathbb{Z}}_\nu^\mu, \quad (2.89)$$

where $\hat{\mathbb{Y}}_\nu^\mu$ consists of the pure scalar terms and $\hat{\mathbb{Z}}_\nu^\mu$ is the combination of tensor, vector and interaction between vector and scalar as follows

$$\hat{\mathbb{Y}}_\nu^\mu \equiv \delta_\nu^\mu - \frac{2}{m^2} \Pi_\nu^\mu + \frac{1}{m^4} \Pi^{\mu\alpha} \Pi_{\alpha\nu} \quad (2.90)$$

$$\hat{\mathbb{Z}}_\nu^\mu \equiv -h_\nu^\mu - \frac{1}{m} (\partial^\mu A_\nu + \partial_\nu A^\mu) + \frac{1}{m^2} \partial^\mu A^\alpha \partial_\nu A_\alpha + \frac{2}{m^3} \partial^\mu A^\alpha \Pi_{\nu\alpha}. \quad (2.91)$$

Then we factorize the scalar terms to obtain

$$\begin{aligned}\hat{\mathbb{Y}}_\nu^\mu &= \delta_\nu^\mu - \frac{2}{m^2}\Pi_\nu^\mu + \frac{1}{m^4}\Pi^{\mu\alpha}\Pi_{\alpha\nu} \\ &= \left(\delta_\rho^\mu - \frac{1}{m^2}\partial^\mu\partial_\rho\pi\right)\left(\delta_\nu^\rho - \frac{1}{m^2}\partial^\rho\partial_\nu\pi\right) = \hat{\mathbb{M}}_\rho^\mu\hat{\mathbb{M}}_\nu^\rho.\end{aligned}\quad (2.92)$$

The relation between the tensor $\hat{\mathbb{M}}_\nu^\mu$ and Π_ν^μ is given by

$$\Pi_\nu^\mu = \partial^\mu\partial_\nu\pi = m^2\left(\delta_\nu^\mu - \hat{\mathbb{M}}_\rho^\mu\right) = m^2\left(\delta_\nu^\mu - \sqrt{\hat{\mathbb{Y}}_\nu^\mu}\right).\quad (2.93)$$

To generalize the ghost-free Lagrangian in Eq. (2.88), we replace Π_ν^μ with a new tensor defined as follow

$$\hat{\mathbb{K}}_\nu^\mu \equiv m^2\left(\delta_\nu^\mu - \sqrt{\hat{\mathbb{X}}_\nu^\mu}\right) = m^2\left(\delta_\nu^\mu - \sqrt{g^{-1}\hat{f}_\nu^\mu}\right).\quad (2.94)$$

The ghost-free nonlinear massive gravity Lagrangian is given by

$$\begin{aligned}L_{\text{NLMG}}^{\text{TD}} &= \left(\left[\hat{\mathbb{K}}\right]^2 - \left[\hat{\mathbb{K}}^2\right]\right) + \alpha_3\left(\left[\hat{\mathbb{K}}\right]^3 - 3\left[\hat{\mathbb{K}}\right]\left[\hat{\mathbb{K}}\right]^2 + 2\left[\hat{\mathbb{K}}^3\right]\right) \\ &+ \alpha_4\left(\left[\hat{\mathbb{K}}\right]^4 - 6\left[\hat{\mathbb{K}}^2\right]\left[\hat{\mathbb{K}}\right]^2 + 8\left[\hat{\mathbb{K}}^3\right]\left[\hat{\mathbb{K}}\right] + 3\left[\hat{\mathbb{K}}^2\right]^2 - 6\left[\hat{\mathbb{K}}^4\right]\right).\end{aligned}\quad (2.95)$$

Presence of the ghost in the model is a major problem for the massive gravity until de Rham, Gabadadze and Tolley (dRGT) handled this problem and introduced the Lagrangian in Eq. (2.96) as the ghost-free nonlinear massive gravity theory [17, 39]. Here the authors generalized the model at the complete level. The further reading for the ghost-free nonlinear massive gravity and its applications are in Refs. [40, 41, 42]. We set $M_P^2 = 1/8\pi G$ for the rest of this section.

The action of the dRGT model is given by

$$S_{\text{dRGT}} = \frac{M_P^2}{2} \int d^4x \sqrt{-g} (R + m_g^2 \mathcal{U}(g, \phi^a)),\quad (2.96)$$

where m_g is the graviton mass and the potential \mathcal{U} is defined by

$$\mathcal{U} = \mathcal{U}_2 + \alpha_3 \mathcal{U}_3 + \alpha_4 \mathcal{U}_4, \quad (2.97)$$

where \mathcal{U}_2 , \mathcal{U}_3 and \mathcal{U}_4 are given by

$$\begin{aligned} \mathcal{U}_2 &= [\mathcal{K}]^2 - [\mathcal{K}^2], \\ \mathcal{U}_3 &= [\mathcal{K}]^3 - 3[\mathcal{K}][\mathcal{K}^2] + 2[\mathcal{K}^3], \\ \mathcal{U}_4 &= [\mathcal{K}]^4 - 6[\mathcal{K}]^2[\mathcal{K}^2] + 8[\mathcal{K}][\mathcal{K}^3] + 3[\mathcal{K}^2]^2 - 6[\mathcal{K}^4], \end{aligned} \quad (2.98)$$

where $\mathcal{K} = \hat{\mathbb{K}}/m_g^2$, $\mathcal{K}_\nu^\mu = \delta_\nu^\mu - \sqrt{g^{\mu\sigma}} f_{ab} \partial_\sigma \phi^a \partial_\nu \phi^b$. Here a bracket [] represents the trace of the tensor, $[\mathcal{K}] \equiv \mathcal{K}_\mu^\mu$, $[\mathcal{K}^2] \equiv \mathcal{K}_{\alpha_1}^\mu \mathcal{K}_\mu^{\alpha_1}$, $[\mathcal{K}^3] \equiv \mathcal{K}_{\alpha_1}^\mu \mathcal{K}_{\beta_1}^{\alpha_1} \mathcal{K}_\mu^{\beta_1}$ and $[\mathcal{K}^4] \equiv \mathcal{K}_{\alpha_1}^\mu \mathcal{K}_{\beta_1}^{\alpha_1} \mathcal{K}_{\alpha_2}^{\beta_1} \mathcal{K}_\mu^{\alpha_2}$. Note here that parameters α_3 and α_4 of the dRGT theory are related to the graviton mass. Performing variation of the gravitational action in Eq.(2.96) with respect to the metric, $g_{\mu\nu}$, yields the equation of motion of the dRGT massive gravity given by

$$G_{\mu\nu} + m_g^2 X_{\mu\nu} = 0, \quad (2.99)$$

where $X_{\mu\nu}$ is defined by

$$\begin{aligned} X_{\mu\nu} &= \frac{1}{\sqrt{-g}} \frac{\delta \sqrt{-g} \mathcal{U}}{\delta g^{\mu\nu}} \\ &= \mathcal{K}_{\mu\nu} - \alpha \left[(\mathcal{K}^2)_{\mu\nu} - [\mathcal{K}] \mathcal{K}_{\mu\nu} + \frac{1}{2} g_{\mu\nu} ([\mathcal{K}]^2 - [\mathcal{K}^2]) \right] \\ &\quad + 3\beta \left[(\mathcal{K}^3)_{\mu\nu} - [\mathcal{K}] (\mathcal{K}^2)_{\mu\nu} + \frac{1}{2} \mathcal{K}_{\mu\nu} ([\mathcal{K}]^2 - [\mathcal{K}^2]) \right. \\ &\quad \left. - \frac{1}{6} g_{\mu\nu} ([\mathcal{K}]^3 - 3[\mathcal{K}][\mathcal{K}^2] + 2[\mathcal{K}^3]) \right], \end{aligned} \quad (2.100)$$

where the parameters α and β are related to $\alpha_{3,4}$ from the action in Eq.(2.96) via

$$\alpha = 1 + 3\alpha_3, \quad \beta = \alpha_3 + 4\alpha_4. \quad (2.101)$$

They are simply defined as the unitary gauge $\phi^a = x^\mu \delta_\mu^a$. The homogeneity and isotropy on the spatial sphere is needed to preserve. Then the choice for f_{ab} is the SU(2)-invariant as follows [25, 43, 44, 45, 46]:

$$f_{ab} = \text{diag}(0, 0, k^2, k^2 \sin^2 \theta), \quad (2.102)$$

where k is a constant. Assume the ansatz as the static and spherically symmetric as follows:

$$ds^2 = g_{\mu\nu} dx^\mu dx^\nu = -n(r)dt^2 + \frac{dr^2}{f(r)} + r^2 d\Omega^2, \quad (2.103)$$

where $n(r)$ and $f(r)$ are arbitrary functions of r , $d\Omega^2 = d\theta^2 + \sin^2\theta d\phi^2$ and the metric in Eq. (2.103) is the vacuum solution of massive gravity theory without any other kind of matter. With the metric tensor in Eq. (2.103), the components of Einstein tensor $G_{\mu\nu}$ in Eq. (2.99) become

$$G_t^t = \frac{f'}{r} + \frac{f}{r^2} - \frac{1}{r^2}, \quad (2.104)$$

$$G_r^r = \frac{f(rn' + n)}{nr^2} - \frac{1}{r^2}, \quad (2.105)$$

$$G_\theta^\theta = G_\phi^\phi = f' \left(\frac{n'}{4n} + \frac{1}{2r} \right) + f \left(\frac{n''}{2n} + \frac{n'}{2nr} - \frac{(n')^2}{4n^2} \right). \quad (2.106)$$

The components of tensor X_ν^μ are

$$m^2 X_t^t = -m_g^2 \left(\frac{3r - 2k}{r} + \frac{\alpha(3r - k)(r - k)}{r^2} + \frac{3\beta(r - k)^2}{r^2} \right), \quad (2.107)$$

$$m^2 X_r^r = -m_g^2 \left(\frac{3r - 2k}{r} + \frac{\alpha(3r - k)(r - k)}{r^2} + \frac{3\beta(r - k)^2}{r^2} \right), \quad (2.108)$$

$$m^2 X_{\theta,\phi}^{\theta,\phi} = -m_g^2 \left(\frac{3r - k}{r} + \frac{\alpha(3r - 2k)}{r} + \frac{3\beta(r - k)}{r} \right). \quad (2.109)$$

To find the solution of function $f(r)$, we use (tt) and (rr) components of Eq. (2.99)

with Eq. (2.104), Eq. (2.105), Eq. (2.107) and Eq. (2.108) [25]

$$\frac{f'}{r} + \frac{f}{r^2} - \frac{1}{r^2} = m_g^2 \left(\frac{3r - 2k}{r} + \frac{\alpha(3r - k)(r - k)}{r^2} + \frac{3\beta(r - k)^2}{r^2} \right), \quad (2.110)$$

and

$$\frac{f(rn' + n)}{nr^2} - \frac{1}{r^2} = m_g^2 \left(\frac{3r - 2k}{r} + \frac{\alpha(3r - k)(r - k)}{r^2} + \frac{3\beta(r - k)^2}{r^2} \right). \quad (2.111)$$

The right hand sides of Eq. (2.110) and Eq. (2.111) are exactly the same. We match the terms only on their left hand sides

$$\frac{f'(r)n(r)}{r} = \frac{f(r)n'(r)}{r}. \quad (2.112)$$

This implies that $f(r) = n(r)$. According to Ref. [25], the ansatz of $f(r)$ becomes

$$f(r) = 1 - \frac{2GM}{r} - \frac{\Lambda r^2}{3} + \gamma r + \zeta, \quad (2.113)$$

where M is the mass parameter, Λ is the effective cosmological constant, and γ and ζ are new parameters. By substituting the ansatz of function $f(r)$ into Eq. (2.110), we obtain the parameters in the dRGT massive gravity via the following relations,

$$\Lambda \equiv -3m_g^2(1 + \alpha + \beta), \quad \gamma \equiv -m_g^2 k(1 + 2\alpha + 3\beta), \quad \zeta \equiv m_g^2 k^2(\alpha + 3\beta). \quad (2.114)$$

The parameter k , α , and β are rewritten in terms of Λ , γ , and ζ by

$$\begin{aligned} k &= \frac{\gamma + \sqrt{\gamma^2 + (m_g^2 + \Lambda)\zeta}}{m_g^2 + \Lambda}, \\ \alpha &= -\frac{\gamma^2 + (2m_g^2 + \Lambda)\zeta - \gamma\sqrt{\gamma^2 + (m_g^2 + \Lambda)\zeta}}{m_g^2\zeta}, \\ \beta &= \frac{2\Lambda}{3m_g^2} + \frac{\gamma^2 + m_g^2\zeta - \gamma\sqrt{\gamma^2 + (m_g^2 + \Lambda)\zeta}}{m_g^2\zeta}. \end{aligned} \quad (2.115)$$

For convenience in the test of this thesis, we set $\zeta = 0$ and obtain

$$k = \frac{2\gamma}{m_g^2 + \Lambda}, \quad \alpha = -3\beta = -\frac{3}{2} - \frac{\Lambda}{2m_g^2}. \quad (2.116)$$

The energy density and pressure can be defined by the components of tensor $X_{\mu\nu}$ from Eq. (2.107), Eq. (2.108) and Eq. (2.109) as follows:

$$\rho_g(r) \equiv \frac{m_g^2}{8\pi G} X_t^t = -M_P^2 \left(\frac{2\gamma - \Lambda r}{r} \right) \quad (2.117)$$

$$p_g^{(r)}(r) \equiv -\frac{m_g^2}{8\pi G} X_r^r = M_P^2 \left(\frac{2\gamma - \Lambda r}{r} \right) \quad (2.118)$$

$$p_g^{(\theta,\phi)}(r) \equiv -\frac{m_g^2}{8\pi G} X_{\theta,\phi}^{\theta,\phi} = M_P^2 \left(\frac{\gamma - \Lambda r}{r} \right) \quad (2.119)$$

For the black hole solution in dRGT model, the cosmological constant Λ is written in terms of graviton mass m_g . Thus, the massive graviton is responsible for the accelerated expansion of the Universe. According to the first detection of gravitational waves in 2017 [47], a lower bound on the graviton Compton wave length λ_g is 1.6×10^{13} km which is equivalent to the upper bound on the graviton mass 7.7×10^{-23} eV/c². In 2019, a new constraint for graviton mass with the planetary ephemeris INPOP is $\lambda_g > 1.83 \times 10^{13}$ km or $m_g < 6.76 \times 10^{-23}$ eV/c² [48].

CHAPTER III

Wormholes in General Relativity

In this thesis, we theoretically construct wormholes by using two standard methods for theoretical wormhole construction; the traversable wormhole and the thin-shell wormhole. The detail of construction, the stability condition and the parameters for the energy conditions will be discussed in this chapter.

3.1 The Lorentzian traversable wormhole

This type of wormhole is a two-way bridge that connects two points in spacetime of the Universe or two points from different Universes. To begin the study, we would like to introduce the properties of the Lorentzian traversable wormhole in the fundamental setup. Then, we provide detailed construction of the traversable wormholes.

3.1.1 Fundamental setup of traversable wormholes

To construct traversable wormholes, we consider the spherical coordinate which is suitable to describe the line element of wormholes. It was proposed by Morris

and Thorne in 1988 given by

$$ds^2 = -e^{2\Phi(r)} dt^2 + \left(1 - \frac{b(r)}{r}\right)^{-1} dr^2 + r^2(d\theta^2 + \sin^2\theta d\phi^2), \quad (3.1)$$

where r, θ , and ϕ are the spherical coordinates, $\Phi(r)$ and $b(r)$ are arbitrary functions of r , $\Phi(r)$ is called the redshift function since it is related to the gravitational redshift, and $b(r)$ is called the shape function because the function determines the shape of traversable wormholes via embedding diagram. To construct traversable wormholes, the coordinate singularity or horizon must be eliminated. Thus $e^{2\Phi(r)} \neq 0$, then $\Phi(r)$ must be finite everywhere. Even though $(1 - b(r)/r)^{-1}$ diverges at the throat of the wormhole $b(r_0) = r_0$, it is just the coordinate singularity where can be eliminated by considering the proper radial distance

$$l(r) = \pm \int_{r_0}^r \left(1 - \frac{b(r)}{r}\right)^{-1/2} dr. \quad (3.2)$$

The proper radial distance is required to be finite everywhere. The metric tensor in Eq. (3.1) can be rewritten as [7]

$$ds^2 = -e^{2\Phi(l)} dt^2 + dl^2 + r^2(l)(d\theta^2 + \sin^2\theta d\phi^2), \quad (3.3)$$

where $l = 0$ is at the throat of the wormhole, and $l > 0$ ($l < 0$) is on the upper (lower) side of the throat.

3.1.2 Embedding diagram for traversable wormholes

To visualize the wormhole spacetime, we consider the slice of the line element given in Eq. (3.1) at $t = \text{constant}$ and $\theta = \pi/2$. The two-dimensional surface is

embedded into three-dimensional Euclidean space (cylindrical coordinate) [49, 50]

$$ds^2 = \left(1 - \frac{b(r)}{r}\right)^{-1} dr^2 + r^2 d\phi^2 = dr^2 + r^2 d\phi^2 + dz^2. \quad (3.4)$$

We obtain the relation

$$\frac{dz}{dr} = \pm \left(\frac{r}{b(r)} - 1\right)^{-1/2}, \quad (3.5)$$

where dz/dr diverges at the throat $b(a) = a$. To avoid the imaginary value of z , we apply the first properties of a traversable wormhole shape function:

$$b(r) < r \text{ for } r > a, \quad (3.6)$$

and

$$b(a) = a. \quad (3.7)$$

Notice that the traditional background metric tensor of traversable wormhole satisfies the asymptotic flatness condition. In general, the background metric tensor might be de-Sitter or anti de-Sitter spacetimes which satisfy the asymptotic de-Sitter condition or the asymptotic anti de-Sitter condition, respectively.

3.1.3 The flaring-out condition for traversable wormhole

The throat of wormhole must be the narrowest part. Generally, we can apply the criteria by considering the second derivative $\left(\frac{d^2r}{dz^2}\right)$ around the wormhole throat as

$$\frac{d^2r}{dz^2} = \frac{b(r) - rb'(r)}{2b^2(r)} > 0 \text{ for } r > a. \quad (3.8)$$

At the throat, the relation of Eq. (3.8) reduces to

$$b'(a) < 1. \quad (3.9)$$

These relations are called the flaring-out condition and hold near and at the wormhole throat.

3.1.4 No-horizon conditions

To make the wormhole possible for transportation, we must set no-horizon condition in spacetime. According to the line element of wormhole, the characteristic of the shape function $b(r)$ is determined by the embedding diagram and the flaring-out condition. In this thesis, we use the static and spherically symmetric metric. Thus, a horizon might appear on the term g_{tt} and g_{rr} . On g_{tt} , it is easy to handle since as long as the red shift function $\Phi(r)$ is finite from throat a to infinity, there is no horizon. To avoid the horizon on g_{rr} , we are able to choose the shape function $b(r)$ that has no root between the throat and infinity.

3.1.5 The construction of the Lorentzian traversable wormhole

The line element follows the Morris Throne wormhole in Eq. (3.1). Generally, the shape function $b(r)$ and the redshift function $\Phi(r)$ are arbitrary as long as they follow the properties in section (3.1). The action of the Lorentzian traversable wormhole in four-dimensional spacetime consists of the geometry of the Universe

$R/16\pi G$ and the matter $\mathcal{L}_{\text{matter}}$ is given by

$$S_{\text{total}} = \int d^4x \sqrt{-g} \left(\frac{R}{16\pi G} + \mathcal{L}_{\text{matter}} \right). \quad (3.10)$$

Performing the variation of the action with respect to $g^{\mu\nu}$, it is not surprising that the equation of motion for the Lorentzian traversable wormhole is governed by the Einstein equation

$$R_{\mu\nu} - \frac{1}{2}g_{\mu\nu}R = 8\pi GT_{\mu\nu}, \quad (3.11)$$

where the energy-momentum tensor of matter source of the wormhole is $T_{\mu\nu} = -\frac{2}{\sqrt{-g}} \frac{\partial(\sqrt{-g}\mathcal{L}_{\text{matter}})}{\partial g^{\mu\nu}}$ which is written in term of anisotropic perfect fluid as

$$T_{\mu\nu} = (\rho + P_t)u_\mu u_\nu + P_t g_{\mu\nu} + (P_r - P_t)\chi_\mu \chi_\nu, \quad (3.12)$$

where u_μ is a four-velocity, χ_μ is the spacelike unit vector orthogonal to the u_μ with the normalization condition $u_\mu u^\mu = -1$, $\chi_\mu \chi^\mu = 1$, ρ is the energy density, P_r and P_t are the radial and tangential pressure, respectively.

The energy conditions for the anisotropic fluid are given by [51]

- Null energy condition

$$\rho + P_r \geq 0, \text{ and } \rho + P_t \geq 0. \quad (3.13)$$

- Weak energy condition

$$\rho + P_r \geq 0, \rho + P_t \geq 0, \text{ and } \rho \geq 0. \quad (3.14)$$

- Strong energy condition

$$\rho + P_r \geq 0, \rho + P_t \geq 0, \text{ and } \rho + P_r + 2P_t \geq 0. \quad (3.15)$$

Substituting the Morris and Thorne line element in Eq. (3.1) into Eq. (3.10), we obtain the equations of state of the source matter for Lorentzian traversable wormhole

$$\rho = \frac{b'(r)}{16\pi Gr^2} \quad (3.16)$$

$$P_r = -\frac{b(r)}{16\pi Gr^3} + \frac{1}{8\pi G} \left(1 - \frac{b(r)}{r}\right) \frac{\Phi'(r)}{r} \quad (3.17)$$

$$P_t = \frac{1}{2r^3} (b(r) - rb'(r)) + \left(\frac{1}{2r} \left(1 - \frac{b(r)}{r}\right) + \frac{1}{2r} (1 - b'(r)) \right) \Phi'(r) \\ + \left(1 - \frac{b(r)}{r}\right) \Phi'^2(r) + \left(1 - \frac{b(r)}{r}\right) \Phi''(r). \quad (3.18)$$

In this thesis, these three variables will be applied into all three energy conditions (NEC, WEC, and SEC) for quantifying the violation the Lorentzian traversable wormhole.

3.2 Thin-shell wormhole

The concept of thin-shell wormhole was first proposed by M. Visser [52]. This class of wormhole can be obtained by a cut-and-paste procedure and structures are called thin-shell wormholes where they distort the two different spacetimes and connect them at wormhole throat which is called the thin shell. This method is called the Darmonis-Israel formalism or the thin-shell formalism [49, 53]. M. Visser proposed the analysis of the thin-shell wormhole's stability and found the stable configurations from the equation-of-state of an exotic matter residing on the throat. Unlike the traversable wormhole technique, the thin-shell spacetimes have no differentiability for its metric at the throat. Then the spacetime at the

throat or thin shell is not smooth.

In this section, we will review a thin-shell wormhole method through the procedure of the thin-shell wormhole construction and the method to measure its stability.

3.2.1 The fundamental setup for thin-shell wormhole

In order to study the thin-shell wormhole and its stability, we have to use the appropriate mathematical tools to construct the two manifolds and the surface. We follow the standard approach in Refs. [49, 54, 55]. The two different spacetimes (upper and lower spacetimes) are described by two manifolds (\mathcal{M}_+ and \mathcal{M}_- , respectively) where \mathcal{M}_+ (\mathcal{M}_-) is described by the metric $g_{\mu\nu}^+$ ($g_{\mu\nu}^-$) with the coordinate x_+^μ (x_-^μ). The plus and minus signs denote the upper and lower spacetimes, respectively. A total manifold $\mathcal{M} = \mathcal{M}_+ \cup \mathcal{M}_-$ results from gluing \mathcal{M}_+ and \mathcal{M}_- at their boundaries $\partial\mathcal{M}_+$ and $\partial\mathcal{M}_-$ respectively. The boundary $\partial\mathcal{M}_+$ ($\partial\mathcal{M}_-$) is described by the induced metric h_{ab}^+ (h_{ab}^-) with the coordinate y_a^+ (y_a^-). The hypersurface Σ separates \mathcal{M} into \mathcal{M}_+ and \mathcal{M}_- such that $\Sigma = \mathcal{M}_+ \cap \mathcal{M}_-$ and is described by the metric $g_{\mu\nu} = g_{\mu\nu}^\pm(r = a)$ where a is the throat of the thin-shell wormhole. Both manifold surfaces ($\partial\mathcal{M}_+$ and $\partial\mathcal{M}_-$) are linked by the (co-moving) thin-shell or hypersurface Σ .

We impose the static and spherically symmetric spacetimes. Then, the line elements of both manifolds read

$$ds_\pm^2 = g_{\mu\nu}^\pm dx^\mu dx^\nu = -f_\pm(r)dt^2 + \frac{dr^2}{f_\pm(r)} + r^2 d\theta^2 + r^2 \sin^2 \theta d\phi^2, \quad (3.19)$$

where r is the radial coordinate in both manifolds covering the range between the throat of thin-shell wormhole to infinity ($r \in (a, \infty)$), $f_{\pm}(r)$ is the vacuum solution on manifolds (\mathcal{M}_{\pm}), for instance, $f_{\pm}(r) = 1$ for flat spacetime, and $f_{\pm}(r) = 1 - 2M/r$ for the Schwarzschild case.

The line element on the thin-shell is given by

$$\begin{aligned} ds_{\Sigma}^2 &= g_{\alpha\beta} dx^{\alpha} dx^{\beta} |_{r=a} = g_{\alpha\beta} \left(\frac{\partial x^{\alpha}}{\partial y^a} dy^a \right) \left(\frac{\partial x^{\beta}}{\partial y^b} dy^b \right) = h_{ab} dy^a dy^b \\ &= -d\tau^2 + a^2(\tau) d\Omega^2, \quad d\Omega^2 = d\theta^2 + \sin^2 \theta d\phi^2, \end{aligned} \quad (3.20)$$

where τ is the proper time on the hypersurface Σ . $y^a = y^a(x^{\mu})$ is a coordinate on the hypersurface Σ , $h_{ab} \equiv g_{\alpha\beta} e_a^{\alpha} e_b^{\beta}$, $e_a^{\alpha} \equiv \partial x^{\alpha} / \partial y^a$ is a tangent vector on curves on a hypersurface, and τ is a local time on the thin-shell.

We consider the dynamics at the throat by comparing the line elements on the thin-shell from Eq. (3.20) and on the manifolds from Eq. (3.19) with limit $r \rightarrow a$,

$$\begin{aligned} -f_{\pm}(a) dt^2 + \frac{dr^2}{f_{\pm}(r)} + a^2 d\Omega^2 &= -d\tau^2 + a^2 d\Omega^2 \\ -f_{\pm}(a) \dot{t}^2 + \frac{\dot{a}^2}{f_{\pm}(a)} &= -1 \\ \dot{t} &\equiv \frac{dt}{d\tau} = \frac{(f_{\pm}(a) + \dot{a}^2)^{1/2}}{f(a)}, \end{aligned} \quad (3.21)$$

where dots denote the derivative with respect to τ . The induced metric h_{ab} is a tangent component of $g_{\alpha\beta}$ on the hypersurface Σ . Then, the normal vector component on $g_{\alpha\beta}^{\pm}$ is defined as follow [49, 50, 54]

$$n_{\alpha}^{\pm} \equiv \pm \frac{F(r, a(\tau))_{,\alpha}}{|F(r, a(\tau))_{,\beta} F(r, a(\tau))^{,\beta}|^{1/2}}, \quad (3.22)$$

where $F(r, a(\tau)) \equiv r - a(\tau) = 0$ is the hypersurface function and the normal vector n_α is perpendicular to a tangent vector e_a^α i.e. $e_a^\alpha n_\alpha = 0$. The Greek indices $(x^\alpha, x^\beta, \dots)$ represent the coordinates on Manifold \mathcal{M} where as the Latin indices (y^a, y^b, \dots) represent the coordinates on hypersurface Σ . The metric tensor of the manifold at the hypersurface can be written in terms of tangent and normal vectors [49, 50, 54]

$$g_{ab} = h_{ab} + \epsilon n_a n_b, \quad (3.23)$$

where ϵ represents the types of thin-shell with $\epsilon = -1, 0, +1$ being the spacelike, nulllike and timelike, respectively.

Now we calculate the elements of n_α by considering

$$\begin{aligned} F_\pm(r, a(\tau))_{,\beta} F_\pm(r, a(\tau))^{,\beta} &= g^{tt} \partial_t F_\pm \partial_t F_\pm + g^{rr} \partial_r F_\pm \partial_r F_\pm \\ &= \frac{f_\pm(a)^2}{f_\pm(a) + \dot{a}^2}. \end{aligned} \quad (3.24)$$

We substitute Eq. (3.24) into Eq. (3.22)

$$\begin{aligned} n_\alpha^\pm &= \left(-\frac{da(\tau)}{dt}, 1, 0, 0 \right) \frac{\sqrt{f_\pm(a) + \dot{a}^2}}{f_\pm(a)} \\ &= \left(-\frac{\dot{a}(\tau)}{\dot{t}}, 1, 0, 0 \right) \frac{\sqrt{f_\pm(a) + \dot{a}^2}}{f_\pm(a)} \\ &= \left(-\dot{a}(\tau), \frac{\sqrt{f_\pm(a) + \dot{a}^2}}{f_\pm(a)}, 0, 0 \right), \end{aligned} \quad (3.25)$$

where we also make use of \dot{t} from Eq. (3.21) for the last line. This is the elements of the normal vector on the hypersurface of manifolds (\mathcal{M}^+ and \mathcal{M}^-).

3.2.2 The embedding diagram for thin-shell wormhole

To visualize the thin-shell wormhole spacetime, we consider the slice of the line element given in Eq. (3.19) at $t = \text{constant}$ and $\theta = \pi/2$. The two-dimensional surface is embedded into three dimensional Euclidean space (cylindrical coordinate)

$$ds^2 = \frac{dr}{f_{\pm}(r)} + r^2 d\phi^2 = dr^2 + r^2 d\phi^2 + dz^2. \quad (3.26)$$

Then, we obtain the relation

$$\frac{dz}{dr} = \sqrt{\frac{1 - f_{\pm}(r)}{f_{\pm}(r)}}, \quad (3.27)$$

where a choice of function $f_{\pm}(r)$ must satisfies $0 < f_{\pm}(r) < 1$ because z must be a real number.

3.2.3 The flaring-out condition for thin-shell wormhole

Furthermore, we apply the following criteria to determine the condition for the narrowest radius of the thin-shell wormhole. We consider the second order derivative as follow

$$\frac{d^2 r}{dz^2} = \frac{f'_{\pm}(r)}{2(1 - f_{\pm}(r))^2} > 0, \quad (3.28)$$

where this relation holds at or near the throat of the thin-shell wormhole to guarantee that the wormhole throat is the narrowest part.

3.2.4 Junction condition

The thin-shell on the hypersurface Σ plays the major role to link two manifolds via the boundaries of two manifolds $\partial\mathcal{M}_\pm$. We study the dynamics of the thin shell by solving the junction condition from an action containing the bulks (manifolds), boundaries and the hypersurface as follow [55, 56]

$$\begin{aligned}
 S_{\text{total}} = & \int_{\mathcal{M}_+} d^4x \sqrt{-g^+} \left(\frac{R}{16\pi G} + \mathcal{L}_{\text{matter}}^+ \right) + \frac{1}{8\pi G} \int_{\partial\mathcal{M}_+} d^3y \sqrt{-h^+} K^+ \\
 & + \int_{\mathcal{M}_-} d^4x \sqrt{-g^-} \left(\frac{R}{16\pi G} + \mathcal{L}_{\text{matter}}^- \right) + \frac{1}{8\pi G} \int_{\partial\mathcal{M}_-} d^3y \sqrt{-h^-} K^- \\
 & + \int_{\Sigma} d^3y \sqrt{-h} \mathcal{L}_{\text{matter}}^\Sigma, \tag{3.29}
 \end{aligned}$$

where $\sqrt{-h}$ is the volume element on the 3-dimensional hypersurface, the boundary terms are called Gibbons-Hawking terms and K is the trace of the extrinsic curvature K_{ab} on the thin-shell with $K \equiv K_a^a = h_{ab}K_a^b$. $\mathcal{L}_{\text{matter}}$ is the Lagrangian density on the thin shell of the material for wormhole construction. Inside the bulk, the line element is described by the metric tensor $g_{\mu\nu}^\pm$ while, on the thin-shell hypersurface, the line element is determined by the induced metric h_{ab} . However, the form of Lagrangian density in bulks is exactly the same as on the hypersurface. With the variational principle to the total action in Eq. (3.29), the equation of

motion reads

$$\begin{aligned}
\delta S &= \int_{\mathcal{M}_+} d^4x \sqrt{-g^+} \left(\frac{G_{\alpha\beta}^+}{16\pi G} + T_{\alpha\beta}^{(f),+} \right) \delta g_+^{\alpha\beta} \\
&+ \int_{\partial\mathcal{M}_+} d^3y \frac{\sqrt{-h^+}}{8\pi G} (K_{ab}^+ - h_{ab}^+ K^+) \delta h_+^{ab} \\
&+ \int_{\mathcal{M}_-} d^4x \sqrt{-g^-} \left(\frac{G_{\alpha\beta}^-}{16\pi G} + T_{\alpha\beta}^{(f),-} \right) \delta g_-^{\alpha\beta} \\
&+ \int_{\partial\mathcal{M}_-} d^3y \frac{\sqrt{-h^-}}{8\pi G} (K_{ab}^- - h_{ab}^- K^-) \delta h_-^{ab} \\
&- \int_{\Sigma} d^3y \sqrt{-h} t_{ab} \delta h^{ab}, \tag{3.30}
\end{aligned}$$

where the energy momentum tensor of the matter in bulks is

$$T_{\alpha\beta}^{(f),\pm} = -\frac{2}{\sqrt{-g}} \frac{\delta(\sqrt{-g} \mathcal{L}_{\text{matter}}^{\pm})}{\delta g_{\pm}^{\alpha\beta}}, \tag{3.31}$$

and the energy momentum tensor of the matter on the thin-shell can be written in terms of perfect fluid as follow

$$\begin{aligned}
t_{ab} &= -\frac{2}{\sqrt{-h}} \frac{\delta(\sqrt{-h} \mathcal{L}_{\text{matter}}^{\Sigma})}{\delta h_{\pm}^{ab}} \\
&= (\rho + p) u^a u_b + p h_b^a. \tag{3.32}
\end{aligned}$$

In order to solve for the junction condition, we consider the variation of the action on the hypersurface Σ and boundaries $\partial\mathcal{M}_{\pm}$ with respect to the induced metric h^{ab}

$$\begin{aligned}
0 = \frac{\delta S}{\delta h^{ab}} &= \int_{\partial\mathcal{M}_+} d^3y \sqrt{-h^+} \frac{1}{8\pi G} (K_{cd}^+ - h_{cd}^+ K^+) \frac{\delta h_+^{cd}}{\delta h^{ab}} \\
&+ \int_{\partial\mathcal{M}_-} d^3y \sqrt{-h^-} \frac{1}{8\pi G} (K_{cd}^- - h_{cd}^- K^-) \frac{\delta h_-^{cd}}{\delta h^{ab}} \\
&- \int_{\Sigma} d^3y \sqrt{-h} t_{ab}. \tag{3.33}
\end{aligned}$$

The normal vector n^a of the hypersurface points from \mathcal{M}_- to \mathcal{M}_+ . Then we can choose $n_-^a = n^a = -n_+^a$ in which the extrinsic curvature on each side is related to

each other via [55, 56]

$$K_{ab}^+(n_+^a) = -K_{ab}^+(n^a), \quad (3.34)$$

and

$$K_{ab}^-(n_-^a) = K_{ab}^-(n^a). \quad (3.35)$$

Moreover, the induced metric h_{ab} are the same on both sides of the boundaries, i.e., $h_{ab}^+ = h_{ab} = h_{ab}^-$. Eq. (3.33) becomes

$$\frac{\delta S_{\text{total}}}{\delta h^{ab}} = \int_{\Sigma} d^3y \sqrt{-h} \frac{1}{8\pi G} \left(h_{ab} \Delta K - \Delta K_{ab} - 8\pi G t_{ab} \right) = 0, \quad (3.36)$$

where the notation $\Delta A \equiv A_+ - A_-$ represents the difference of A in both manifolds.

Eventually the junction condition on the thin-shell is given by

$$\delta_b^a \Delta K - \Delta K_b^a = 8\pi G t_b^a, \quad (3.37)$$

where the matrix form of energy momentum tensor of matter reads

$$t_b^a = \begin{pmatrix} -\rho & 0 & 0 \\ 0 & P_t & 0 \\ 0 & 0 & P_t \end{pmatrix}, \quad (3.38)$$

where ρ is the energy density of wormhole material on the thin shell and P_t is the pressure in the tangential directions of wormhole material on the thin shell. Thus, junction condition will provide the detail of the matter that holds the thin-shell wormhole sustainably.

Now we consider the left hand side of the junction condition in Eq. (3.37).

The extrinsic curvature can be calculated via the following equation:

$$\begin{aligned}
K_{ab} &\equiv e_a^\alpha e_b^\beta \nabla_\beta n_\alpha \\
&= e_b^\beta \nabla_\beta (n_\alpha e_a^\alpha) - n_\alpha e_b^\beta \nabla_\beta (e_a^\alpha) \\
&= 0 - n_\alpha \nabla_b e_a^\alpha \\
&= -n_\alpha \nabla_b \left(\frac{dx^\alpha}{dy^a} \right) \\
&= -n_\alpha \left[\frac{d^2 x^\alpha}{dy^a dy^b} + \Gamma_{\beta\gamma}^\alpha \frac{dx^\beta}{dy^a} \frac{dx^\gamma}{dy^b} \right], \tag{3.39}
\end{aligned}$$

where the normal vector n_α from Eq. (3.22) with the spherical symmetric metric tensor from Eq. (3.19) is given by

$$n_{\alpha\pm} = \pm \left(-\dot{a}(\tau), \frac{\sqrt{f(a) + \dot{a}^2}}{f(a)}, 0, 0 \right). \tag{3.40}$$

Therefore all non-zero components of the extrinsic curvature are

$$K_\tau^{\tau\pm} = \pm \frac{1}{\sqrt{f_\pm + \dot{a}^2}} \left(\ddot{a} + \frac{f'_\pm}{2} \right), \tag{3.41}$$

$$K_\theta^{\theta\pm} = K_\phi^{\phi\pm} = \pm \frac{1}{a} (\sqrt{f_\pm + \dot{a}^2}). \tag{3.42}$$

The continuity condition of the metric tensor on thin-shell implies that the metric tensor of both manifolds are continuous at the throat of the wormhole implying [49, 50]

$$g_{\mu\nu}^+ = g_{\mu\nu}^-. \tag{3.43}$$

This leads to $f_+(a) = f_-(a) = f(a)$. The $(\tau\tau)$ component of the junction condition of the thin-shell wormhole in Eq.(3.37) reads

$$\frac{2}{a} (\sqrt{f + \dot{a}^2}) = -8\pi G\rho. \tag{3.44}$$

Moreover, the $(\theta\theta)$ and $(\phi\phi)$ components of the junction condition are given by

$$\frac{1}{\sqrt{f + \dot{a}^2}}(2\ddot{a} + f') = 8\pi G P_t. \quad (3.45)$$

In addition, the continuity of the perfect fluid matter gives a relation between the energy density in Eq. (3.44) and pressure in Eq. (3.45) on the thin-shell as

$$\frac{d}{d\tau}(a\rho) + P_t \frac{da}{d\tau} = 0. \quad (3.46)$$

It is also written in terms of the first order derivative of ρ with respect to a as

$$\frac{d\rho}{da} = -\left(\frac{\rho + P_t}{a}\right). \quad (3.47)$$

The second order derivative of ρ with respect to a yields

$$\frac{d^2\rho}{da^2} = \frac{\rho + p}{a^2} \left(2 + \frac{dP_t}{d\rho}\right), \quad (3.48)$$

where $P_t = P_t(\rho)$. Above equations are useful for analysing the stability of the wormhole with several types of the perfect fluid matters.

3.2.5 Stability of the thin-shell wormhole

We use the junction conditions of the thin-shell wormhole to investigate its the stability. The $(\tau\tau)$ component of the junction condition in Eq. (3.44) can be written in term of kinetic and potential terms of throat a

$$\frac{1}{2}\dot{a}^2 + V(a) = 0, \quad (3.49)$$

where the effective potential $V(a)$ is given by

$$V(a) = \frac{1}{2}f(a) - 8\pi^2 G^2 \rho^2 a^2. \quad (3.50)$$

The dynamics of the wormhole throat is determined by Eq. (3.49). To investigate the stability of the wormhole, we consider the small perturbation on the thin shell while it is at the equilibrium point $a = a_0$. The effective potential $V(a)$ describes the type of equilibrium point a_0 whether it is a stable equilibrium or unstable equilibrium. To do so, the effective potential is expanded by Taylor series around the static throat a_0

$$V(a) = V(a_0) + V'(a_0)(a - a_0) + \frac{1}{2}V''(a_0)(a - a_0)^2 + \mathcal{O}((a - a_0)^3). \quad (3.51)$$

It is straightforward to show that $V(a_0) = 0$ and $V'(a_0) = 0$ by considering Eq. (3.49) and its first derivative with a at the static throat a_0 . The non-zero leading term from the perturbation of effective potential becomes

$$V(a) = \frac{1}{2}V''(a_0)(a - a_0)^2 + \mathcal{O}((a - a_0)^3). \quad (3.52)$$

Therefore, the equation of motion for the wormhole throat approximately takes the form

$$\dot{a}^2 + V''(a_0)(a - a_0)^2 = 0. \quad (3.53)$$

The perturbed thin-shell wormhole is stable if and only if $V''(a_0) > 0$ with the frequency of the oscillation $\omega = \sqrt{V''(a_0)}$. Otherwise, the dynamics of wormhole throat a will be exponentially grow or collapse. Note that $V(a_0)$ has the minimum at a_0 . We finally obtain the stability condition of the thin-shell wormhole throat by using the definition of the effective potential in Eq. (3.50) and substituting the first and second order derivatives of energy density with a from Eq. (3.47) and Eq. (3.48)

$$0 < V''(a_0) = \frac{1}{2}f''(a_0) + \frac{dP_t}{d\rho} \left(-16G^2\pi^2\rho(P_t + \rho) \right) - 16G^2P_t^2\pi^2. \quad (3.54)$$

The last puzzle to investigate the stability of wormhole is the equation of state of the matter which explains the relation between the energy density ρ and pressure P_t of the matter. We apply interesting types of fluid model in the following section.



CHAPTER IV

Wormholes in Massive Gravity

In this chapter, we present two methods to construct wormholes in the dRGT massive gravity and investigate their stability. The first method is the Lorentzian traversable wormhole where the characteristic of wormhole is determined by the shape function and the red-shift function. The second method is the thin-shell wormhole which connects hypersurfaces of two different Universes. To check the requirement of the exotic matter for wormhole construction, we apply the energy conditions to study the properties of matter content in the wormhole throat whether it is physical or not.

The following sets of parameters in this work might violate the Vainshtein mechanism since the models here are designed to investigate the effects on exotic matter by variation of parameters in the modified gravity and dRGT massive gravity [57, 58]. In the other words, we study a toy model of the wormholes in $f(R)$ and dRGT massive gravity. However, we realize the major caveat and will apply all parameters to satisfy the Vainshtein mechanism in the future research.

According to section 2.5, the nonlinear Fierz-Pauli theory faces the BD ghost instability causing the extra degree of freedom. From the dRGT massive gravity,

the higher order potential terms in Eq. (2.97) can get rid of the BD ghost problem at least in the decoupling limit [16, 17]. In the decoupling limit, the coupling cutoff is set to eliminate the scalar self-interactions in any order. The cutoff would be raised to $\Lambda_3 = (M_P m_g^2)^{1/3}$. Thus, the dRGT massive gravity is still functional without the quantum effects until the distance is smaller than $r_Q \sim 1/\Lambda_3$. In addition, we note that the factor $m_g^{2/3} = \Lambda_3$ carries [mass]¹ dimension since we have set $M_P = 1$ for the present analysis.

We are using the dRGT massive gravity theory with a UV cutoff Λ_3 , therefore we should not worry about the BD instabilities until the mass of the BD ghost is below Λ_3 . This happens at the quantum length scale [16]

$$r_Q = r_{\text{ghost}} \sim \frac{1}{\Lambda_3} = \left(\frac{1}{m_g^2} \right)^{1/3}. \quad (4.1)$$

For a source mass M for building the traversable wormhole, the non-linearities of the dRGT massive gravity becomes important at the radius [16]

$$r_V = \frac{M^{1/3}}{\Lambda_3} = \left(\frac{M}{m_g^2} \right)^{1/3}. \quad (4.2)$$

Generally the Vainshtein radius r_V is larger than the quantum length scale r_Q , therefore we could use the dRGT theory at the distance $r > r_V$ without concerning the quantum correction to the wormhole's solutions.

4.1 Lorentzian Traversable Wormhole in dRGT massive gravity theory

Modified gravity theories have been a major role for study wormholes. $f(R)$ theory, which generalizes the Einstein general relativity to the higher orders, has been used to study the traversable wormhole [9, 10]. The investigation of NEC and WEC for wormholes in $f(R)$ gravity with various the shape functions $b(r)$ and the red-shift functions $\Phi(r)$ are found in Refs. [11, 59]. The study of the effect of cosmological constant on the Morris-Thorne wormholes was explored in Ref. [60]. There are numerous types of wormholes with modified gravity, for instance, Einstein-Gauss-Bonnet gravity [61], $f(R, \phi)$ gravity [62], both $f(R)$ and $f(R, T)$ theories [63, 64], Born-Infeld gravity [65], Eddington-inspired Born-Infeld gravity [66], and even in non-commutative geometry [67, 68].

In this section, we apply the modified $f(R)$ gravity and dRGT massive gravity to find the solution of traversable wormhole. We consider the Starobinsky inflation model [69] which is used to understand the inflation in the early Universe and the acceleration of the Universe in the late-time acceleration. The modified gravity function is $f(R) = R + \alpha_1 R^n$ where α_1 and n are arbitrary constants.

4.1.1 Equation of motion for Lorentzian traversable wormhole

The action of $f(R)$ gravity with the dRGT massive gravity theory is given by [57]

$$S = \int d^4x \sqrt{-g} \left(\frac{1}{16\pi G} \left[f(R) + m_g^2 \mathcal{U}(g, \phi^a) \right] \right) + \int d^4x \sqrt{-g} \mathcal{L}_{\text{matter}}, \quad (4.3)$$

where $f(R) = R + \alpha_1 R^n$ is the modified gravity by Starobinsky and $\mathcal{U}(g, \phi^a)$ is the ghost-free effective potential from dRGT massive gravity theory in Eq. (2.97).

According to the variational principle, we vary the action with respect to $g^{\mu\nu}$ to obtain the equation of motion

$$F(R)R_{\mu\nu} - \frac{1}{2}f(R)g_{\mu\nu} - \nabla_\mu \nabla_\nu F + g_{\mu\nu} \square F = -m_g^2 X_{\mu\nu} + 8\pi G T_{\mu\nu}^{(m)}, \quad (4.4)$$

where the energy-momentum tensor of the matter field is

$$\begin{aligned} T_{\mu\nu}^{(m)} &= \frac{-2}{\sqrt{-g}} \frac{\delta(\sqrt{-g} \mathcal{L}_{\text{matter}})}{\delta g^{\mu\nu}} \\ &= \text{diag}(-\rho, P_r, P_t, P_t), \end{aligned} \quad (4.5)$$

$F = F(R) \equiv df(R)/dR$ and $\square F = g^{\mu\nu} \nabla_\mu \nabla_\nu F$. The energy momentum tensor for the matter constructing the traversable wormhole is written in terms of anisotropic perfect fluid as Eq. (3.12). $X_{\mu\nu}$ is the dRGT massive gravity tensor defined in Eq. (2.100). Each non-zero components of $X_{\mu\nu}$ serves the energy density and pressure of the massive graviton from Eq. (2.117), Eq. (2.118) and Eq. (2.119).

The field equation in Eq. (4.4) can be written in the following form [57]

$$G_{\mu\nu} = R_{\mu\nu} - \frac{1}{2}Rg_{\mu\nu} = -m_g^2 X_{\mu\nu} + 8\pi G \left(T_{\mu\nu}^{(f(R))} + T_{\mu\nu}^{(m)} \right), \quad (4.6)$$

where

$$8\pi GT_{\mu\nu}^{(f(R))} = \frac{1}{2}g_{\mu\nu}(f(R) - R) + \nabla_\mu \nabla_\nu F - g_{\mu\nu} \square F + (1 - F)R_{\mu\nu}. \quad (4.7)$$

To study the traversable wormhole, we use the line element of the Morris-and-Thorne traversable wormhole from Eq. (3.1)

$$ds^2 = -e^{2\Phi(r)} dt^2 + \left(1 - \frac{b(r)}{r}\right)^{-1} dr^2 + r^2(d\theta^2 + \sin^2\theta d\phi^2),$$

Considering the field equation in Eq. (4.6) with the Morris-and-Thorne line element, one obtains the energy density, pressure in radial and tangential directions as follows [57],

$$\begin{aligned} \rho = & \frac{dF(R)}{dr} \left(\frac{rb'(r) + 3b(r) - 4r}{16\pi Gr^2} - \frac{1}{8\pi G} \left(1 - \frac{b(r)}{r}\right) \Phi'(r) \right) + \frac{f(R)}{16\pi G} \\ & + \frac{2\gamma r - \Lambda r^2}{8\pi Gr^2} + F(R) \left(\frac{(r(-b'(r)) - 3b(r) + 4r) \Phi'(r)}{16\pi Gr^2} \right. \\ & \left. + \frac{1}{8\pi G} \left(1 - \frac{b(r)}{r}\right) (\Phi''(r) + \Phi'^2(r)) \right) - \frac{1}{8\pi G} \left(1 - \frac{b(r)}{r}\right) \frac{d^2 F(R)}{dr^2}, \end{aligned} \quad (4.8)$$

$$\begin{aligned} P_r = & \frac{dF(R)}{dr} \left(\frac{1}{8\pi G} \left(1 - \frac{b(r)}{r}\right) \Phi'(r) + \frac{1}{4\pi Gr} \left(1 - \frac{b(r)}{r}\right) \right) - \frac{f(R)}{16\pi G} \\ & + \frac{\Lambda r^2 - 2\gamma r}{8\pi Gr^2} + F(R) \left(\frac{1}{8\pi Gr^3} (rb'(r) - b(r)) \left(1 + \frac{r\Phi'(r)}{2}\right) \right. \\ & \left. - \frac{1}{8\pi G} \left(1 - \frac{b(r)}{r}\right) (\Phi''(r) + \Phi'^2(r)) \right), \end{aligned} \quad (4.9)$$

$$\begin{aligned} P_t = & F(R) \left(\frac{1}{8\pi G} \left(1 - \frac{b(r)}{r}\right) \Phi'(r) + \frac{1}{16\pi Gr^3} (b(r) + rb'(r)) \right) - \frac{f(R)}{16\pi G} \\ & + \frac{dF(R)}{dr} \left(\frac{1}{8\pi G} \left(1 - \frac{b(r)}{r}\right) \Phi'(r) + \frac{1}{16\pi Gr^3} (4r^2 - 3rb(r) - r^2b'(r)) \right) \\ & + \frac{\Lambda r^2 - 2\gamma r}{8\pi Gr^2} + \frac{1}{8\pi G} \left(1 - \frac{b(r)}{r}\right) \frac{d^2 F(R)}{dr^2}. \end{aligned} \quad (4.10)$$

4.1.2 Analyze the energy conditions for Lorentzian traversable wormholes

To analyze the energy conditions of the matter constructing the traversable wormhole, we have to choose the shape function and red-shift function that satisfy the wormhole properties in section [3]. In our study, we choose the shape function as

$$b(r) = \frac{r}{\exp(\alpha(r - r_0))}, \quad (4.11)$$

where r_0 is the radius of the wormhole throat, α is the arbitrary constant. It is straightforward to show that the shape function in Eq. (4.11) satisfies the wormhole properties in embedding diagram, flaring-out condition and no-horizon condition. According to Refs.[63, 70], the choice of α is unity to construct the traversable wormhole. The embedding diagram of the metric Eq. (3.4) is illustrated in Fig. 4.1 which is the function of $z(r)$ (by integration of Eq. (3.5)) for the slices $t = \text{constant}$, $\theta = \pi/2$. The chosen shape function of the traversable satisfies the embedding diagram and the flaring-out condition demonstrated in Fig. (4.2) [57].

In this thesis, we select these three types of the red-shift function $\Phi(r) = \text{constant} = p$, $\Phi(r) = \frac{\gamma_1}{r}$, and $\Phi(r) = \log\left(1 + \frac{\gamma_2}{r}\right)$ where γ_1 and γ_2 are arbitrary real constants. We apply three cases of the red-shift functions with the shape function to calculate null energy condition (NEC), weak energy condition (WEC) and strong energy condition (SEC) introduced in subsection (1.3).

There are four sets of the dRGT parameters which are ($\Lambda = -1.0$ and $\gamma = 0.5$), ($\Lambda = -0.5$ and $\gamma = 0.5$), ($\Lambda = -1.0$ and $\gamma = 0.1$), and ($\Lambda = -0.5$

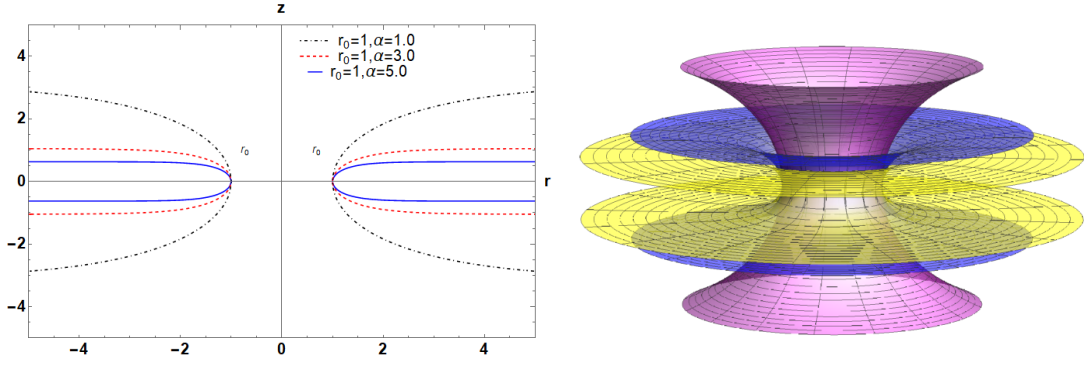


Figure 4.1: Plots show embedding diagrams of the metric (3.4) for slices $t = \text{const}, \theta = \pi/2$. The left panel shows the 2-dimensional diagram of the traversable wormhole using $r_0 = 1.0$, and $\alpha = 1.0$ (a black dot-dashed line), $r_0 = 1.0$, and $\alpha = 3.0$ (a red dot line) and $r_0 = 1.0$, and $\alpha = 5.0$ and (a blue solid line). The right panel displays 3-dimensional diagram of the traversable wormholes using the same three sets of parameters.

and $\gamma = 0.1$), then their Vainshtein radiuses are 0.794, 0.874, 0.941 and 1.126, respectively. Because we set $G = 1$ and $M = 1$, the Vainshtein radiuses equal the quantum length scales. Additionally, we set the throat of the traversable wormhole at $r_0 = 1$, then the first three cases have no problem with all range except for the last case where the distance from the throat ($r_0 = 1$) to its Vainshtein radius ($r_V = 1.126$) cannot be trusted due to the involvement of the quantum correction.

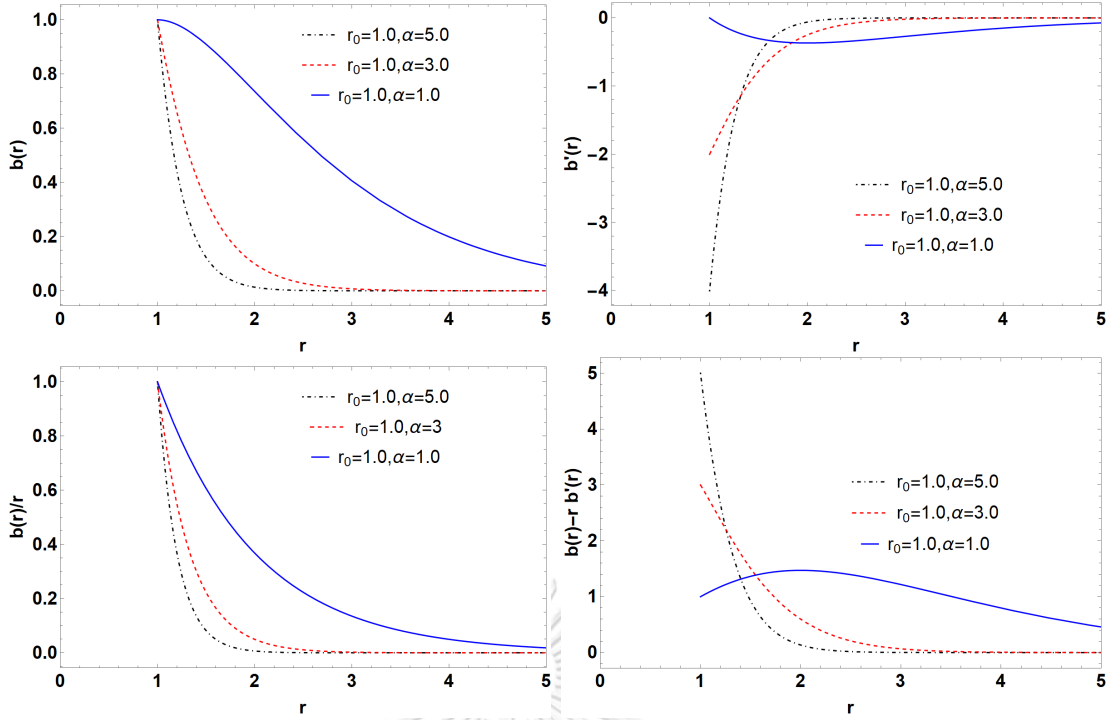


Figure 4.2: We verify the properties of the shape function introduced in Eq. (4.11). The plots show behaviors of the proposed shape function against the requirements given by the embedding diagram and the flaring-out condition for traversable wormhole in Eqs. (3.6 - 3.9) using various values of $\alpha = 1.0, 3.0, 5.0$ and $r_0 = 1$. We find that the shape function of the wormhole is completely satisfied the requirements.

The first case: $\Phi(r) = \text{constant} = p$

With the shape function from Eq. (4.11) and the constant red shift function, we find [57]

$$\rho = F'(r) \left(\frac{b'(r)}{16\pi Gr} + \frac{3b(r)}{16\pi Gr^2} - \frac{1}{4\pi Gr} \right) + \left(\frac{b(r)}{8\pi Gr} - \frac{1}{8\pi G} \right) F''(r) + \frac{f(R(r))}{16\pi G} - \frac{\Lambda}{8\pi G} + \frac{\gamma}{4\pi Gr}, \quad (4.12)$$

$$P_r = F(r) \left(\frac{b'(r)}{8\pi Gr^2} - \frac{b(r)}{8\pi Gr^3} \right) + \left(\frac{1}{4\pi Gr} - \frac{b(r)}{4\pi Gr^2} \right) F'(r) - \frac{f(R(r))}{16\pi G} + \frac{\Lambda}{8\pi G} - \frac{\gamma}{4\pi Gr}, \quad (4.13)$$

$$\begin{aligned}
P_t = & F'(r) \left(-\frac{b'(r)}{16\pi Gr} - \frac{3b(r)}{16\pi Gr^2} + \frac{1}{4\pi Gr} \right) + F(r) \left(\frac{b'(r)}{16\pi Gr^2} + \frac{b(r)}{16\pi Gr^3} \right) \\
& + \left(\frac{1}{8\pi G} - \frac{b(r)}{8\pi Gr} \right) F''(r) - \frac{f(R(r))}{16\pi G} + \frac{\Lambda}{8\pi G} - \frac{\gamma}{8\pi Gr}. \quad (4.14)
\end{aligned}$$

The combinations of Eqs. (4.12 - 4.14) yield the following relations among ρ, P_r , and P_t :

$$\begin{aligned}
\rho + P_r = & F'(r) \left(\frac{b'(r)}{16\pi Gr} - \frac{b(r)}{16\pi Gr^2} \right) + F(r) \left(\frac{b'(r)}{8\pi Gr^2} - \frac{b(r)}{8\pi Gr^3} \right) \\
& + \left(\frac{b(r)}{8\pi Gr} - \frac{1}{8\pi G} \right) F''(r), \quad (4.15)
\end{aligned}$$

$$\rho + P_t = \frac{F(r)b'(r)}{16\pi Gr^2} + \frac{b(r)F(r)}{16\pi Gr^3} + \frac{\gamma}{8\pi Gr}, \quad (4.16)$$

$$\begin{aligned}
\rho - |P_r| = & - \left| -\frac{\gamma}{4G\pi r} + \frac{\Lambda}{8G\pi} - \frac{f(R(r))}{16G\pi} + F(r) \left(\frac{b'(r)}{8G\pi r^2} - \frac{b(r)}{8G\pi r^3} \right) \right. \\
& + \left. \left(\frac{1}{4G\pi r} - \frac{b(r)}{4G\pi r^2} \right) F'(r) \right| + F'(r) \left(\frac{b'(r)}{16\pi Gr} + \frac{3b(r)}{16\pi Gr^2} \right. \\
& - \left. \frac{1}{4\pi Gr} \right) + \left(\frac{b(r)}{8\pi Gr} - \frac{1}{8\pi G} \right) F''(r) + \frac{f(R(r))}{16\pi G} - \frac{\Lambda}{8\pi G} \\
& + \frac{\gamma}{4\pi Gr}, \quad (4.17)
\end{aligned}$$

$$\begin{aligned}
\rho - |P_t| = & F'(r) \left(\frac{b'(r)}{16\pi Gr} + \frac{3b(r)}{16\pi Gr^2} - \frac{1}{4\pi Gr} \right) + \frac{f(R(r))}{16\pi G} - \frac{\Lambda}{8\pi G} \\
& + \left(\frac{b(r)}{8\pi Gr} - \frac{1}{8\pi G} \right) F''(r) + \frac{\gamma}{4\pi Gr} - \left| F'(r) \left(-\frac{b'(r)}{16\pi Gr} \right. \right. \\
& - \left. \left. \frac{3b(r)}{16\pi Gr^2} + \frac{1}{4\pi Gr} \right) + F(r) \left(\frac{b'(r)}{16\pi Gr^2} + \frac{b(r)}{16\pi Gr^3} \right) \right. \\
& + \left. \left(\frac{1}{8\pi G} - \frac{b(r)}{8\pi Gr} \right) F''(r) - \frac{f(R(r))}{16\pi G} + \frac{\Lambda}{8\pi G} - \frac{\gamma}{8\pi Gr} \right|, \quad (4.18)
\end{aligned}$$

$$\begin{aligned} \rho + 2P_t = & F'(r) \left(-\frac{b'(r)}{16\pi Gr} - \frac{3b(r)}{16\pi Gr^2} + \frac{1}{4\pi Gr} \right) \\ & + F(r) \left(\frac{b'(r)}{8\pi Gr^2} + \frac{b(r)}{8\pi Gr^3} \right) + \left(\frac{1}{8\pi G} - \frac{b(r)}{8\pi Gr} \right) F''(r) \\ & - \frac{f(R(r))}{16\pi G} + \frac{\Lambda}{8\pi G}, \end{aligned} \quad (4.19)$$

$$\begin{aligned} \rho + P_r + 2P_t = & F'(r) \left(-\frac{b'(r)}{16\pi Gr} - \frac{7b(r)}{16\pi Gr^2} + \frac{1}{2\pi Gr} \right) + \frac{F(r)b'(r)}{4\pi Gr^2} \\ & + \left(\frac{1}{8\pi G} - \frac{b(r)}{8\pi Gr} \right) F''(r) - \frac{f(R(r))}{8\pi G} + \frac{\Lambda}{4\pi G} - \frac{\gamma}{4\pi Gr} \end{aligned} \quad (4.20)$$

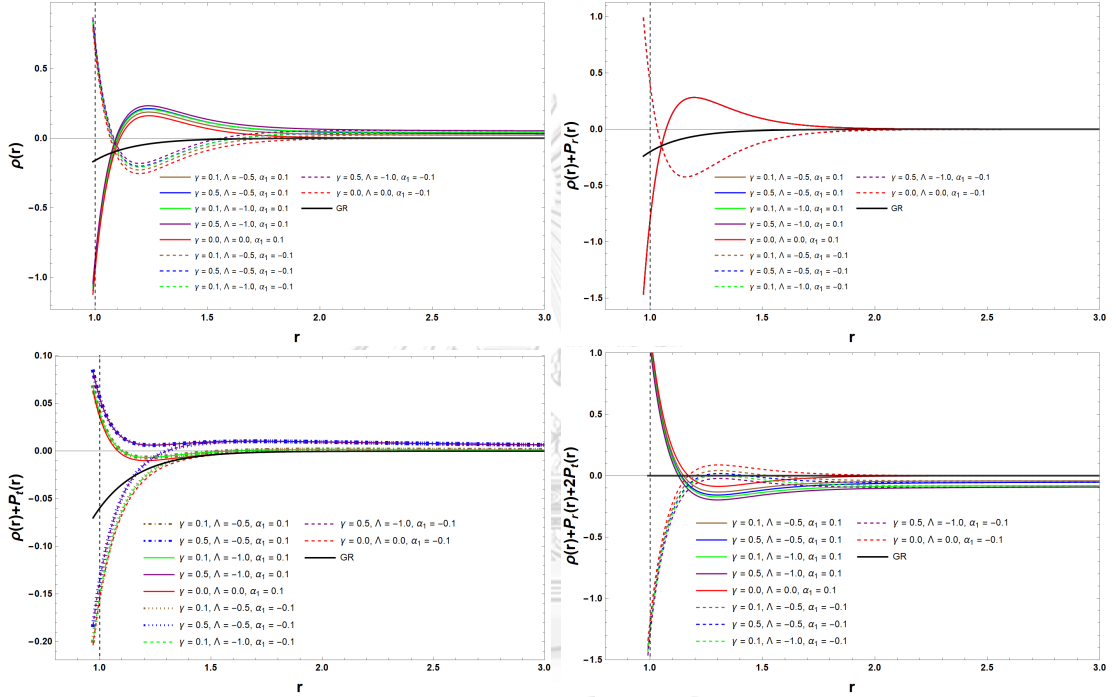


Figure 4.3: Figures demonstrate the variation of ρ , $\rho + P_r$, $\rho + P_t$, $\rho + P_r + 2P_t$ as a function of r with $\Phi(r) = p = 1$, $\alpha_1 = \pm 0.1$ and $n = 2$. We have used $\alpha = 5.0$, $r_0 = 1$, $G = 1$ and various values of γ and Λ .

We consider the red-shift function of the wormhole metric as $\Phi(r) = 1$. We split results by the strength of Starobinsky model into two figures shown in Fig.4.3 ($\alpha = \pm 0.1$) and Fig.4.4 ($\alpha = \pm 0.01$). In each panel in figures, there are three main cases of traversable wormholes; general relativity, positive α_1 and negative α_1 .

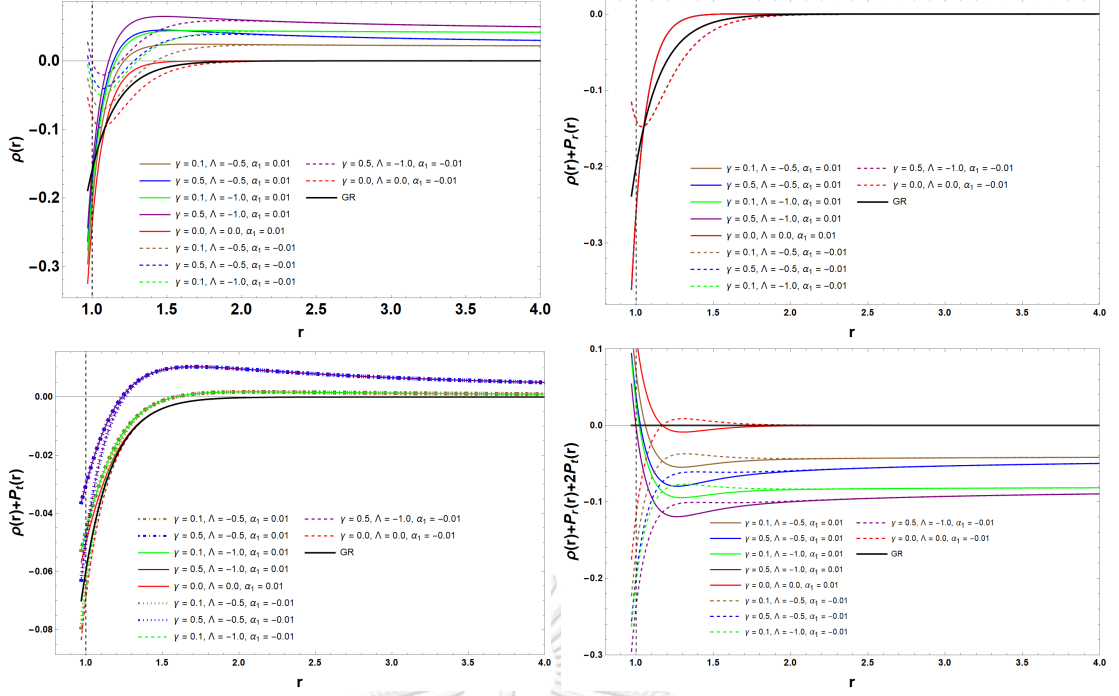


Figure 4.4: Figures demonstrate the variation of ρ , $\rho + P_r$, $\rho + P_t$, $\rho + P_r + 2P_t$ as a function of r with $\Phi(r) = 1$, $\alpha_1 = \pm 0.01$ and $n = 2$. We have used $\alpha = 5.0$, $r_0 = 1$, $G = 1$ and various values of γ and Λ .

Let consider Fig.4.3 ($\Phi(r) = 1$ and $\alpha_1 = \pm 0.1$). The first case in this figure is the traversable wormhole in GR represented by the black solid lines of ρ , $\rho + P_r$, $\rho + P_t$, and $\rho + P_r + 2P_t$ as functions of r . It violates WEC, NEC and SEC for all range from its throat to the cosmological horizon.

The second case in Fig.4.3 is the modified gravity with dRGT and Starobinsky models with $\alpha_1 = 0.1$ represented in color solid lines. The positive value of α_1 limits the negative zones of ρ and $\rho + P_r$ around the throat of the wormhole. The zone of negative energy density reduces when the value of γ increases and the value of Λ decreases. While both parameters do not effect the negative zone of $\rho + P_r$. $\rho + P_t$ is positive at the throat and becomes a decrease function near the

Table 4.1: Table shows a summary of energy/pressure conditions for $\Phi(r) = p = 1.0, n = 2, \alpha = 5.0, r_0 = 1, G = 1, \gamma = 0.5,$ and $\Lambda = -1.0$.

No.	Terms	$\alpha_1 = 0.1$	$\alpha_1 = -0.1$
1	ρ	≥ 0 , for $r \in [1.1, \infty)$ < 0 , for $r \in [1.0, 1.1)$	≥ 0 , for $r \in [1.0, 1.1] \cup [1.55, \infty)$ < 0 , for $r \in [1.1, 1.55)$
2	$\rho + P_r$	≥ 0 , for $r \in [1.1, \infty)$ < 0 , for $r \in [1.0, 1.1)$	≥ 0 , for $r \in [1.0, 1.05] \cup [2.5, \infty)$ < 0 , for $r \in (1.05, 2.5)$
3	$\rho + P_t$	≥ 0 , for $r \in [1.0, \infty)$	≥ 0 , for $r \in [1.3, \infty)$ < 0 , for $r \in [1.0, 1.3)$
4	$\rho + P_r + 2P_t$	≥ 0 , for $r \in [1.0, 1.15]$ < 0 , for $r \in (1.15, \infty)$	< 0 , for $\forall r$
5	$\rho - P_r $	≥ 0 , for $r \in [1.1, \infty)$ < 0 , for $r \in [1.0, 1.1)$	≥ 0 , for $r \in [1.0, 1.05] \cup [2.5, \infty)$
6	$\rho - P_t $	< 0 , for $\forall r$	< 0 , for $\forall r$

throat where its value goes below zero for low value of γ while Λ does not effect much. $\rho + P_r + 2P_t$, which is one for analysing SEC, is above zero only near the throat and becomes negative for the rest of the the spacetime. The effects from dRGT and Starobinsky on $\rho + P_r + 2P_t$ seem to be contradict to the energy density since $\rho + P_r + 2P_t$ is more negative for more positive γ and more negative Λ .

For the last case in Fig.4.3, the modified gravity with dRGT and Starobinsky models with $\alpha_1 = -0.1$ is represented in color dashed lines. All results are mostly opposite to the positive α_1 case. The energy density is positive around the throat

and becomes negative for the rest of the spacetime. The zone of negative energy density reduces when the value of γ increases and the value of Λ decreases like the previous case. The trend of $\rho + P_r$ is similar to its energy density; however, it is invariant under the change of γ and Λ . If the value of γ is not high enough, $\rho + P_t$ remains negative when the distance from the throat increases. For analysing $\rho + P_r + 2P_t$, it is negative around the throat and increasing to converge to some constants as the distance increases. The violation zone will be limited if the value of γ decreases and Λ increases.

Now consider Fig.4.4 ($\alpha_1 = \pm 0.01$). The only significant difference from this one to Fig.4.3 is the values of ρ , $\rho + P_r$, $\rho + P_t$, and $\rho + P_r + 2P_t$ near the throat of wormhole. It is evident that the less magnitude of α_1 is, the more violation zone near the throat becomes. The characteristic of energy density for $\alpha_1 = 0.01$ is still similar to the previous case but energy density is negative for all range from throat to the cosmological constant. The values of $\rho + P_r$ for $\alpha_1 = \pm 0.01$, are mostly negative except some small region of positiveness for $\alpha_1 = 0.01$. The values of $\rho + P_t$ for all cases are negative near the throat. However, the characteristic of $\rho + P_r + 2P_t$ is still the same but small magnitude near the throat.

The second case: $\Phi(r) = \frac{\gamma_1}{r}$

With the shape function from Eq. (4.11) and $\Phi(r) = \frac{\gamma_1}{r}$, we find [57]

$$\begin{aligned} \rho = & F'(r) \left(\frac{b'(r)}{16\pi Gr} - \frac{\gamma_1 b(r)}{8\pi Gr^3} + \frac{3b(r)}{16\pi Gr^2} + \frac{\gamma_1}{8\pi Gr^2} - \frac{1}{4\pi Gr} \right) \\ & + F(r) \left(\frac{\gamma_1 b'(r)}{16\pi Gr^3} - \frac{\gamma_1^2 b(r)}{8\pi Gr^5} - \frac{\gamma_1 b(r)}{16\pi Gr^4} + \frac{\gamma_1^2}{8\pi Gr^4} \right) \\ & + \left(\frac{b(r)}{8\pi Gr} - \frac{1}{8\pi G} \right) F''(r) + \frac{f(R(r))}{16\pi G} - \frac{\Lambda}{8\pi G} + \frac{\gamma}{4\pi Gr}, \end{aligned} \quad (4.21)$$

$$\begin{aligned} P_r = & F(r) \left(-\frac{\gamma_1 b'(r)}{16\pi Gr^3} + \frac{b'(r)}{8\pi Gr^2} + \frac{\gamma_1^2 b(r)}{8\pi Gr^5} + \frac{5\gamma_1 b(r)}{16\pi Gr^4} - \frac{b(r)}{8\pi Gr^3} \right. \\ & \left. - \frac{\gamma_1^2}{8\pi Gr^4} - \frac{\gamma_1}{4\pi Gr^3} \right) + F'(r) \left(\frac{\gamma_1 b(r)}{8\pi Gr^3} - \frac{b(r)}{4\pi Gr^2} - \frac{\gamma_1}{8\pi Gr^2} + \frac{1}{4\pi Gr} \right) \\ & - \frac{f(R(r))}{16\pi G} + \frac{\Lambda}{8\pi G} - \frac{\gamma}{4\pi Gr}, \end{aligned} \quad (4.22)$$

$$\begin{aligned} P_t = & F'(r) \left(-\frac{b'(r)}{16\pi Gr} + \frac{\gamma_1 b(r)}{8\pi Gr^3} - \frac{3b(r)}{16\pi Gr^2} - \frac{\gamma_1}{8\pi Gr^2} + \frac{1}{4\pi Gr} \right) \\ & + F(r) \left(\frac{b'(r)}{16\pi Gr^2} - \frac{\gamma_1 b(r)}{8\pi Gr^4} + \frac{b(r)}{16\pi Gr^3} + \frac{\gamma_1}{8\pi Gr^3} \right) \\ & + \left(\frac{1}{8\pi G} - \frac{b(r)}{8\pi Gr} \right) F''(r) - \frac{f(R(r))}{16\pi G} + \frac{\Lambda}{8\pi G} - \frac{\gamma}{8\pi Gr}. \end{aligned} \quad (4.23)$$

The combinations of Eqs. (4.21 - 4.23) yield the following relations among ρ , P_r , and P_t :

$$\begin{aligned} \rho + P_r &= F'(r) \left(\frac{b'(r)}{16\pi Gr} - \frac{b(r)}{16\pi Gr^2} \right) + \left(\frac{b(r)}{8\pi Gr} - \frac{1}{8\pi G} \right) F''(r) \\ &+ F(r) \left(\frac{b'(r)}{8\pi Gr^2} + \frac{\gamma_1 b(r)}{4\pi Gr^4} - \frac{b(r)}{8\pi Gr^3} - \frac{\gamma_1}{4\pi Gr^3} \right), \end{aligned} \quad (4.24)$$

$$\begin{aligned} \rho + P_t &= F(r) \left(\frac{\gamma_1 b'(r)}{16\pi Gr^3} + \frac{b'(r)}{16\pi Gr^2} - \frac{\gamma_1^2 b(r)}{8\pi Gr^5} - \frac{3\gamma_1 b(r)}{16\pi Gr^4} \right. \\ &\left. + \frac{b(r)}{16\pi Gr^3} + \frac{\gamma_1^2}{8\pi Gr^4} + \frac{\gamma_1}{8\pi Gr^3} \right) + \frac{\gamma}{8\pi Gr}, \end{aligned} \quad (4.25)$$

$$\begin{aligned} \rho - |P_r| &= - \left| -\frac{\gamma}{4G\pi r} + \frac{\Lambda}{8G\pi} - \frac{f(R(r))}{16G\pi} + F(r) \left(\frac{b(r)\gamma_1^2}{8G\pi r^5} - \frac{\gamma_1^2}{8G\pi r^4} \right. \right. \\ &+ \frac{5b(r)\gamma_1}{16G\pi r^4} - \frac{b'(r)\gamma_1}{16G\pi r^3} - \frac{\gamma_1}{4G\pi r^3} - \frac{b(r)}{8G\pi r^3} + \frac{b'(r)}{8G\pi r^2} \left. \right) \\ &+ \left(\frac{\gamma_1 b(r)}{8G\pi r^3} - \frac{b(r)}{4G\pi r^2} - \frac{\gamma_1}{8G\pi r^2} + \frac{1}{4G\pi r} \right) F'(r) \left| \right. \\ &+ F'(r) \left(\frac{b'(r)}{16\pi Gr} - \frac{\gamma_1 b(r)}{8\pi Gr^3} + \frac{3b(r)}{16\pi Gr^2} + \frac{\gamma_1}{8\pi Gr^2} - \frac{1}{4\pi Gr} \right) \\ &+ F(r) \left(\frac{\gamma_1 b'(r)}{16\pi Gr^3} - \frac{\gamma_1^2 b(r)}{8\pi Gr^5} - \frac{\gamma_1 b(r)}{16\pi Gr^4} + \frac{\gamma_1^2}{8\pi Gr^4} \right) \\ &+ \left(\frac{b(r)}{8\pi Gr} - \frac{1}{8\pi G} \right) F''(r) + \frac{f(R(r))}{16\pi G} - \frac{\Lambda}{8\pi G} + \frac{\gamma}{4\pi Gr}, \end{aligned} \quad (4.26)$$

$$\begin{aligned} \rho - |P_t| &= - \left| -\frac{\gamma}{8G\pi r} + \frac{\Lambda}{8G\pi} - \frac{f(R(r))}{16G\pi} + F(r) \left(-\frac{\gamma_1 b(r)}{8G\pi r^4} + \frac{b(r)}{16G\pi r^3} \right. \right. \\ &+ \frac{\gamma_1 b'(r)}{8G\pi r^3} + \frac{b'(r)}{16G\pi r^2} \left. \right) + \left(\frac{\gamma_1 b(r)}{8G\pi r^3} - \frac{3b(r)}{16G\pi r^2} - \frac{\gamma_1}{8G\pi r^2} \right. \\ &\left. - \frac{b'(r)}{16G\pi r} + \frac{1}{4G\pi r} \right) F'(r) + \left(\frac{1}{8G\pi} - \frac{b(r)}{8G\pi r} \right) F''(r) \left| \right. \\ &+ F'(r) \left(\frac{b'(r)}{16\pi Gr} - \frac{\gamma_1 b(r)}{8\pi Gr^3} + \frac{3b(r)}{16\pi Gr^2} + \frac{\gamma_1}{8\pi Gr^2} - \frac{1}{4\pi Gr} \right) \\ &+ F(r) \left(\frac{\gamma_1 b'(r)}{16\pi Gr^3} - \frac{\gamma_1^2 b(r)}{8\pi Gr^5} - \frac{\gamma_1 b(r)}{16\pi Gr^4} + \frac{\gamma_1^2}{8\pi Gr^4} \right) \\ &+ \left(\frac{b(r)}{8\pi Gr} - \frac{1}{8\pi G} \right) F''(r) + \frac{f(R(r))}{16\pi G} - \frac{\Lambda}{8\pi G} + \frac{\gamma}{4\pi Gr}, \end{aligned} \quad (4.27)$$

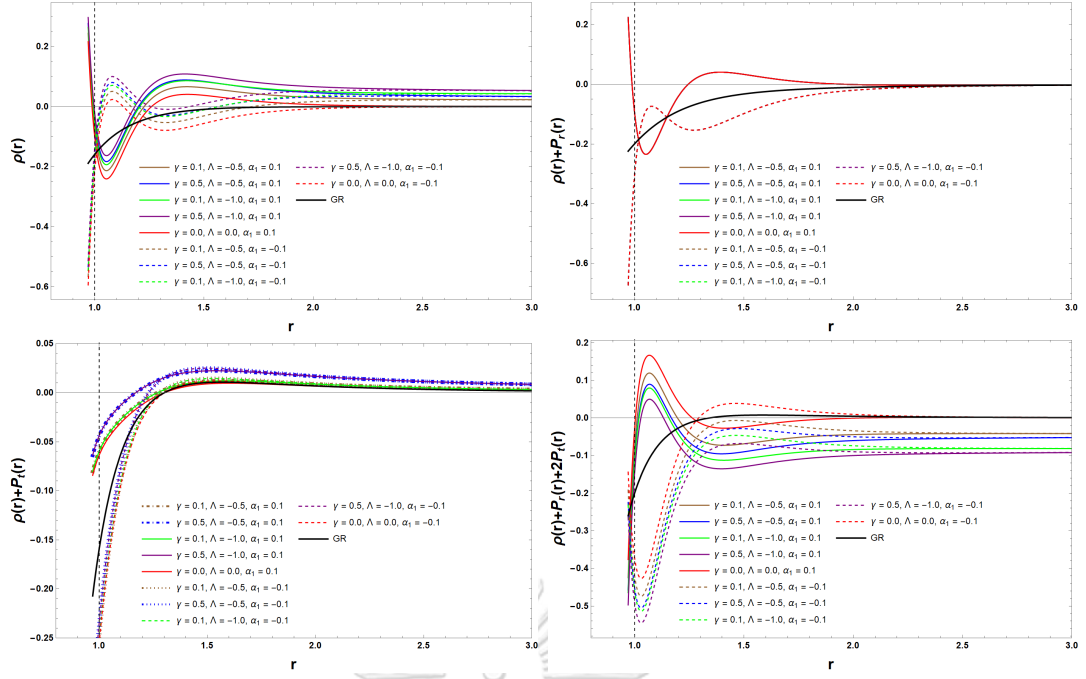


Figure 4.5: Figures illustrate the variation of ρ , $\rho + P_r$, $\rho + P_t$, $\rho + P_r + 2P_t$ as a function of r with $\Phi(r) = \gamma_1/r$. Here we have used $\alpha_1 = \pm 0.1$, $n = 2\alpha = 5.0$, $r_0 = 1$, $G = 1$, $\gamma_1 = 1.0$ and various values of γ and Λ .

$$\begin{aligned}
 \rho + 2P_t &= F'(r) \left(-\frac{b'(r)}{16\pi Gr} + \frac{\gamma_1 b(r)}{8\pi Gr^3} - \frac{3b(r)}{16\pi Gr^2} - \frac{\gamma_1}{8\pi Gr^2} + \frac{1}{4\pi Gr} \right) \\
 &+ F(r) \left(\frac{\gamma_1 b'(r)}{16\pi Gr^3} + \frac{b'(r)}{8\pi Gr^2} - \frac{\gamma_1^2 b(r)}{8\pi Gr^5} - \frac{5\gamma_1 b(r)}{16\pi Gr^4} + \frac{b(r)}{8\pi Gr^3} \right. \\
 &\left. + \frac{\gamma_1^2}{8\pi Gr^4} + \frac{\gamma_1}{4\pi Gr^3} \right) + \left(\frac{1}{8\pi G} - \frac{b(r)}{8\pi Gr} \right) F''(r) \\
 &- \frac{f(R(r))}{16\pi G} + \frac{\Lambda}{8\pi G}, \tag{4.28}
 \end{aligned}$$

$$\begin{aligned}
 \rho + P_r + 2P_t &= F'(r) \left(-\frac{b'(r)}{16\pi Gr} + \frac{\gamma_1 b(r)}{4\pi Gr^3} - \frac{7b(r)}{16\pi Gr^2} - \frac{\gamma_1}{4\pi Gr^2} + \frac{1}{2\pi Gr} \right) \\
 &+ \frac{F(r)b'(r)}{4\pi Gr^2} + \left(\frac{1}{8\pi G} - \frac{b(r)}{8\pi Gr} \right) F''(r) - \frac{f(R(r))}{8\pi G} + \frac{\Lambda}{4\pi G} \\
 &- \frac{\gamma}{4\pi Gr}. \tag{4.29}
 \end{aligned}$$

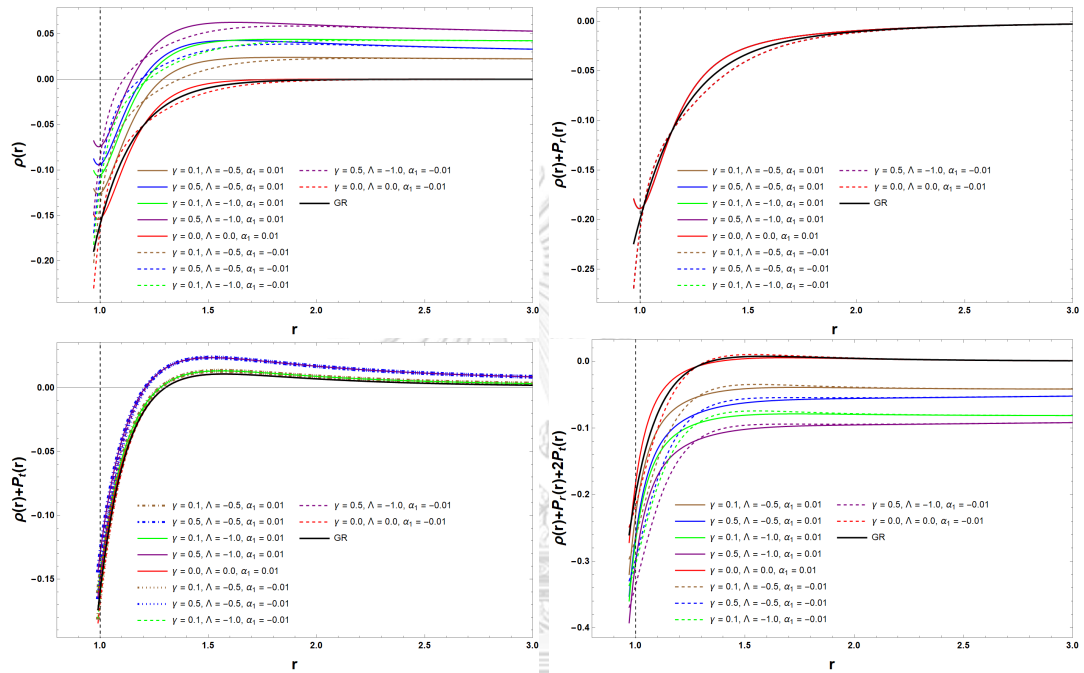


Figure 4.6: Figures illustrate the variation of ρ , $\rho + P_r$, $\rho + P_t$, $\rho + P_r + 2P_t$ as a function of r with $\Phi(r) = \gamma_1/r$. Here we have used $\alpha_1 = \pm 0.01$, $n = 2$, $\alpha = 5.0$, $r_0 = 1$, $G = 1$, $\gamma_1 = 1.0$ and various values of γ and Λ .

Table 4.2: Table shows a summary of energy/pressure conditions for $\Phi(r) = \gamma_1/r, n = 2, \alpha = 5.0, r_0 = 1, G = 1, \gamma_1 = 1.0, \gamma = 0.5,$ and $\Lambda = -1.0$.

No.	Terms	$\alpha_1 = 0.1$	$\alpha_1 = -0.1$
1	ρ	$\geq 0,$ for $r \in [1.2, \infty)$ $< 0,$ for $r \in [1.0, 1.2)$	$\geq 0,$ for $r \in [1.02, 1.25] \cup [1.45, \infty)$ $< 0,$ for $r \in [1.0, 1.02) \cup (1.25, 1.45)$
2	$\rho + P_r$	$\geq 0,$ for $r \in [1.25, \infty)$ $< 0,$ for $r \in [1.0, 1.25)$	$< 0,$ for $\forall r$
3	$\rho + P_t$	$\geq 0,$ for $r \in [1.15, \infty)$ $< 0,$ for $r \in [1.0, 1.15)$	$\geq 0,$ for $r \in [1.3, \infty)$ $< 0,$ for $r \in [1.0, 1.3)$
4	$\rho + P_r + 2P_t$	$\geq 0,$ for $r \in [1.02, 1.12]$ $< 0,$ for $r \in [1.0, 1.02) \cup (1.12, \infty)$	$< 0,$ for $\forall r$
5	$\rho - P_r $	$\geq 0,$ for $r \in [1.22, 1.9]$ $< 0,$ for $r \in [1.0, 1.22) \cup (1.9, \infty)$	$< 0,$ for $\forall r$
6	$\rho - P_t $	$< 0,$ for $\forall r$	$< 0,$ for $\forall r$

For the red-shift function of the wormhole metric as $\Phi(r) = 1/r$, there are still three main cases of traversable wormholes categorized by the strength of Starobinsky model; GR ($\alpha = 0$), positive α , and negative α .

Let consider Fig.4.5 ($\Phi(r) = 1/r$ and $\alpha_1 = \pm 0.1$). The first case is the traversable wormhole in GR with $\Phi(r) = 1/r$ which are demonstrated in the black solid lines. It violates WEC, NEC and SEC for all range from its throat to the cosmological horizon.

The second case in Fig.4.5 is the modified gravity with dRGT and Starobinsky models with $\alpha_1 = \pm 0.1$ represented in color solid lines. Since the red-shift function is inversely proportional to r , the amount of negative energy density and

negative $\rho + P_r$ reduce significantly near the throat compared to the constant red-shift function. Additionally the negative region of energy density is reduced by the increasing value of γ and the decreasing value of Λ . However, those parameters do not effect on the negative zone of $\rho + P_r$. $\rho + P_t$ is negative at the throat but increases as distance increases until reaching the top before reducing and converging to positive constant. Λ does not effect the region but γ plays a major role to reduce the negative region. While $\rho + P_r + 2P_t$ has an opposite effect of dRGT and Starobinsky from the energy density because $\rho + P_r + 2P_t$ has more negative region for more positive γ and more negative Λ .

For the last case in Fig.4.5, the modified gravity with dRGT and Starobinsky models with $\alpha_1 = -0.1$ is represented in color dashed lines. All results for this case look like upside down when compared to $\alpha_1 = 0.1$. The energy density has two negative regions; around the throat and the further region. The region reduces when the value of γ increases and the value of Λ decreases. Note that if γ is high or Λ is low enough, there would be only one negative energy density region which is the one with the throat. $\rho + P_r$ is negative for all region of spacetime regardless of dRGT parameters. $\rho + P_t$ is negative from the throat and increases as the distance increases which converges to positive constant. The negative region reduces as the value of γ increases. At the throat, the value of $\rho + P_t$ for $\alpha_1 = -0.1$ is more negative than the value of $\rho + P_t$ for $\alpha_1 = 0.1$. $\rho + P_r + 2P_t$ is negative near the throat and increases as distance increases. When γ decreases and Λ increases enough, the negative region of $\rho + P_r + 2P_t$ will be limited around the throat.

Now consider Fig.4.6 ($\alpha_1 = \pm 0.01$). It is obvious that the less magnitude

of α is, the less fluctuations in ρ , $\rho + P_r$, $\rho + P_t$ and $\rho + P_r + 2P_t$ are. The energy density is an increasing function which is negative at the throat. The negative region decreases as the value of γ increases or the value of Λ decreases. While $\rho + P_r$ is negative for all spacetime region where the dRGT parameters do not effect the characteristic at all. The value of $\rho + P_t$ is negative at the throat and increases to be positive as the distance increases. The violation region reduces with the increase of γ and the decrease of Λ . However, the dRGT and Starobinsky models provide the opposite results on $\rho + P_r + 2P_t$ where it is more negative with the increase of γ and the decrease of Λ .

The third case: $\Phi(r) = \log\left(1 + \frac{\gamma_2}{r}\right)$

With the shape function from Eq. (4.11) and $\Phi(r) = \log\left(1 + \frac{\gamma_2}{r}\right)$, we find [57]

$$\begin{aligned} \rho = & F'(r) \left(\frac{b'(r)}{16\pi Gr} - \frac{\gamma_2 b(r)}{8\pi Gr^3 \left(\frac{\gamma_2}{r} + 1\right)} + \frac{3b(r)}{16\pi Gr^2} + \frac{\gamma_2}{8\pi Gr^2 \left(\frac{\gamma_2}{r} + 1\right)} - \frac{1}{4\pi Gr} \right) \\ & + F(r) \left(\frac{\gamma_2 b'(r)}{16\pi Gr^3 \left(\frac{\gamma_2}{r} + 1\right)} - \frac{\gamma_2 b(r)}{16\pi Gr^4 \left(\frac{\gamma_2}{r} + 1\right)} \right) + \left(\frac{b(r)}{8\pi Gr} - \frac{1}{8\pi G} \right) F''(r) \\ & + \frac{f(R(r))}{16\pi G} - \frac{\Lambda}{8\pi G} + \frac{\gamma}{4\pi Gr}, \end{aligned} \quad (4.30)$$

$$\begin{aligned} P_r = & F(r) \left(-\frac{\gamma_2(b'(r) + 4)}{16\pi Gr^3 \left(\frac{\gamma_2}{r} + 1\right)} + \frac{b'(r)}{8\pi Gr^2} + \frac{5\gamma_2 b(r)}{16\pi Gr^4 \left(\frac{\gamma_2}{r} + 1\right)} - \frac{b(r)}{8\pi Gr^3} \right) \\ & + F'(r) \left(\frac{\gamma_2 b(r)}{8\pi Gr^3 \left(\frac{\gamma_2}{r} + 1\right)} - \frac{b(r)}{4\pi Gr^2} - \frac{\gamma_2}{8\pi Gr^2 \left(\frac{\gamma_2}{r} + 1\right)} + \frac{1}{4\pi Gr} \right) \\ & - \frac{f(R(r))}{16\pi G} + \frac{\Lambda}{8\pi G} - \frac{\gamma}{4\pi Gr}, \end{aligned} \quad (4.31)$$

$$\begin{aligned}
P_t = & F'(r) \left(-\frac{b'(r)}{16\pi Gr} + \frac{\gamma_2 b(r)}{8\pi Gr^3 \left(\frac{\gamma_2}{r} + 1\right)} - \frac{3b(r)}{16\pi Gr^2} - \frac{\gamma_2}{8\pi Gr^2 \left(\frac{\gamma_2}{r} + 1\right)} + \frac{1}{4\pi Gr} \right) \\
& + F(r) \left(\frac{b'(r)}{16\pi Gr^2} - \frac{\gamma_2 b(r)}{8\pi Gr^4 \left(\frac{\gamma_2}{r} + 1\right)} + \frac{b(r)}{16\pi Gr^3} + \frac{\gamma_2}{8\pi Gr^3 \left(\frac{\gamma_2}{r} + 1\right)} \right) \\
& + \left(\frac{1}{8\pi G} - \frac{b(r)}{8\pi Gr} \right) F''(r) - \frac{f(R(r))}{16\pi G} + \frac{\Lambda}{8\pi G} - \frac{\gamma}{8\pi Gr}. \tag{4.32}
\end{aligned}$$

The combinations of Eqs. (4.30 - 4.32) yield the following relations among ρ , P_r , and P_t :

$$\begin{aligned}
\rho + P_r = & F'(r) \left(\frac{b'(r)}{16\pi Gr} - \frac{b(r)}{16\pi Gr^2} \right) + F(r) \left(\frac{b'(r)}{8\pi Gr^2} + \frac{\gamma_2 b(r)}{4\pi Gr^4 \left(\frac{\gamma_2}{r} + 1\right)} - \frac{b(r)}{8\pi Gr^3} \right. \\
& \left. - \frac{\gamma_2}{4\pi Gr^3 \left(\frac{\gamma_2}{r} + 1\right)} \right) + \left(\frac{b(r)}{8\pi Gr} - \frac{1}{8\pi G} \right) F''(r), \tag{4.33}
\end{aligned}$$

$$\begin{aligned}
\rho + P_t = & F(r) \left(\frac{\gamma_2 b'(r)}{16\pi Gr^3 \left(\frac{\gamma_2}{r} + 1\right)} + \frac{b'(r)}{16\pi Gr^2} - \frac{3\gamma_2 b(r)}{16\pi Gr^4 \left(\frac{\gamma_2}{r} + 1\right)} + \frac{b(r)}{16\pi Gr^3} \right. \\
& \left. + \frac{\gamma_2}{8\pi Gr^3 \left(\frac{\gamma_2}{r} + 1\right)} \right) + \frac{\gamma}{8\pi Gr}, \tag{4.34}
\end{aligned}$$

$$\begin{aligned}
\rho - |P_r| = & - \left| -\frac{\gamma}{4G\pi r} + \frac{\Lambda}{8G\pi} - \frac{f(R(r))}{16G\pi} + F(r) \left(\frac{5\gamma_2 b(r)}{16G\pi r^4 \left(\frac{\gamma_2}{r} + 1\right)} - \frac{b(r)}{8G\pi r^3} \right. \right. \\
& - \frac{\gamma_2 b'(r)}{16G\pi r^3 \left(\frac{\gamma_2}{r} + 1\right)} + \frac{b'(r)}{8G\pi r^2} - \frac{\gamma_2}{4G\pi r^3 \left(\frac{\gamma_2}{r} + 1\right)} \left. \right) + \left(\frac{\gamma_2 b(r)}{8G\pi r^3 \left(\frac{\gamma_2}{r} + 1\right)} \right. \\
& \left. - \frac{b(r)}{4G\pi r^2} + \frac{1}{4G\pi r} - \frac{\gamma_2}{8G\pi r^2 \left(\frac{\gamma_2}{r} + 1\right)} \right) F'(r) \left| + F'(r) \left(\frac{b'(r)}{16\pi Gr} \right. \right. \\
& \left. - \frac{\gamma_2 b(r)}{8\pi Gr^3 \left(\frac{\gamma_2}{r} + 1\right)} + \frac{3b(r)}{16\pi Gr^2} + \frac{\gamma_2}{8\pi Gr^2 \left(\frac{\gamma_2}{r} + 1\right)} - \frac{1}{4\pi Gr} \right) \\
& + F(r) \left(\frac{\gamma_2 b'(r)}{16\pi Gr^3 \left(\frac{\gamma_2}{r} + 1\right)} - \frac{\gamma_2 b(r)}{16\pi Gr^4 \left(\frac{\gamma_2}{r} + 1\right)} \right) \\
& + \left(\frac{b(r)}{8\pi Gr} - \frac{1}{8\pi G} \right) F''(r) + \frac{f(R(r))}{16\pi G} - \frac{\Lambda}{8\pi G} + \frac{\gamma}{4\pi Gr}, \tag{4.35}
\end{aligned}$$

$$\begin{aligned}
\rho - |P_t| = & - \left| -\frac{\gamma}{8G\pi r} + \frac{\Lambda}{8G\pi} - \frac{f(R(r))}{16G\pi} + F(r) \left(-\frac{\gamma_2(b(r)+r)}{8G\pi r^4 \left(\frac{\gamma_2}{r} + 1\right)} \right. \right. \\
& + \left. \frac{b(r)}{16G\pi r^3} + \frac{b'(r)}{16G\pi r^2} \right) + F'(r) \left(\frac{\gamma_2(b(r)+r)}{8G\pi r^3 \left(\frac{\gamma_2}{r} + 1\right)} - \frac{3b(r)}{16G\pi r^2} \right. \\
& - \left. \frac{b'(r)}{16G\pi r} + \frac{1}{4G\pi r} \right) F'(r) + \left(\frac{1}{8G\pi} - \frac{b(r)}{8G\pi r} \right) F''(r) \Big| \\
& + F'(r) \left(\frac{b'(r)}{16\pi Gr} - \frac{\gamma_2(b(r)-r)}{8\pi Gr^3 \left(\frac{\gamma_2}{r} + 1\right)} + \frac{3b(r)}{16\pi Gr^2} - \frac{1}{4\pi Gr} \right) \\
& + F(r) \left(\frac{\gamma_2 b'(r)}{16\pi Gr^3 \left(\frac{\gamma_2}{r} + 1\right)} - \frac{\gamma_2 b(r)}{16\pi Gr^4 \left(\frac{\gamma_2}{r} + 1\right)} \right) \\
& + \left(\frac{b(r)}{8\pi Gr} - \frac{1}{8\pi G} \right) F''(r) + \frac{f(R(r))}{16\pi G} - \frac{\Lambda}{8\pi G} + \frac{\gamma}{4\pi Gr}, \quad (4.36)
\end{aligned}$$

$$\begin{aligned}
\rho + 2P_t = & F'(r) \left(-\frac{b'(r)}{16\pi Gr} + \frac{\gamma_2(b(r)+r)}{8\pi Gr^3 \left(\frac{\gamma_2}{r} + 1\right)} - \frac{3b(r)}{16\pi Gr^2} + \frac{1}{4\pi Gr} \right) \\
& + F(r) \left(\frac{\gamma_2 b'(r)}{16\pi Gr^3 \left(\frac{\gamma_2}{r} + 1\right)} + \frac{b'(r)}{8\pi Gr^2} - \frac{5\gamma_2 b(r)}{16\pi Gr^4 \left(\frac{\gamma_2}{r} + 1\right)} \right. \\
& + \left. \frac{b(r)}{8\pi Gr^3} + \frac{\gamma_2}{4\pi Gr^3 \left(\frac{\gamma_2}{r} + 1\right)} \right) + \left(\frac{1}{8\pi G} - \frac{b(r)}{8\pi Gr} \right) F''(r) \\
& - \frac{f(R(r))}{16\pi G} + \frac{\Lambda}{8\pi G}, \quad (4.37)
\end{aligned}$$

$$\begin{aligned}
\rho + P_r + 2P_t = & F'(r) \left(-\frac{b'(r)}{16\pi Gr} + \frac{\gamma_2(b(r)-r)}{4\pi Gr^3 \left(\frac{\gamma_2}{r} + 1\right)} - \frac{7b(r)}{16\pi Gr^2} + \frac{1}{2\pi Gr} \right) \\
& + \frac{F(r)b'(r)}{4\pi Gr^2} + \left(\frac{1}{8\pi G} - \frac{b(r)}{8\pi Gr} \right) F''(r) - \frac{f(R(r))}{8\pi G} \\
& + \frac{\Lambda}{4\pi G} - \frac{\gamma}{4\pi Gr}. \quad (4.38)
\end{aligned}$$

In this case, the red-shift function in the wormhole metric is $\Phi(r) = \log(1 + \frac{\gamma_2}{r})$. There are still three main cases of traversable wormholes categorized by the strength of Starobinsky model; GR ($\alpha = 0$), positive α , and negative α .

Let consider Fig.4.7 ($\Phi(r) = \log(1 + \frac{\gamma_2}{r})$ and $\alpha_1 = \pm 0.1$). The first case is the traversable wormhole in GR which are illustrated in the black solid lines of ρ , $\rho + P_r$, $\rho + P_t$, and $\rho + P_r + 2P_t$. It violates WEC, NEC and SEC for all range

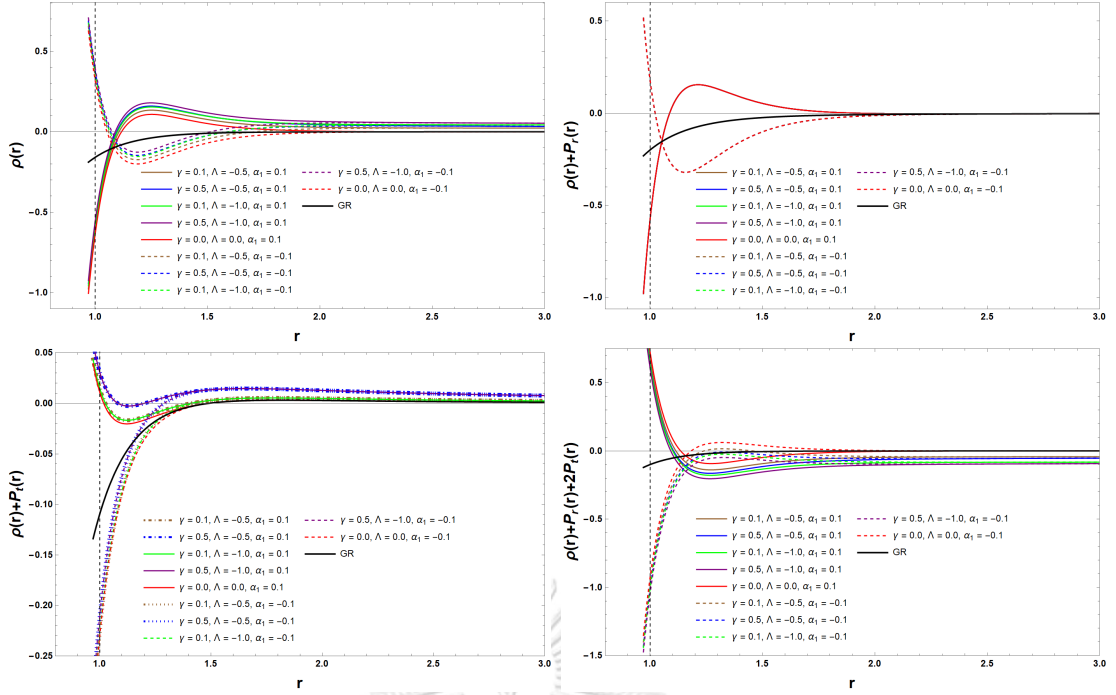


Figure 4.7: Figures illustrate the variation of ρ , $\rho + P_r$, $\rho + P_t$, $\rho + P_r + 2P_t$ as a function of r with $\Phi(r) = \log(1 + \frac{\gamma_2}{r})$. Here we have used $\alpha_1 = \pm 0.1$, $n = 2$, $\alpha = 5.0$, $r_0 = 1$, $G = 1$ and $\gamma_2 = 1.0$ and various values of γ and Λ .

from its throat to the cosmological horizon.

The second case in Fig.4.7 is the modified gravity with dRGT and Starobinsky models with $\alpha_1 = 0.1$ represented in color solid lines. The negative regions of ρ and $\rho + P_r$ are limited only near the throat where this region is reduced by increasing γ and decreasing Λ . Note that the dRGT parameters do not effect the negative region of $\rho + P_r$. $\rho + P_t$ is positive at the throat and decreases as moving further from the throat before increasing and converging to positive constants. The negative region is depleted with more positive γ and more negative Λ enough. $\rho + P_r + 2P_t$ is a decrease function with positive value at the throat. It converges to a negative value as distance increases. The trend of $\rho + P_r + 2P_t$ is contradict

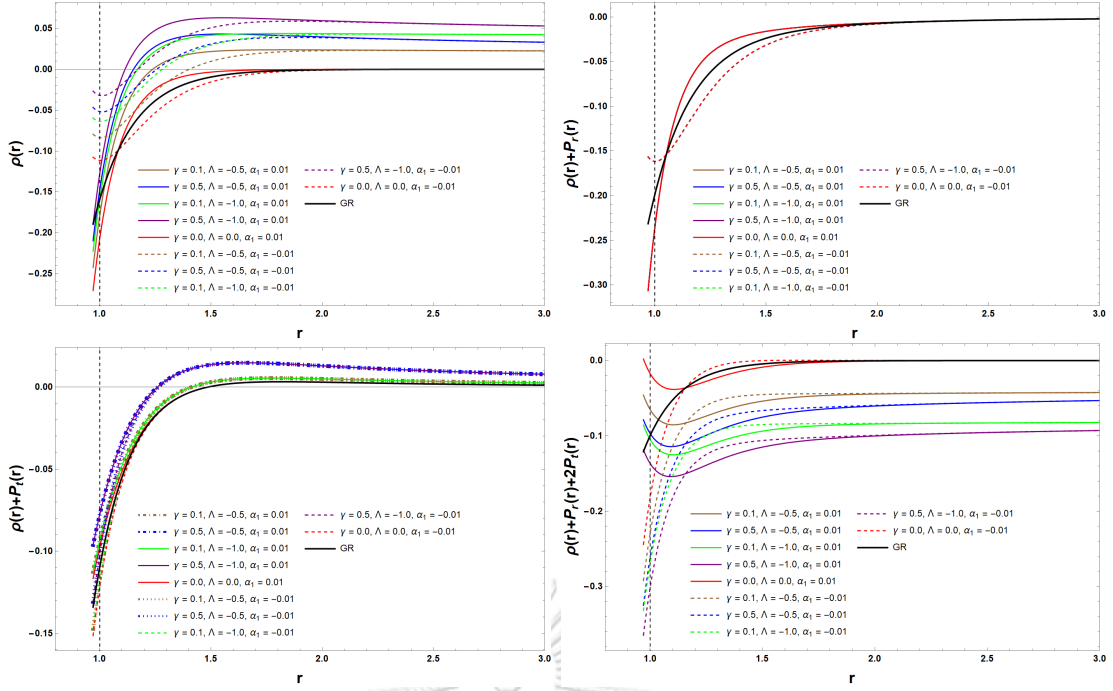


Figure 4.8: Figures illustrate the variation of ρ , $\rho + P_r$, $\rho + P_t$, $\rho + P_r + 2P_t$ as a function of r with $\Phi(r) = \log(1 + \frac{\gamma_2}{r})$. Here we have used $\alpha_1 = \pm 0.01$, $n = 2$, $\alpha = 5.0$, $r_0 = 1$, $G = 1$, and $\gamma_2 = 1.0$.

to the energy density since it has longer negative region with more positive γ and more negative Λ .

For the last case in Fig.4.7, $\alpha_1 = -0.1$ case is represented in color dashed lines. The characteristics of ρ , $\rho + P_r$, $\rho + P_t$ and $\rho + P_r + 2P_t$ are upside down compared to $\alpha_1 = 0.1$. The energy density and $\rho + P_r$ have negative regions further from the throat and converges to positive value as distance increases. The negative region of energy density is reduced with more positive γ and more negative Λ while $\rho + P_r$ is not effected by the variation of dRGT parameters. $\rho + P_t$ is negative at the throat and increases over zero as distance increases before converging to some positive constant. The negative region is reduced with more positive γ where Λ

Table 4.3: Table shows a summary of energy/pressure conditions for $\Phi(r) = \log(1 + \gamma_2/r)$, $n = 2$, $\alpha = 5.0$, $r_0 = 1$, $G = 1$, $\gamma_2 = 1.0$, $\gamma = 0.5$, and $\Lambda = -1.0$.

No.	Terms	$\alpha_1 = 0.1$	$\alpha_1 = -0.1$
1	ρ	≥ 0 , for $r \in [1.07, \infty)$ < 0 , for $r \in [1.0, 1.07)$	≥ 0 , for $r \in [1.0, 1.05] \cup [1.50, \infty)$ < 0 , for $r \in (1.05, 1.5)$
2	$\rho + P_r$	≥ 0 , for $r \in [1.07, \infty]$ < 0 , for $r \in [1.0, 1.07)$	≥ 0 , for $r \in [1.0, 1.02]$ < 0 , for $r \in (1.02, \infty)$
3	$\rho + P_t$	≥ 0 , for $r \in [1.0, 1.07] \cup [1.2, \infty)$ < 0 , for $r \in (1.07, 1.2)$	≥ 0 , for $r \in [1.3, \infty)$ < 0 , for $r \in [1.0, 1.3)$
4	$\rho + P_r + 2P_t$	≥ 0 , for $r \in [1.0, 1.1]$ < 0 , for $r \in (1.1, \infty)$	< 0 , for $\forall r$
5	$\rho - P_r $	≥ 0 , for $r \in [1.07, \infty]$ < 0 , for $r \in [1.0, 1.07)$	≥ 0 , for $r \in [1.0, 1.02]$ < 0 , for $r \in (1.02, \infty)$
6	$\rho - P_t $	≥ 0 , for $r \in [1.2, \infty)$ < 0 , for $r \in [1.0, 1.20)$	≥ 0 , for $r \in [1.5, \infty)$ < 0 , for $r \in [1.0, 1.5)$

does not effect much. However, the parameter sets that reduce the negative region for energy density support the negative region for $\rho + P_r + 2P_t$.

Now consider Fig.4.8 ($\alpha_1 \pm 0.01$). Overall, the less magnitude of α_1 makes ρ , $\rho + P_r$, $\rho + P_t$ and $\rho + P_r + 2P_t$ negative near the throat. For example, the energy density is negative for all choices of dRGT parameters. Even if it increases over zero for further distance and converges to positive constant. The negative region decreases as the more positive γ or the more negative Λ . While $\rho + P_r$ is below zero for all range and has no effect on dRGT parameters. $\rho + P_t$ is negative at

the throat for all cases and increases over zero as moving further from the throat which finally converges to some positive constant. The more positive γ reduces the negative region for $\rho + P_t$ while Λ does not involve. $\rho + P_r + 2P_t$ is negative for all range and has the opposite effect of dRGT parameters contrasting to the energy density.

4.2 The thin-shell Wormhole in dRGT massive gravity theory

In this section, we find the solution of the thin-shell wormhole in the dRGT spacetime [58]. As we discussed in section (3.2), thin-shell wormhole solution can be constructed by gluing together two boundaries of spacetimes. Here we apply the same trick to the case of massive gravity in which the ghost-free massive gravity terms in Eq. (2.96) is added in to the total action. Consider two spacetime manifolds denoted by \mathcal{M}_\pm with boundary $\partial\mathcal{M}_\pm$. Suppose the two boundaries are connected (or glued) by the hypersurface Σ . The total action can be written as [58]

$$\begin{aligned}
S_{\text{total}} = & \int_{\mathcal{M}_+} d^4x \sqrt{-g^+} \left(\frac{1}{16\pi G} (R^+ + m_g^2 \mathcal{U}(g^+, \phi^a)) + \mathcal{L}_{\text{matter}}^+ \right) \\
& + \frac{1}{8\pi G} \int_{\partial\mathcal{M}_+} d^3y \sqrt{-h^+} K^+ \\
& + \int_{\mathcal{M}_-} d^4x \sqrt{-g^-} \left(\frac{1}{16\pi G} (R^- + m_g^2 \mathcal{U}(g^-, \phi^a)) + \mathcal{L}_{\text{matter}}^- \right) \\
& + \frac{1}{8\pi G} \int_{\partial\mathcal{M}_-} d^3y \sqrt{-h^-} K^- \\
& + \int_{\Sigma} d^3y \sqrt{-h} \mathcal{L}_{\text{matter}}^\Sigma,
\end{aligned} \tag{4.39}$$

where $\mathcal{L}_{\text{matter}}^\Sigma = \mathcal{L}_f^\Sigma + \mathcal{L}_g^\Sigma$ contains two types of fluids (perfect fluid, \mathcal{L}_f^Σ and massive gravity fluid, \mathcal{L}_g^Σ) which are localized on the hypersurface. The line element is still the same form as Eq. (3.19) in GR, however, $f(r)$ is the vacuum solution of dRGT massive gravity in Eq. (2.113)

$$f(r) = 1 - \frac{2GM}{r} - \frac{\Lambda r^2}{3} + \gamma r + \zeta.$$

In the next step, we apply the variational principle to obtain the equation of motion

$$\begin{aligned} \delta S_{\text{total}} = & \int_{\mathcal{M}_+} d^4x \sqrt{-g^+} \left(\frac{1}{16\pi G} (G_{\alpha\beta}^+ + m_g^2 X_{\alpha\beta}^+) + T_{\alpha\beta}^{(f),+} \right) \delta g_+^{\alpha\beta} \\ & + \int_{\partial\mathcal{M}^+} d^3y \sqrt{-h^+} \frac{1}{8\pi G} (K_{ab}^+ - h_{ab}^+ K^+) \delta h_+^{ab} \\ & + \int_{\mathcal{M}_-} d^4x \sqrt{-g^-} \left(\frac{1}{16\pi G} (G_{\alpha\beta}^- + m_g^2 X_{\alpha\beta}^-) + T_{\alpha\beta}^{(f),-} \right) \delta g_-^{\alpha\beta} \\ & + \int_{\partial\mathcal{M}_-} d^3y \sqrt{-h^-} \frac{1}{8\pi G} (K_{ab}^- - h_{ab}^- K^-) \delta h_-^{ab} \\ & - \int_{\Sigma} d^3y \sqrt{-h} (t_{ab} + Y_{ab}) \delta h^{ab}, \end{aligned} \quad (4.40)$$

where t_{ab} is the energy momentum tensor of the wormhole source defined in Eq. (3.32) and Y_b^a is the massive gravity fluid tensor

$$Y_b^a = -\frac{2}{\sqrt{-h}} \frac{\delta}{\delta h_b^a} \left(\sqrt{-h} \mathcal{L}_g^\Sigma \right) \equiv (\rho_g + p_g^{(\perp)}) u^a u_b + p_g^{(\perp)} h_b^a, \quad (4.41)$$

where ρ_g and $p_g^{(\perp)}$ are the energy density and pressure in tangential directions of the massive gravity fluid. To analyze the thin-shell wormhole, we consider the equation of motion on the hypersurface Σ and boundaries $\partial\mathcal{M}_\pm$. Varying the total

action with respect to the induced metric h^{ab} provides [58]

$$\begin{aligned} \frac{\delta S_{\text{total}}}{\delta h^{ab}} &= \int_{\partial\mathcal{M}_+} d^3y \sqrt{-h^+} \frac{1}{8\pi G} (K_{cd}^+ - h_{cd}^+ K^+) \frac{\delta h_{ab}^+}{\delta h^{ab}} \\ &+ \int_{\partial\mathcal{M}_-} d^3y \sqrt{-h^-} \frac{1}{8\pi G} (K_{cd}^- - h_{cd}^- K^-) \frac{\delta h_{ab}^-}{\delta h^{ab}} \\ &- \int_{\Sigma} d^3y \sqrt{-h} (t_{ab} + Y_{ab}). \end{aligned} \quad (4.42)$$

With the help of the choice of normal vectors (in both spacetime and on thin-shell), the extrinsic curvature tensor from Eq. (3.34) and Eq. (3.35) and the continuity of h_{ab}^{\pm} on the boundaries, we finally obtain the junction condition of the thin-shell wormhole in the dRGT theory

$$\delta_b^a \Delta K - \Delta K_b^a = 8\pi G S_b^a, \quad (4.43)$$

where the new effective energy momentum tensor S_b^a on the thin-shell is defined by [58]

$$S_b^a \equiv t_b^a + Y_b^a. \quad (4.44)$$

Furthermore, it is very convenient to represent the S_b^a tensor in the matrix form

$$S_b^a \equiv \begin{pmatrix} -\rho_{\text{eff.}} & 0 & 0 \\ 0 & P_{\text{eff.}} & 0 \\ 0 & 0 & P_{\text{eff.}} \end{pmatrix} = \begin{pmatrix} -\rho - \rho_g & 0 & 0 \\ 0 & P_t + p_g^{(\perp)} & 0 \\ 0 & 0 & P_t + p_g^{(\perp)} \end{pmatrix}, \quad (4.45)$$

where the explicit forms of the ρ_g and $p_g^{(\perp)} = p_g^{(\theta, \phi)}$ are given in Eq. (2.117) and Eq. (2.119). We will see in the latter that the equation of motion of the dRGT massive gravity wormholes takes very simple form like the standard GR case with two types of fluids. The components of the effective momentum tensor S_b^a in

Eq. (4.44) are given by

$$\begin{aligned} S_\tau^\tau &= -\rho_{\text{eff.}} = -\rho - \rho_g(a) \\ &= -\rho + \frac{1}{8\pi G} \left(\frac{2\gamma}{a} - \Lambda \right), \end{aligned} \quad (4.46)$$

$$\begin{aligned} S_\theta^\theta &= S_\phi^\phi = P_{\text{eff.}} = P_t + p_g^{(\perp)}(a) \\ &= P_t + \frac{1}{8\pi G} \left(\frac{\gamma}{a} - \Lambda \right), \end{aligned} \quad (4.47)$$

where we use the definitions of the energy density, radial and tangent pressure from Eq. (2.117), Eq. (2.118), and Eq. (2.119), respectively.

The non-trivial components of the extrinsic curvature tensor, K_b^a , are the same form in Eq. (3.41) and Eq. (3.42) with $f(a)$ from Eq. (2.113) in dRGT massive gravity theory. The $(\tau\tau)$ component of the junction condition of the thin-shell wormhole in Eq.(4.43) reads

$$\frac{2}{a}(\sqrt{f + \dot{a}^2}) = -8\pi G\rho + \left(\frac{2\gamma}{a} - \Lambda \right). \quad (4.48)$$

On the other hand, the angular component of Eq.(4.43) is given by

$$\frac{1}{\sqrt{f + \dot{a}^2}}(2\ddot{a} + f') = 8\pi G P_t + \left(\frac{\gamma}{a} - \Lambda \right). \quad (4.49)$$

The relation between the energy density and pressure from Eq. (4.48) and Eq. (4.49) as follows:

$$\frac{d}{d\tau}(\rho a) + P_t \frac{da}{d\tau} + \frac{\gamma \dot{a}}{8\pi G a} = 0. \quad (4.50)$$

It is also written in terms of the first order derivative of ρ with respect to a as

$$\frac{d\rho}{da} = -\frac{1}{a}(\rho + P_t) - \frac{\gamma}{8\pi G a^2}. \quad (4.51)$$

The second order derivative of ρ with respect to a becomes

$$\frac{d^2\rho}{da^2} = \left(\frac{\rho + P_t}{a^2}\right) \left(2 + \frac{dP_t}{d\rho}\right) + \frac{3\gamma}{8\pi G a^3} + \frac{dP_t}{d\rho} \left(\frac{\gamma}{8\pi G a^3}\right). \quad (4.52)$$

At the static throat a_0 , the solutions of the energy density $\rho(a_0)$ and pressure of the tangential direction $P_t(a_0)$ are determined by Eq. (4.48) and Eq. (4.49)

$$\rho_0 = -\frac{\sqrt{f(a_0)}}{4\pi G a_0} + \frac{1}{8\pi G} \left(\frac{2\gamma}{a_0} - \Lambda\right) \quad (4.53)$$

$$P_{t(0)} = \frac{1}{8\pi G} \left(\frac{f'(a_0)}{\sqrt{f(a_0)}} - \left(\frac{\gamma}{a_0} - \Lambda\right)\right). \quad (4.54)$$

To investigate the stability of the dRGT thin-shell wormhole, we apply the technique in the subsection 3.2.5. Assuming the static throat of the thin-shell wormhole is located $a = a_0$, the following relation must be satisfied,

$$0 < V''(a_0) = \frac{1}{2}f''(a_0) + \frac{dP_t}{d\rho} \left(-2G(P_t + \rho)\pi\Lambda - 16G^2\pi^2\rho(P_t + \rho) + \frac{4G\pi\gamma(P_t + \rho)}{a_0}\right) - 16G^2P_t^2\pi^2 + 4GP_t\pi\Lambda - \frac{1}{4}\Lambda^2. \quad (4.55)$$

To analyse the function $f(r)$ in Eq. (2.113) from the dRGT massive gravity, we consider the horizons of the metric tensor as the roots of function $f(r)$ which is the cubic polynomial problem. For convenience, we define

$$\begin{aligned} \tilde{f}(r) &\equiv r f(r) \\ &= Ar^3 + Br^2 + Cr + D, \end{aligned} \quad (4.56)$$

where $A = -\frac{\Lambda}{3}$, $B = \gamma$, $C = (1 + \zeta)$ and $D = -2GM$. The function \tilde{f} has three distinct, real roots if and only if

$$-27A^2D^2 + 18ABCD - 4AC^3 - 4B^3D + B^2C^2 > 0 \quad (4.57)$$

or

$$\gamma^2 + 8GM\gamma^3 + \frac{4\Lambda}{3} + 12GM\gamma\Lambda - 12G^2M^2\Lambda^2 > 0. \quad (4.58)$$

For de-Sitter ($\Lambda > 0$) or closed spacetime, the function \tilde{f} still has 3 distinct and real roots since the negative term is small ($\Lambda^2 \ll 1$). For anti de-Sitter ($\Lambda < 0$) or open spacetime, only the first two terms are positive and compensate the other negative terms, then the function \tilde{f} holds the properties with high value of γ and low value of Λ .

Now we consider the analytic solutions of roots in (r) by introducing a new variable

$$t = r + \frac{B}{3A}, \quad (4.59)$$

where the cubic equation in Eq. (4.56) can be rewritten as a depressed cubic equation that has no term in t^2 ,

$$\tilde{f}(t) = t^3 + \tilde{p}t + \tilde{q}, \quad (4.60)$$

where

$$\tilde{p} = \frac{3AC - B^2}{3A^2} = -\frac{3(\gamma^2 + \Lambda)}{\Lambda^2}, \quad (4.61)$$

$$\tilde{q} = \frac{2B^3 - 9ABC + 27A^2D}{27A^3} = -\frac{2\gamma^3 + 3\gamma\Lambda - 6GM\Lambda^2}{\Lambda^3}. \quad (4.62)$$

The real and distinct expressions of solutions to Eq. (4.60) can be obtained by using the cosines and arccosines as shown

$$\begin{aligned} t_k &= 2\sqrt{-\frac{\tilde{p}}{3}} \cos\left(\frac{1}{3} \arccos\left(\frac{3q}{2p}\sqrt{\frac{-3}{p}}\right) - \frac{2\pi k}{3}\right) \\ &= \frac{2\sqrt{\gamma^2 + \Lambda}}{\Lambda} \cos\left(\frac{1}{3} \cos^{-1}\left(\frac{1}{6} \left(3 \left(\frac{1}{\gamma^2 + \Lambda}\right)^{3/2} (2\gamma^3 + 3\gamma\Lambda - 6\Lambda^2GM) - 4\pi k\right)\right)\right), \end{aligned} \quad (4.63)$$

where $k = 1, 2, 3$. While the three distinct and real horizons are

$$r_k = t_k + \frac{\gamma}{\Lambda}. \quad (4.64)$$

According to the line element in Eq. (3.19) and embedding diagram in Eq. (3.27), $f(r)$ must hold the following relation,

$$0 < f(r) \leq 1. \quad (4.65)$$

The following parameters are tuned to satisfy the embedding diagram of the thin-shell wormholes. For thin-shell wormhole, we use the parameters given below:

$$G = 1, \Lambda = 0.0001, \gamma = 0.001, M = 1, \text{ and } \zeta = 0. \quad (4.66)$$

With these parameters, $f(r)$ satisfies the relation(4.65) and reaches zero at the event horizon $r_{\text{EH}} = 2.00$ and the cosmological horizon $r_{\text{CH}} = 187.93$. Moreover, according to the flaring-out condition $f'(r) > 0$, the throat radius has an upper limit which is called the the upper limit of flaring-out condition is $r_{\text{FO}} = 36.96$. Due to the UV cutoff from the dRGT massive gravity, the Vainshtein radius for the set of the thin-shell parameter in Eq. (4.66) is $r_V = (M/m_g^2)^{1/3} = 8.07$. The range that is below the Vainshtein radius r_V cannot be trusted without the UV completion. Therefore, the range of the static throat of thin-shell wormhole for this study case is

$$r_{\text{EH}} = 8.07 < a_0 \leq r_{\text{FO}} = 36.96, \quad (4.67)$$

where the range of the possible value of the static throat is in red shaded area of Fig. (4.9).

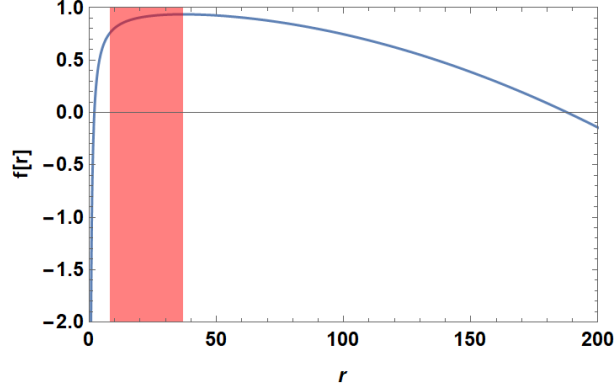


Figure 4.9: This figure represents the characteristic of function $f(r)$ with parameters $G = 1$, $\Lambda = 0.0001$, $\gamma = 0.001$, $M = 1$, and $\zeta = 0$. The red area represents the possible value of the static throat of thin-shell wormhole, $r_{\text{EH}} = 8.07 < a_0 \leq r_{\text{FO}} = 36.96$.

We analyze the energy conditions (NEC, WEC and SEC) of the linear model in the thin-shell wormhole in dRGT massive gravity. The energy conditions are expressed in terms of the effective energy density ($\rho_{\text{eff.}}$) and the effective pressure ($P_{\text{eff.}}$), defined in Eq. (4.46) and Eq. (4.47) respectively.

- I. Null energy condition is expressed in terms of energy density and pressure as follows:

$$\rho_{\text{eff.}} + P_{\text{eff.}} \geq 0, \quad (4.68)$$

which yields [58]

$$\begin{aligned} \rho_{\text{eff.}} + P_{\text{eff.}} &= \rho - \frac{1}{8\pi G} \left(\frac{2\gamma}{a} - \Lambda \right) + P_t + \frac{1}{8\pi G} \left(\frac{\gamma}{a} - \Lambda \right) \\ &= \rho + P_t - \frac{1}{8\pi G} \frac{\gamma}{a} \geq 0. \end{aligned} \quad (4.69)$$

II. Weak energy condition is given by

$$\rho_{\text{eff.}} \geq 0, \quad \rho_{\text{eff.}} + P_{\text{eff.}} \geq 0, \quad (4.70)$$

which gives the following result for the thin-shell wormholes in the dRGT massive gravity [58]

$$\rho_{\text{eff.}} = \rho - \frac{1}{8\pi G} \left(\frac{2\gamma}{a} - \Lambda \right) \geq 0, \quad (4.71)$$

III. Strong energy condition is governed by

$$\rho_{\text{eff.}} + 3P_{\text{eff.}} \geq 0, \quad \rho_{\text{eff.}} + P_{\text{eff.}} \geq 0, \quad (4.72)$$

which gives the following result for the thin-shell wormholes in the dRGT massive gravity [58]

$$\begin{aligned} \rho_{\text{eff.}} + 3P_{\text{eff.}} &= \rho - \frac{1}{8\pi G} \left(\frac{2\gamma}{a} - \Lambda \right) + 3P_t + \frac{3}{8\pi G} \left(\frac{\gamma}{a} - \Lambda \right) \\ &= \rho + 3P_t + \frac{1}{8\pi G} \left(\frac{\gamma}{a} - 2\Lambda \right) \geq 0. \end{aligned} \quad (4.73)$$

Next we assume the four fluid models for studying the stability of the dRGT wormhole: (1) a linear model, (2) a Chaplygin gas model, (3) a generalized Chaplygin gas model and (4) a logarithm model.

4.2.1 Linear model

We start analyzing the stability of the thin-shell wormhole in dRGT [49]:

$$P_t(\rho) = \epsilon_0 \rho, \quad (4.74)$$

where ϵ_0 is dimensionless parameter. It is easy to show that

$$\frac{dP_t}{d\rho} = \epsilon_0. \quad (4.75)$$

Notice that the change in the pressure on the energy density is a constant. Moreover, the throat of the wormhole basically locates between the event and the cosmological horizons. After substituting the above results into the stability condition (4.55), we find [58]

$$0 < V''(a_0) = \frac{1}{2}f''(a_0) - \frac{1}{4}\left(\Lambda^2 + 8\pi(\epsilon_0 - 1)\epsilon_0\Lambda\rho + 64\pi^2\epsilon_0(1 + 2\epsilon_0)\rho^2\right) + \frac{4\pi\gamma\epsilon_0(\epsilon_0 + 1)}{a_0}, \quad (4.76)$$

where $f''(a_0) = -\frac{M}{a_0^3} - \frac{2\Lambda}{3}$. The thin-shell wormhole for the linear model will be stable if the relation (4.76) holds. For the linear model, the more positive value of γ increases the value of $V''(a_0)$, while more magnitude of Λ ($|\Lambda| \gg 1$) decrease the value of $V''(a_0)$. In order to visualize the stability region of the model, we plot the stability contour in terms of ϵ_0 and a_0 . Our result is illustrated in Fig.4.10 for the linear model. We notice that in order to satisfy the stability condition (4.55) the constant ϵ_0 has negative values in the throat radius a_0 between $22.00 < a_0 < 36.96$. Unfortunately, all range of the stable throat has negative values of ϵ_0 which is not the behavior of an ordinary matter.

Substituting the relations of energy density and pressure in Eq. (4.74) and Eq. (4.75) into the relations in NEC, WEC and SEC, we find

$$\rho_{\text{eff.}} = -\frac{\sqrt{f(a)}}{4\pi Ga}, \quad (4.77)$$

$$\rho_{\text{eff.}} + P_{\text{eff.}} = \frac{((1 + 2\epsilon_0)\gamma - a(1 + \epsilon_0)\Lambda) - 2(1 + \epsilon_0)\sqrt{f(a)}}{8\pi Ga}, \quad (4.78)$$

$$\rho_{\text{eff.}} + 3P_{\text{eff.}} = \frac{3((1 + 2\epsilon_0)\gamma - a(1 + \epsilon_0)\Lambda) - 2(1 + \epsilon_0)\sqrt{f(a)}}{8\pi Ga}. \quad (4.79)$$

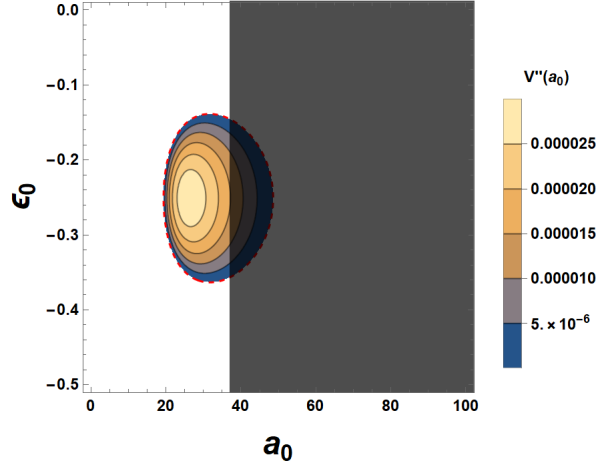


Figure 4.10: The plot shows the stable region of the linear model $P_t(\rho) = \epsilon_0\rho$ with $G = 1$. The contour shows that the constant ϵ_0 has negative values in the throat. The black shaded area is not possible for the thin-shell throat since this zone violates the flaring-out condition shown in cond. (4.67). The red dashed line represents $V''(a_0) = 0$.

In the linear model, the effective energy density, $\rho_{\text{eff.}}$, is non-positive for all cases but the value will increase as further distance from throat to the cosmological horizon for de-Sitter spacetime. For both $\rho_{\text{eff.}} + P_{\text{eff.}}$ and $\rho_{\text{eff.}} + 3P_{\text{eff.}}$, the de-Sitter spacetime would reduce the both values leading to the violation in NEC, WEC and SEC while the anti de-Sitter spacetime and the positive γ tend increase the both values which make less violation on the energy conditions.

In order to analyse the energy conditions, we choose the values of $\epsilon_0 = -0.25$ which is in the stable regions as shown in Fig.4.10 and then verify the energy conditions. Fig.4.11 shows the variation of $\rho_{\text{eff.}}$, $\rho_{\text{eff.}} + P_{\text{eff.}}$ and $\rho_{\text{eff.}} + 3P_{\text{eff.}}$ as a function of a in the linear model $P_t(\rho) = \epsilon_0\rho$. We observe that all energy conditions are violated in this model.

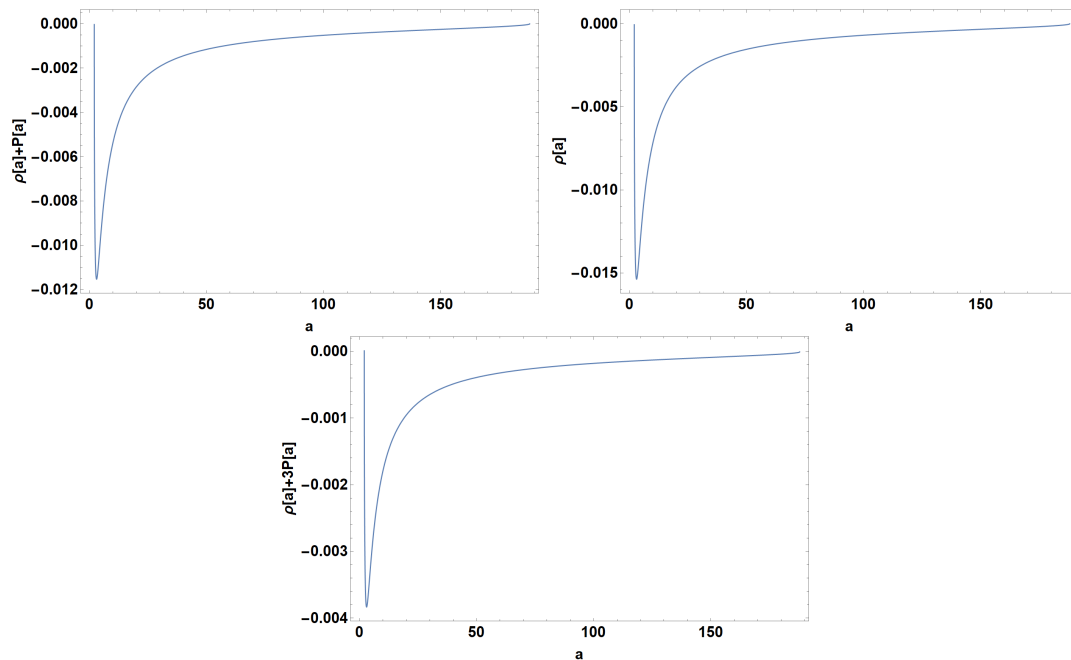


Figure 4.11: The plots show the variation of $\rho_{\text{eff}} + P_{\text{eff}}$, ρ_{eff} , and $\rho_{\text{eff}} + 3P_{\text{eff}}$ as a function of a of the linear model with $P_t(\rho) = \epsilon_0\rho$ with $G = 1$.

4.2.2 Chaplygin gas model

One of the greatest mysteries in high energy physics is the nature of the dark matter and dark energy. Dark matter is proposed to describe the missing mass of galaxies inferred from the viral theorem [72] and to explain the flat rotation curves [73, 74]. Dark energy is applied to explain the acceleration of the expansion of the Universe [75, 76, 77]. Our Universe have been expanding with acceleration, according to the recent year observations of the luminosity of type Ia distant supernovae [22, 23, 78]. The energy density and pressure of the universe violate the strong energy condition. The matter responsible for the acceleration of the universe is referred to as the dark energy [79, 80, 81]. In the standard cold dark matter (Λ CDM) model, the dark matter is represented by a pressureless fluid and

the cosmological constant Λ represents the dark energy.

The pressureless dark matter assumption works well in the weakly interacting massive particles (WIMPs) with a mass range in the order of GeV to TeV. The theory suggests that these particles froze out from the thermal equilibrium in the early era of the Universe. By the result of this decoupling, it cooled off rapidly as the Universe expands. In some models, the dark matter is made of fermions [82, 83] or bosons [84, 85]. These models explain the physics in the scale of galaxies very well but not in the Universe scale.

At the cosmological scale, the Λ CDM model has a problem with cosmological value [86, 87]. The energy density of the cosmological constant Λ is $\rho_\Lambda = \Lambda/8\pi G$ and the equation of state is $P_\Lambda = -\rho_\Lambda$ which is a negative pressure. According to the observational results, the value of energy density of dark energy is $\rho_\Lambda = 6.72 \times 10^{-24} \text{ g m}^{-3}$. On the other hand, the prediction from the theoretical framework provides that the vacuum energy density should be of the order of the Planck density $\rho_P = 5.16 \times 10^{99} \text{ g m}^{-3}$. These quantities are different by 123 orders of magnitude. To solve this problem, some theoretical physicists explain the acceleration of the Universe in terms of a dark energy with time-varying density. In this work [88], they proposed the unification of the dark matter and dark energy in terms of an exotic matter with an equation of state $P = -A/\rho$ called the Chaplygin gas.

The Chaplygin gas model was first proposed by Sergey Chaplygin [89]. It was a mathematical model approximation for calculating the lifting force on a wing of an airplane in aerodynamics. The model was rediscovered later in Refs.

[90, 91]. In the reference [92], they proposed a model of Universe filled with the Chaplygin gas, which is a perfect fluid given by the following equation of state, [92, 93, 94, 95]

$$P_t(\rho) = -\frac{A}{\rho}, \quad (4.80)$$

where $A > 0$. The negative pressure from the Chaplygin gas equation of state can be used to describe certain effects in deformable solids, of strip states in the context of quantum Hall effect and of other phenomena. The equation of state parameter for the Chaplygin gas model is $w \equiv P_t/\rho$, interpolating from $w = 0$ at early times of the Universe when the energy density is very high $\rho \rightarrow \infty$ and $w = -1$ at late times (accelerated expansion) of the Universe when its energy density reaches the minimum value $\rho = A$. In our case, the pressure is already given in Ref.[49]:

$$P_t(\rho) = -\epsilon_1 \left(\frac{1}{\rho} - \frac{1}{\rho_0} \right) + P_{t(0)}, \quad (4.81)$$

where ϵ_1 is a constant with the dimension of pressure² in the natural unit, the parameters ρ_0 and $P_{t(0)}$ are boundary conditions of the energy density and tangential pressure at the throat, respectively and they are determined by using Eq. (4.48) and Eq. (4.49) with $a = a_0$. It is worth to mention a property of the Chaplygin gas which is the positive and bounded squared sound velocity,

$$\frac{dP_t}{d\rho} = \frac{\epsilon_1}{\rho_0^2} \equiv v_s^2, \quad (4.82)$$

where $\rho_0^2 \geq \epsilon_1$ and v_s is the sound velocity of the Chaplygin model. By the definition of the sound velocity in Eq. (4.82), the value of ϵ_1 must be positive.

After substituting the above results into the stability condition (4.55), we

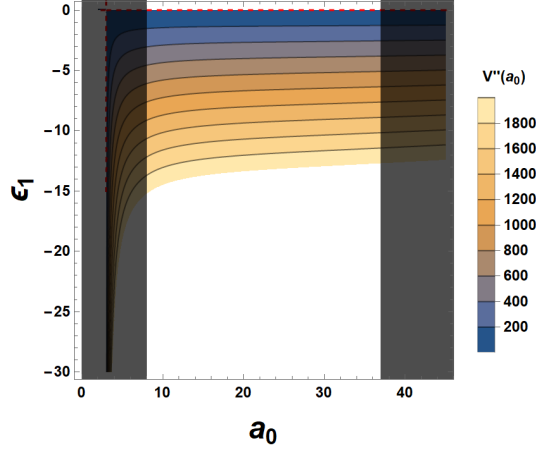


Figure 4.12: The plot shows the stable region of the Chaplygin gas model $p(\sigma) = \epsilon_1(\frac{1}{\rho} - \frac{1}{\rho_0}) + P_{t(0)}$ with $G = 1$ from the Vainshtein radius $r_V = 8.07$ to the upper limit of the flaring-out condition $r_{FO} = 36.96$. The red dashed line represents $V''(a_0) = 0$.

find in this case [58]

$$0 < \frac{f''(a)}{2} + \frac{2\pi G (\rho_0 \epsilon_1 (2\gamma - a\Lambda) + a\Lambda P_{t(0)} (-\epsilon_1 + 2\rho_0^2) + 2\gamma P_{t(0)} \epsilon_1)}{a\rho_0^2} - \frac{16\pi^2 G^2 (P_{t(0)}^2 \rho_0 + (P_{t(0)} + \rho_0) \epsilon_1)}{\rho_0} \frac{\Lambda^2}{4}. \quad (4.83)$$

Here we plot the stability contour in terms of ϵ_1 and a_0 for this model. The stable region for this case is represented in Fig.4.12.

We notice that, in order to satisfy the stability condition (4.55), the Vainshtein radius r_V and the flaring-out condition (4.67), the possible stable throat in this case must be the negative region of ϵ_1 and its radius is in the range $8.07 < a_0 < 36.96$. However, the negative region of ϵ_1 violates the squared sound velocity condition in Eq. (4.82). Therefore, the Chaplygin gas model cannot be an appropriate candidate for the thin-shell wormhole in dRGT massive gravity.

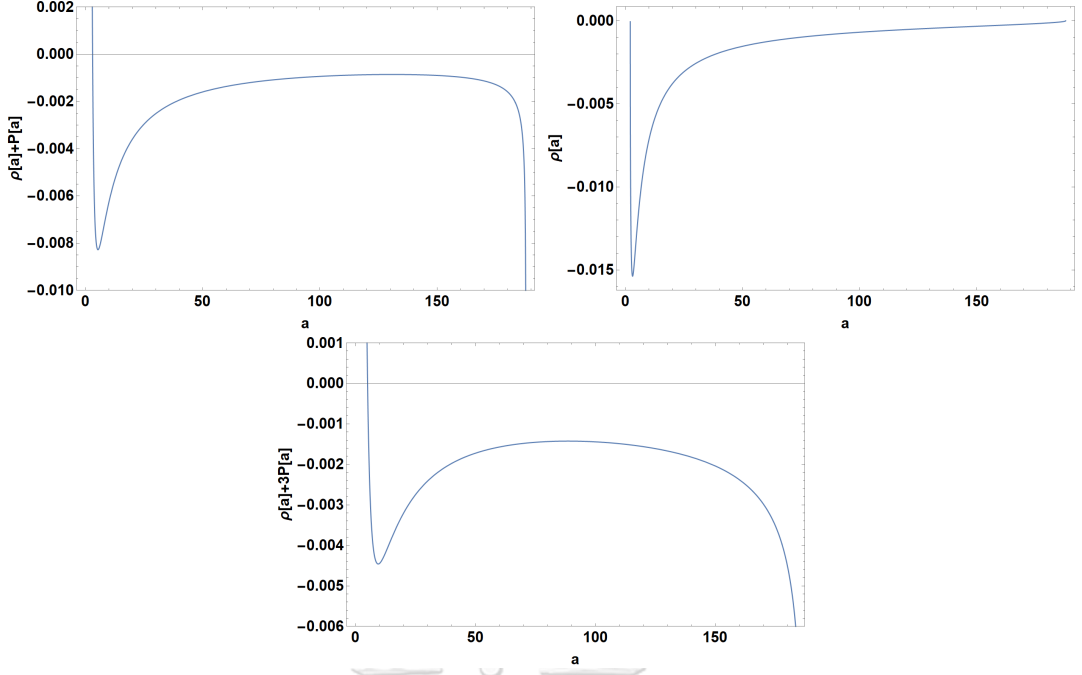


Figure 4.13: The plots show the variation of $\rho_{\text{eff.}} + P_{\text{eff.}}$, $\rho_{\text{eff.}}$ and $\rho_{\text{eff.}} + 3P_{\text{eff.}}$ as a function of a of the Chaplygin gas model with $P_t(\rho) = \epsilon_1 \left(\frac{1}{\rho} - \frac{1}{\rho_0} \right) + P_{t(0)}$ with $G = 1$.

By the relations of the pressure and energy density of the exotic matter in Eq. (4.81) and Eq. (4.82), we find

$$\rho_{\text{eff.}} + P_{\text{eff.}} = \frac{1}{8} \left(\frac{(\gamma - a\Lambda)}{\pi Ga} - \frac{8\epsilon_1((-2\gamma + a\Lambda) + 8aG\pi\rho_0 + 2\sqrt{f(a)})}{\rho_0((2\gamma - a\Lambda) - 2\sqrt{f(a)})} - \frac{2\sqrt{f(a)}}{aG\pi} \right) \geq 0, \quad (4.84)$$

$$\rho_{\text{eff.}} = -\frac{\sqrt{f(a)}}{4\pi Ga} \geq 0, \quad (4.85)$$

$$\rho_{\text{eff.}} + 3P_{\text{eff.}} = \frac{1}{8} \left(\frac{3(\gamma - a\Lambda)}{\pi Ga} - \frac{24\epsilon_1((-2\gamma + a\Lambda) + 8aG\pi\rho_0 + 2\sqrt{f(a)})}{\rho_0((2\gamma - a\Lambda) - 2\sqrt{f(a)})} - \frac{2\sqrt{f(a)}}{aG\pi} \right) \geq 0. \quad (4.86)$$

To quantify the energy conditions, we will choose the values of $\epsilon_1 = -1$ in the stable regions shown in Fig.4.12 and then examine the energy conditions. Fig.4.13

shows the variation of $\rho_{\text{eff.}} + P_{\text{eff.}}$, $\rho_{\text{eff.}}$ and $\rho_{\text{eff.}} + 3P_{\text{eff.}}$ as a function of a in the linear model $P_t(\rho) = \epsilon_1 \left(\frac{1}{\rho} - \frac{1}{\rho_0} \right) + P_{t(0)}$. We observe that all energy conditions are violated for all range in this model.

4.2.3 Generalized Chaplygin gas model

In addition, the Chaplygin gas model given in the previous subsection can be generalized where the relation between $P_t(\rho)$ and ρ takes the form [49]

$$P_t(\rho) = P_{t(0)} \left(\frac{\rho_0}{\rho} \right)^{\epsilon_2}, \quad (4.87)$$

and

$$\frac{dP_t}{d\rho} = -P_{t(0)} \epsilon_2 \frac{\rho_0^{\epsilon_2}}{\rho^{\epsilon_2+1}} \equiv v_s^2, \quad (4.88)$$

where ϵ_2 is the dimensionless parameter and v_s is the sound velocity for the generalized Chaplygin model.

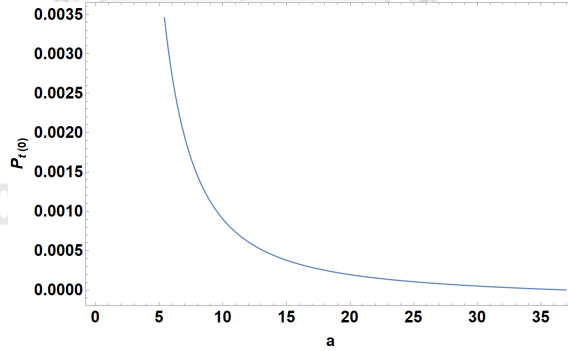


Figure 4.14: This plot illustrates the function of $P_{t(0)}$ against r with the set of parameters as $G = 1, \Lambda = 0.0001, \gamma = 0.001, M = 1$, and $\zeta = 0$. The value of $P_{t(0)}$ is positive for all range of r that satisfies the flaring-out condition ($r \in [2.00, 36.96]$).

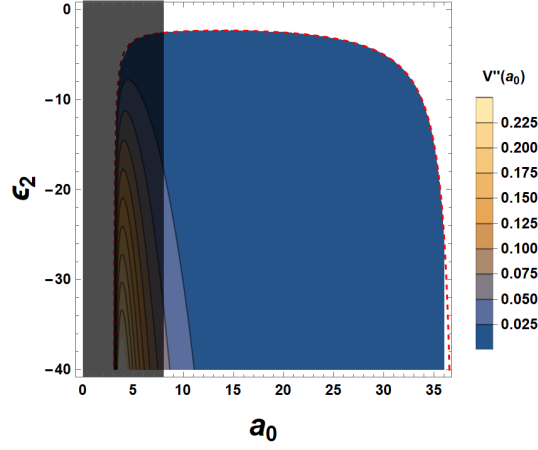


Figure 4.15: The plot shows the stable region of the generalized Chaplygin gas model $P_{t(0)}(\rho) = P_{t(0)}(\frac{\rho_0}{\rho})^{\epsilon_2}$ with $G = 1$ from the Vainshtein radius $r_V = 8.07$ to the upper limit of the flaring-out condition $r_{FO} = 36.96$. The red dashed line represents $V''(a_0) = 0$.

After substituting the above results into the stability condition (4.55), we find in this case [58]

$$0 < \frac{f''(a)}{2} + \frac{2\pi G P_{t(0)} (P_{t(0)} \epsilon_2 (a\Lambda - 2\gamma) + a\Lambda \rho_0 (\epsilon_2 + 2) - 2\gamma \rho_0 \epsilon_2)}{a\rho_0} + 16\pi^2 G^2 P_{t(0)} (P_{t(0)} (\epsilon_2 - 1) + \rho_0 \epsilon_2) - \frac{\Lambda^2}{4} \quad (4.89)$$

In this case, we have an additional condition from the squared sound velocity in Eq. (4.88) as follow

$$P_{t(0)} \epsilon_2 < 0. \quad (4.90)$$

Here $P_{t(0)}$ is the tangential pressure at the throat and it can be determined by using Eq. (4.49) with $a = a_0$. We illustrate the plot of $P_{t(0)}$ in the range that satisfies the Vainshtein radius and the flaring-out condition ($a_0 \in [8.07, 36.96]$) as shown Fig.(4.14) with the set of parameters ($\Lambda = 0.0001, \gamma = 0.001, M =$

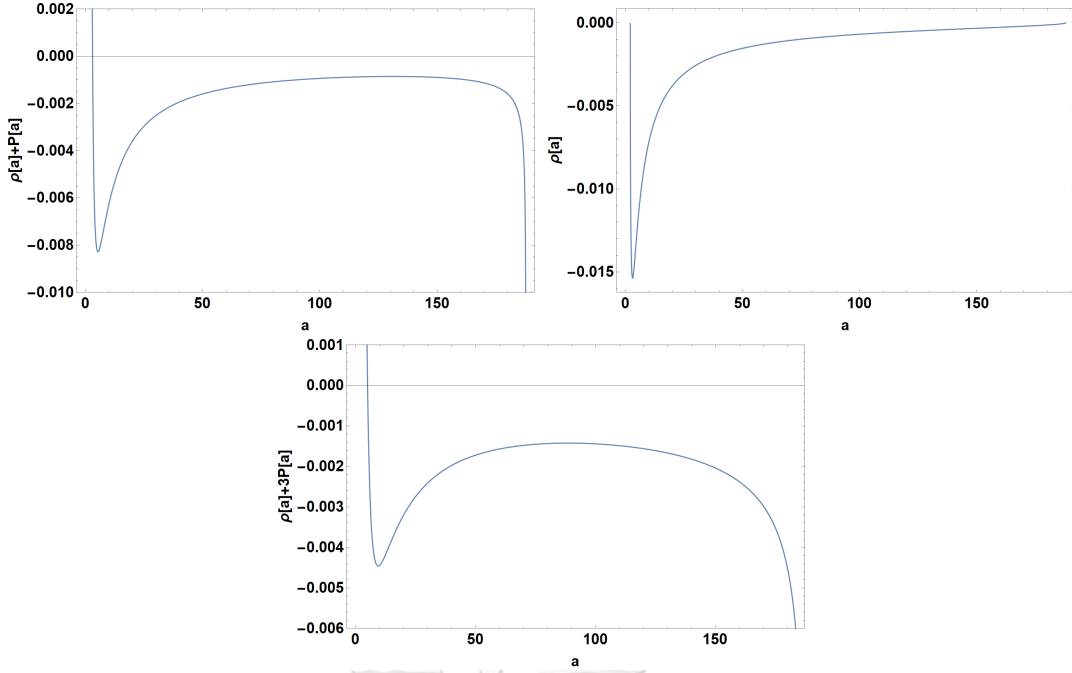


Figure 4.16: The plots show the variation of $\rho_{\text{eff}} + P_{\text{eff}}$, ρ_{eff} , and $\rho_{\text{eff}} + 3P_{\text{eff}}$, as a function of a of the generalized Chaplygin gas model with $P_t(\rho) = P_{t(0)} \left(\frac{\rho_0}{\rho} \right)^{\epsilon_2}$ with $G = 1$.

1, and $\zeta = 0$). The value of $P_{t(0)}$ is positive then this shows no sign of dark energy requirement for the thin-shell wormhole construction in the generalized Chaplygin gas model. Moreover, the allowed value of ϵ_2 is only for negative which means that the exponent of the energy density in Eq. (4.87) is positive.

To find the stability region of the thin-shell wormhole throat, we solve the stability condition (4.55). The squared sound velocity in Eq. (4.88) excludes the region of the wormhole throat that $\epsilon_2 \geq 0$. Moreover, the flaring-out condition and the Vainshtein radius (4.67) limit the possible value of throat radius to $a_0 \in [8.07, 36.96]$. Here we display the stability contour in terms of ϵ_2 and a_0 illustrated in Fig. 4.15. Unlike the Chaplygin gas, the possible region for the stable thin-shell

wormhole throat in dRGT theory satisfies the sound velocity, .

By the relations of the pressure and energy density of the exotic matter in Eq. (4.87) and Eq. (4.88), we find

$$\rho_{\text{eff.}} + P_{\text{eff.}} = \frac{1}{8\pi Ga} \left((\gamma - a\Lambda) - 2\sqrt{f(a)} - Ga(8\pi)^{1+\epsilon_2} \left(-\frac{Ga\rho_0}{(-2\gamma + a\Lambda) + 2\sqrt{f(a)}} \right)^{\epsilon_2} \right) \geq 0, \quad (4.91)$$

$$\rho_{\text{eff.}} = -\frac{\sqrt{f(a)}}{4\pi Ga} \geq 0, \quad (4.92)$$

$$\rho_{\text{eff.}} + 3P_{\text{eff.}} = \frac{1}{8\pi Ga} \left(3(\gamma - 3a\Lambda) - 2\sqrt{f(a)} - 3Ga(8\pi)^{1+\epsilon_2} \left(-\frac{Ga\rho_0}{(-2\gamma + a\Lambda) + 2\sqrt{f(a)}} \right)^{\epsilon_2} \right) \geq 0. \quad (4.93)$$

We here quantify the energy conditions by choosing the values of ϵ_2 in the stable regions shown in Fig. 4.15 and then examine the energy conditions. Fig.4.16 shows the variation of $\rho_{\text{eff.}} + P_{\text{eff.}}$, $\rho_{\text{eff.}}$ and $\rho_{\text{eff.}} + 3P_{\text{eff.}}$ as a function of a in the generalized Chaplygin gas model. We observe that all energy conditions are violated for negative values of ϵ_2 .

4.2.4 Logarithm model

According to the theoretical problems about the dark matter and the dark energy mentioned in the previous model, some works proposed the logotropic equation of state where the pressure $P_t(\rho)$ and the rest-mass density ρ are related via [49, 96]

$$P_t(\rho) = \epsilon_3 \log \left(\frac{\rho}{\rho_0} \right) + P_{t(0)}, \quad (4.94)$$

where ϵ_3 is a constant with the dimension of pressure and

$$\frac{dP_t}{d\rho} = \frac{\epsilon_3}{\rho} \equiv v_s^2, \quad (4.95)$$

where the energy density ρ must not be greater than ϵ_3 and v_s is the sound velocity for the logotropic model.

The logotropic equation of state was used to study the giant molecular clouds (GMCs) and dense cores in astrophysics where the logotropic model describes the turbulent pressure very well in given by Ref. [97]. Moreover, the dynamics of the logotropic gas was studied in the static and dynamical properties of a generalized Smoluchowski equation where it can be interpreted as a limiting form of the polytropic equation of state or the generalized Chaplygin model of the form $P = K\rho^\gamma$ (where P is the isotropic pressure and ρ is the energy density of gas) with $\gamma \rightarrow 0$, $K \rightarrow \infty$ and $B = \gamma K$ is finite [98]. Another application of the logotropic equation of state is in a scalar field theory which is a candidate for the dark fluid in Bose-Einstein condensates. The dynamics of the dark fluid is described in the non-relativistic regime of the Gross-Pitaevskii equation [99].

Now we demonstrate the unification of the dark energy and dark matter for the logotropic gas model by considering the Friedmann equations for a flat Universe without the cosmological constant

$$\frac{dE}{dt} + 3\frac{\dot{a}}{a}(E + P_t) = 0, \quad (4.96)$$

where $E(t)$ is the total energy density, $P_t(t)$ is the pressure and $a(t)$ is the scale factor. The first law of thermodynamics in the adiabatic process reduces to

$$dE = \frac{P_t + E}{\rho} d\rho, \quad (4.97)$$

where ρ is the energy density of the rest mass. Then we have the continuity

equation as follows:

$$\frac{d\rho}{dt} + 3\frac{\dot{a}}{a}\rho = 0, \quad (4.98)$$

where the solution of the continuity equation is $\rho = \rho_0/a^3$ and ρ_0 is the present value of the energy density of the rest mass. The following ansatz satisfies Eq. (4.97)

$$E = \rho + \rho \int^\rho \frac{P_t(\rho')}{\rho'^2} d\rho' = \rho + u(\rho), \quad (4.99)$$

where $u(\rho)$ is the internal energy density. Then the total energy density E is the sum of the energy density of the rest mass ρ and the internal energy $u(\rho)$. By the choice of the logotropic model in Eq. (4.94), the total energy density becomes

$$E = \rho - \epsilon_3 \log\left(\frac{\rho}{\rho_0}\right) - P_{t(0)} - \epsilon_3 = \rho + u(\rho). \quad (4.100)$$

The total energy density is the sum of 2 terms; the energy density of the rest mass $\rho \propto a^{-3}$ representing the dark matter and the internal energy term $u(\rho) = -\epsilon_3 \log\left(\frac{\rho}{\rho_0}\right) - P_{t(0)} - \epsilon_3$ representing the dark energy.

In the early Universe where the dark matter dominates over other kinds of matter ($a \rightarrow 0, \rho \rightarrow +\infty$), the total energy density is approximated by

$$E \sim \rho, \quad P_t \sim \epsilon_3 \log\left(\frac{\rho}{\rho_0}\right). \quad (4.101)$$

In the late time Universe ($a \rightarrow +\infty, \rho \rightarrow 0$), the dark energy or, in this case, the internal energy dominates

$$E \sim -\epsilon_3 \log\left(\frac{\rho}{\rho_0}\right), \quad P_t \sim -E. \quad (4.102)$$

We also note that the asymptotic behavior of the pressure of the late time Universe recovers $P_t \sim -\rho$ from the logotropic model because it is the exotic matter equation of state.

We apply the logotropic equation of state in Eq. (4.94) into the stability condition (4.55) as shown [58]

$$0 < \frac{f''(a)}{2} + \frac{2\pi G (\rho_0 \epsilon_3 (2\gamma - a\Lambda) - a\Lambda P_{t(0)} (\epsilon_3 - 2\rho_0) + 2\gamma P_{t(0)} \epsilon_3)}{a\rho_0} - 16\pi^2 G^2 ((P_{t(0)} + \rho_0) \epsilon_3 + P_{t(0)}^2) - \frac{\Lambda^2}{4} \quad (4.103)$$

Here we display the stability contour in terms of ϵ_3 and a_0 illustrated in Fig.4.17. The stable region for this case is represented in Fig.4.17 for the logarithm model model. We observe that in order to satisfy the stability condition (4.55) ϵ_3 is

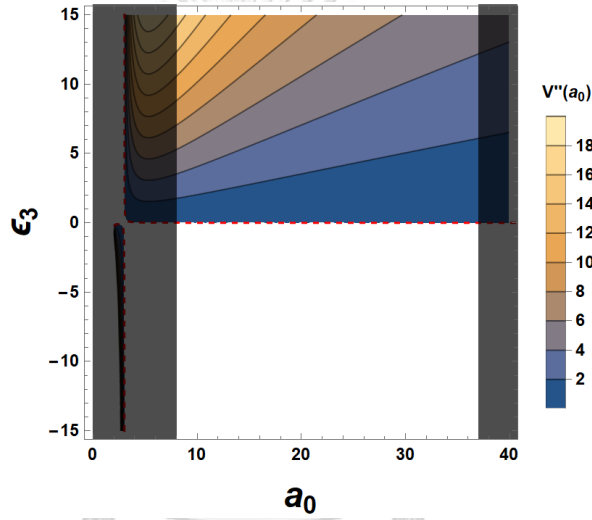


Figure 4.17: The plot shows the stable region of the linear model $P_t(\rho) = \epsilon_3 \log(\frac{\rho}{\rho_0}) + P_{t(0)}$ with $G = 1$. The result shows that ϵ_3 can have both negative values and positive ones in the throat with radius a_0 . The red dashed line represents $V''(a_0) = 0$.

positive and the possible throat of the wormhole in dRGT massive gravity is in the range $r \in [8.07, 36.96]$.

By the relations of the pressure and energy density of the exotic matter in

Eq. (4.87) and Eq. (4.88), we find

$$\begin{aligned} \rho_{\text{eff.}} + P_{\text{eff.}} &= \frac{1}{8\pi Ga} \left((\gamma - a\Lambda) - 2\sqrt{f(a)} \right. \\ &\quad \left. + P_{t(0)} + \epsilon_3 \log \left(\frac{2\gamma - a\Lambda + 2\sqrt{f(a)}}{8\pi Ga\rho_0} \right) \right) \geq 0, \end{aligned} \quad (4.104)$$

$$\rho_{\text{eff.}} = -\frac{\sqrt{f(a)}}{4\pi Ga} \geq 0, \quad (4.105)$$

$$\begin{aligned} \rho_{\text{eff.}} + 3P_{\text{eff.}} &= \frac{1}{8\pi Ga} \left(3(\gamma - a\Lambda) - 2\sqrt{f(a)} \right. \\ &\quad \left. + 3P_{t(0)} + 3\epsilon_3 \log \left(\frac{2\gamma - a\Lambda + 2\sqrt{f(a)}}{8\pi Ga\rho_0} \right) \right) \geq 0. \end{aligned} \quad (4.106)$$

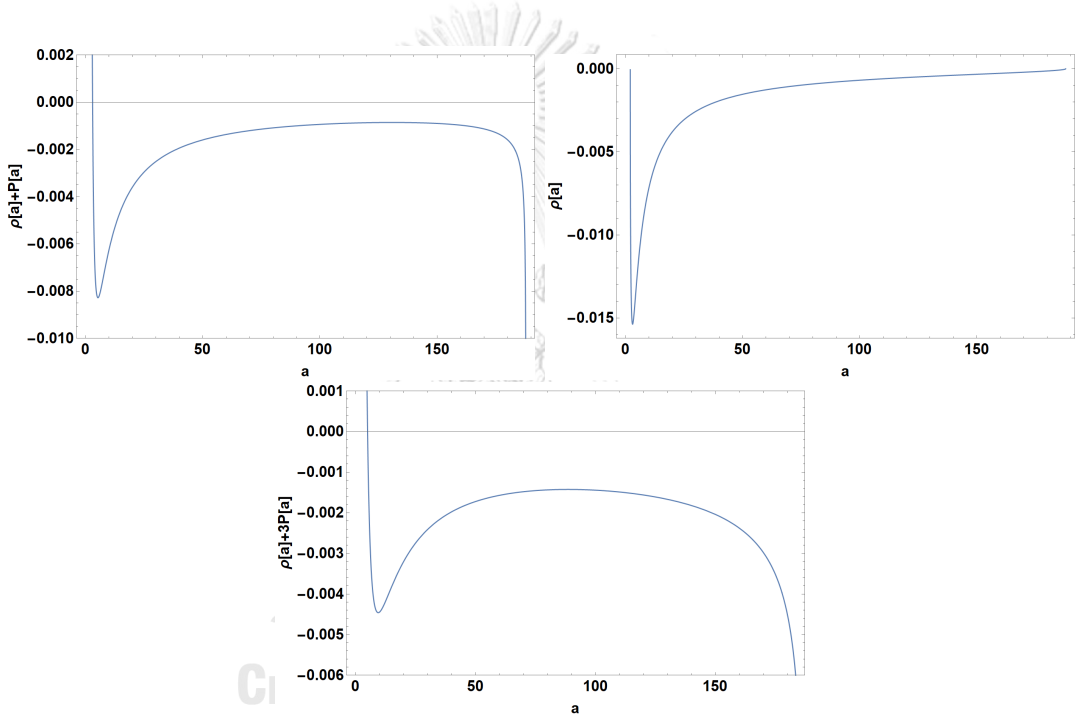


Figure 4.18: The plots show the variation of $\rho_{\text{eff.}} + P_{\text{eff.}}$, $\rho_{\text{eff.}}$ and $\rho_{\text{eff.}} + 3P_{\text{eff.}}$ as a function of a of the generalized Chaplygin gas model with $P_t(\rho) = P_{t(0)} \left(\frac{\rho_0}{\rho} \right)^{\epsilon_3}$ with $G = 1$.

We here quantify the energy conditions by choosing the values of ϵ_3 in the stable regions shown in Fig.4.17 and then examine the energy conditions. Fig.4.18 shows the variation of $\rho_{\text{eff.}} + P_{\text{eff.}}$, $\rho_{\text{eff.}}$ and $\rho_{\text{eff.}} + 3P_{\text{eff.}}$ as a function of a in the

ogarithm model $P_t(\sigma) = \epsilon_3 \log(\frac{\rho}{\rho_0})$. We observe that all energy conditions are violated for all range.



CHAPTER V

Discussions and conclusions

In this thesis, we have reviewed the massive gravity theory from the linear theory or FP theory. The discrepancy between the FP theory at the massless limit and GR is revealed by the Stueckelberg trick. Even in the massless limit, the additional scalar field does not disappear in FP theory. This leads to the new way to construct the massive theory via non-linearity with help of the Vanstein mechanism. The effect of non-linear theory overwhelms the effect of linear inside the Vainstein radius which is approximately infinity when graviton mass $m_g \rightarrow 0$. However, the major caveat for the non-linear massive gravity is the appearance of ghost or the wrong sign of kinetic terms in action. However, de Rham, Gabadadze and Tolley have succeeded to find the ghost-free nonlinear massive gravity theory called dRGT theory. With the great effort to search the signal of gravitation wave by LIGO, the results show that the graviton is not completely massless and the upper bound of the graviton mass is below 10^{-24} eV/c². The mass of graviton is very small from the constraint of the gravitational waves observations. This implies that the dRGT is not a trivial theory and it is worth for further study.

There still remain numerous questions about the dRGT theory. One of them

is the black hole characteristic in dRGT theory which has been widely studied in the following references; the class and the thermodynamics properties of black holes in dRGT [25], the prediction of the black hole perturbation in quasinormal modes [100, 101, 102, 103], and the Greybody factor technique of the black hole in dRGT massive gravity [104]. The study of this topic will reveal an interesting and advantage of the dRGT massive gravity. While, in this thesis, we have investigated the possibilities of the existences of the wormholes from the spherical symmetric solutions in the dRGT theory. This study will also extensively explore more salient features and properties of the dRGT massive gravity. Moreover, there are two types of wormholes investigated in this thesis; the Lorentzian traversable wormhole and the thin-shell wormhole.

The Lorentzian traversable wormhole is the shortcut that links two points in spacetime where its characteristic depends on the shape function $b(r)$ and the red-shift function $\Phi(r)$. We have chosen the form of $b(r)$ as $b(r) = r \exp(-\alpha(r-r_0))$ and three types of the red-shift functions; constant, linear and logarithm. We apply the $f(R)$ gravity and dRGT to find the traversable wormhole solutions. To analyze the material for the traversable wormhole construction, we consider the energy conditions; NEC ($\rho + P_r \geq 0$ and $\rho + P_t \geq 0$), WEC ($\rho \geq 0$, $\rho + P_r \geq 0$ and $\rho + P_t \geq 0$), and SEC ($\rho + P_r + 2P_t \geq 0$, $\rho + P_r \geq 0$ and $\rho + P_t \geq 0$). According to the results of three red-shift functions; $\Phi(r) = 1$, $\Phi(r) = 1/r$, and $\Phi(r) = \log(1 + 1/r)$, the regions, which violate the energy conditions, vary on the strength of the Starobinsky model (α_1) and the dRGT parameters (γ and Λ). Let consider the effect of α_1 on energy conditions. For low magnitudes of $\alpha = \pm 0.01$,

NEC, WEC and SEC are violated near the throat regions except for $\alpha_1 = 0.01$ that SEC is satisfied near the throat but violated in the rest of the spacetime region. For $\alpha = -0.1$, NEC and WEC are not violated at the throat but some finite region further away from it while SEC is, on the other hand, violated almost all spacetime region except some finite region. For $\alpha = 0.1$, The only violated region of NEC and WEC is only the finite region around the throat but SEC is violated almost all of the spacetime region. Now we conclude the effect of dRGT parameters (γ and Λ). Overall results point that the violated regions of NEC and WEC reduce by the more positive γ and more negative Λ which affect totally opposite on SEC violation region. In the future work, one might obtain numerous solutions of the wormhole by considering other choices of ρ , P_r and P_t , for instance, varying the shape function $b(r)$, the red-shift function $\Phi(r)$ and the $f(R)$ theory.

The other type of wormhole is the thin-shell wormhole in the dRGT spacetime. This wormhole acts as the glue between two hypersurfaces of two Universe. The technique is called cut-and-paste procedure [52]. To study the thin-shell wormhole in the massive gravity, we have to investigate the junction condition between two dRGT spacetimes for the stability. The matter to construct the thin-shell wormhole in dRGT model must satisfy the four following criteria; the no-horizon condition, the flaring-out condition, the Vainshtein radius and the sound velocity. Then, we analyze the stable thin-shell wormhole in dRGT spacetime with energy conditions (NEC, WEC, and SEC). We have considered the variation of $\rho_{\text{eff.}} + P_{\text{eff.}}$, $\rho_{\text{eff.}}$ and $\rho_{\text{eff.}} + 3P_{\text{eff.}}$ as a function of a in all models: (1) a linear model $P_t(\rho) = \epsilon_0\rho$, (2) a Chaplygin gas model $P_t(\rho) = \epsilon_0\left(\frac{1}{\rho} - \frac{1}{\rho_0}\right) + P_{t(0)}$, (3) a

generalized Chaplygin gas model $P_t(\rho) = P_{t(0)} \left(\frac{\rho_0}{\rho} \right)^{\epsilon_0}$ and (4) a logarithm model $P_t(\rho) = \epsilon_0 \log \left(\frac{\rho}{\rho_0} \right) + P_{t(0)}$. In the linear model, the exotic matter is necessary for building the thin-shell wormhole in dRGT model. Even though the Chaplygin gas model is a candidate for the dark matter, it is not an appropriate candidate for the thin-shell wormhole material in the dRGT model. While a generalized Chaplygin gas model shows that the requirement of the dark matter is not necessary to construct a thin-shell wormhole in dRGT model. In the last case, the exotic matter that satisfies the logotropic model can form the thin-shell wormhole in dRGT model. Choosing the values of ϵ_0 in the stable regions, we have observed that in general the classical energy conditions are violated by introducing all existing models of the exotic fluids.

Before closing discussion, we would like to clarify and comment the results in the published works [57, 58] of this thesis. The sets of parameters in this work might not be compatible with the Vainshtein mechanism for dRGT massive gravity and $f(R)$ gravity. Since we focus on the investigations of the effects on exotic matter in the wormholes by variation of parameters in the models and they are toy models in the study of the wormholes. However, we realize the major caveat and we plan to improve all parameters that satisfy the Vainshtein mechanism in the future research works.

References

- [1] K. Schwarzschild, Sitzungsber. Preuss. Akad. Wiss. Berlin (Math. Phys.) **1916** (1916) 189 [physics/9905030].
- [2] L. Flamm, Physikalische Zeitschrift, **17**, 448 (1916). Note: This article is unavailable online. The editorial note on the Ludwig Flamm's work is given online: G. W. Gibbons, Gen. Relativ. Gravit. **47** (2015) 71.
- [3] A. Einstein and N. Rosen, Phys. Rev. **48** (1935) 73.
- [4] C. W. Misner and J. A. Wheeler, Annals Phys. **2**, 525 (1957).
- [5] H. G. Ellis, J. Math. Phys. **14**, 104 (1973).
- [6] K. A. Bronnikov, Acta Phys. Polon. B **4**, 251 (1973).
- [7] M. S. Morris and K. S. Thorne, Am. J. Phys. **56**, 395 (1988).
- [8] M. S. Morris, K. S. Thorne and U. Yurtsever, Phys. Rev. Lett. **61**, 1446 (1988).
- [9] F. S. N. Lobo and M. A. Oliveira, Phys. Rev. D **80**, 104012 (2009)
- [10] K. A. Bronnikov, M. V. Skvortsova and A. A. Starobinsky, Grav. Cosmol. **16** (2010), 216-222 doi:10.1134/S0202289310030047 [arXiv:1005.3262 [gr-qc]].
- [11] H. Saeidi and B. N. Esfahani, Mod. Phys. Lett. A **26** (2011), 1211-1219 doi: 10.1142/S0217732311035547 [arXiv:1409.2176 [physics.gen-ph]].

- [12] M. Fierz and W. Pauli, Proc. Roy. Soc. Lond. A **A173** (1939), 211-232 doi:
10.1098/rspa.1939.0140
- [13] V. I. Zakharov, JETP Lett. **12** (1970), 312
- [14] H. van Dam and M. J. G. Veltman, Nucl. Phys. B **22** (1970), 397-411 doi:
10.1016/0550-3213(70)90416-5
- [15] A. I. Vainshtein, Phys. Lett. B **39** (1972), 393-394 doi:10.1016/0370-
2693(72)90147-5
- [16] K. Hinterbichler, Rev. Mod. Phys. **84** (2012), 671-710 doi:10.1103/RevMod-
Phys.84.671 [arXiv:1105.3735 [hep-th]].
- [17] C. de Rham, G. Gabadadze and A. J. Tolley, Phys. Rev. Lett. **106** (2011),
231101 doi:10.1103/PhysRevLett.106.231101 [arXiv:1011.1232 [hep-th]].
- [18] U. I. Uggerhoj and R. E. Mikkelsen and J. Faye, Eur. J. Phys. **37**, 035602
(2016) doi:10.1088/0143-0807/37/3/035602
- [19] H. M. Schwartz, Am. J. Phys. **45**, 512 (1977). doi:10.1119/1.10949
- [20] G. M. Clemence, Am. J. Phys. **19**, 361 (1947). doi:10.1103/RevModPhys.
19.361
- [21] B. P. Abbott *et al.* [LIGO Scientific and Virgo Collaborations], Phys. Rev.
Lett. **116**, no. 6, 061102 (2016) doi:10.1103/PhysRevLett.116.061102
[arXiv:1602.03837 [gr-qc]].

- [22] A. G. Riess *et al.* [Supernova Search Team], *Astron. J.* **116**, 1009 (1998) doi: 10.1086/300499 [astro-ph/9805201].
- [23] S. Perlmutter *et al.* [Supernova Cosmology Project Collaboration], *Astrophys. J.* **517**, 565 (1999) doi:10.1086/307221 [astro-ph/9812133].
- [24] K. Konno, T. Matsuyama, Y. Asano and S. Tanda, *Phys. Rev. D* **78**, 024037 (2008) doi:10.1103/PhysRevD.78.024037 [arXiv:0807.0679 [gr-qc]].
- [25] S. G. Ghosh, L. Tannukij and P. Wongjun, *Eur. Phys. J. C* **76** (2016) no.3, 119 doi:10.1140/epjc/s10052-016-3943-x [arXiv:1506.07119 [gr-qc]].
- [26] E. Babichev and R. Brito, *Class. Quant. Grav.* **32** (2015), 154001 doi: 10.1088/0264-9381/32/15/154001 [arXiv:1503.07529 [gr-qc]].
- [27] S. Chougule, S. Dey, B. Pourhassan and M. Faizal, *Eur. Phys. J. C* **78** (2018) no.8, 685 doi:10.1140/epjc/s10052-018-6172-7 [arXiv:1809.00868 [gr-qc]].
- [28] S. D. Forghani, S. H. Mazharimousavi and M. Halilsoy, *Eur. Phys. J. C* **79** (2019) no.6, 449 doi:10.1140/epjc/s10052-019-6964-4 [arXiv:1812.05074 [gr-qc]].
- [29] S. M. Carroll, [arXiv:gr-qc/9712019 [gr-qc]].
- [30] R. Arnowitt, S. Deser, and C. W. Misner, *Phys. Rev.* **117** (1960), 1595 doi: 10.1103/PhysRev.117.1595
- [31] R. Arnowitt, S. Deser and C. W. Misner, *Gen. Rel. Grav.* **40** (2008), 1997-2027 doi:10.1007/s10714-008-0661-1 [arXiv:gr-qc/0405109 [gr-qc]].

- [32] S. Kurekci, *Basics of Massive Spin-2 Theories*, Ph.D. thesis, The graduate School of Natural and Applied Sciences of Middle East Technical University, Turkey, 2015.
- [33] E. Dyer and K. Hinterbichler, *Phys. Rev. D* **79** (2009), 024028 doi:10.1103/PhysRevD.79.024028 [arXiv:0809.4033 [gr-qc]].
- [34] D. G. Boulware and S. Deser, *Phys. Rev. D* **6** (1972), 3368-3382 doi:10.1103/PhysRevD.6.3368
- [35] P. Creminelli, A. Nicolis, M. Papucci and E. Trincherini, *JHEP* **09** (2005), 003 doi:10.1088/1126-6708/2005/09/003 [arXiv:hep-th/0505147 [hep-th]].
- [36] C. de Rham, *Living Rev. Rel.* **17** (2014), 7 doi:10.12942/lrr-2014-7 [arXiv:1401.4173 [hep-th]].
- [37] A. Nicolis, R. Rattazzi and E. Trincherini, *Phys. Rev. D* **79** (2009), 064036 doi:10.1103/PhysRevD.79.064036 [arXiv:0811.2197 [hep-th]].
- [38] K. Hinterbichler, M. Trodden and D. Wesley, *Phys. Rev. D* **82** (2010), 124018 doi:10.1103/PhysRevD.82.124018 [arXiv:1008.1305 [hep-th]].
- [39] C. de Rham and G. Gabadadze, *Phys. Rev. D* **82** (2010), 044020 doi:10.1103/PhysRevD.82.044020 [arXiv:1007.0443 [hep-th]].
- [40] S. F. Hassan and R. A. Rosen, *JHEP* **07** (2011), 009 doi:10.1007/JHEP07(2011)009 [arXiv:1103.6055 [hep-th]].
- [41] S. F. Hassan and R. A. Rosen, *JHEP* **02** (2012), 126 doi:10.1007/JHEP02(2012)126 [arXiv:1109.3515 [hep-th]].

- [42] S. F. Hassan and R. A. Rosen, Phys. Rev. Lett. **108** (2012), 041101 doi:10.1103/PhysRevLett.108.041101 [arXiv:1106.3344 [hep-th]].
- [43] D. Vegh, [arXiv:1301.0537 [hep-th]].
- [44] A. Adams, D. A. Roberts and O. Saremi, Phys. Rev. D **91** (2015) no.4, 046003 doi:10.1103/PhysRevD.91.046003 [arXiv:1408.6560 [hep-th]].
- [45] R. G. Cai, Y. P. Hu, Q. Y. Pan and Y. L. Zhang, Phys. Rev. D **91** (2015) no. 2, 024032 doi:10.1103/PhysRevD.91.024032 [arXiv:1409.2369 [hep-th]].
- [46] J. Xu, L. M. Cao and Y. P. Hu, Phys. Rev. D **91** (2015) no.12, 124033 doi:10.1103/PhysRevD.91.124033 [arXiv:1506.03578 [gr-qc]].
- [47] B. P. Abbott *et al.* [LIGO Scientific and VIRGO], Phys. Rev. Lett. **118** (2017) no.22, 221101 doi:10.1103/PhysRevLett.118.221101 [arXiv:1706.01812 [gr-qc]].
- [48] L. Bernus, O. Minazzoli, A. Fienga, M. Gastineau, J. Laskar and P. Deram, Phys. Rev. Lett. **123** (2019) no.16, 161103 doi:10.1103/PhysRevLett.123.161103 [arXiv:1901.04307 [gr-qc]].
- [49] A. Övgün, doi:10.13140/RG.2.1.2655.8966/1 [arXiv:1610.08118 [gr-qc]].
- [50] T. Kokubu and T. Harada, [arXiv:2002.02577 [gr-qc]].
- [51] E. Curiel, Einstein Stud. **13** (2017), 43-104 doi:10.1007/978-1-4939-3210-8_3 [arXiv:1405.0403 [physics.hist-ph]].
- [52] M. Visser, Woodbury, USA: AIP (1995) 412 p.

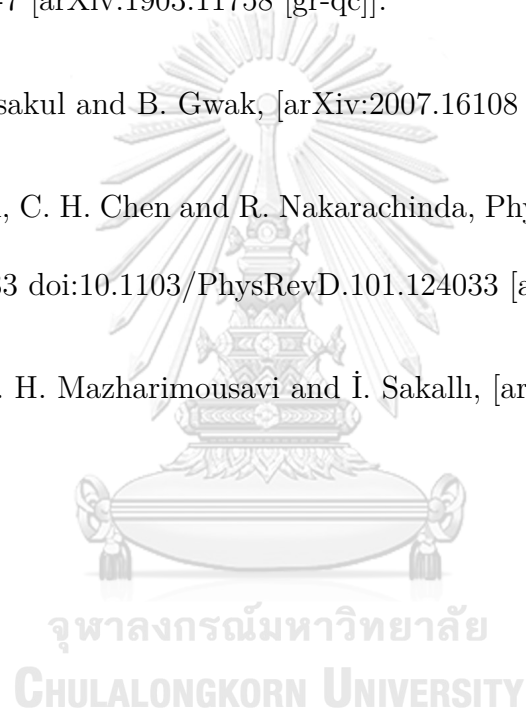
- [53] W. Israel, *Nuovo Cim. B* **44S10** (1966), 1 doi:10.1007/BF02710419
- [54] E. Poisson, doi:10.1017/CBO9780511606601
- [55] L. Avilés, H. Maeda and C. Martinez, *Class. Quant. Grav.* **37** (2020) no.7, 075022 doi:10.1088/1361-6382/ab728a [arXiv:1910.07534 [gr-qc]].
- [56] A. Padilla and V. Sivanesan, *JHEP* **08** (2012), 122 doi: 10.1007/JHEP08(2012)122 [arXiv:1206.1258 [gr-qc]].
- [57] T. Tangphati, A. Chatrabhuti, D. Samart and P. Channuie, *Phys. Rev. D* **102** (2020) no.8, 084026 doi:10.1103/PhysRevD.102.084026 [arXiv:2003.01544 [gr-qc]].
- [58] T. Tangphati, A. Chatrabhuti, D. Samart and P. Channuie, *Eur. Phys. J. C* **80** (2020) no.8, 722 doi:10.1140/epjc/s10052-020-8294-y [arXiv:1912.12208 [gr-qc]].
- [59] P. K. F. Kuhfittig, *J. Phys.* **92** (2018), 1207-1212 doi:10.1007/s12648-018-1213-5 [arXiv:1801.10474 [gr-qc]].
- [60] J. P. S. Lemos, F. S. N. Lobo and S. Quinet de Oliveira, *Phys. Rev. D* **68** (2003), 064004 doi:10.1103/PhysRevD.68.064004 [arXiv:gr-qc/0302049 [gr-qc]].
- [61] H. Maeda and M. Nozawa, *Phys. Rev. D* **78** (2008), 024005 doi:10.1103/PhysRevD.78.024005 [arXiv:0803.1704 [gr-qc]].
- [62] M. Zubair, F. Kousar and S. Bahamonde, *Eur. Phys. J. Plus* **133** (2018) no. 12, 523 doi:10.1140/epjp/i2018-12344-y [arXiv:1712.05699 [gr-qc]].

- [63] G. C. Samanta, N. Godani and K. Bamba, “Traversable Wormholes with Exponential Shape Function in Modified Gravity and in General Relativity: A Comparative Study,” [arXiv:1811.06834 [gr-qc]].
- [64] P. K. Sahoo, P. H. R. S. Moraes and P. Sahoo, Eur. Phys. J. C **78** (2018) no. 1, 46 doi:10.1140/epjc/s10052-018-5538-1 [arXiv:1709.07774 [gr-qc]].
- [65] R. Shaikh, Phys. Rev. D **98** (2018) no.6, 064033 doi:10.1103/PhysRevD.98.064033 [arXiv:1807.07941 [gr-qc]].
- [66] T. Harko, F. S. N. Lobo, M. K. Mak and S. V. Sushkov, Mod. Phys. Lett. A **30**, no. 35, 1550190 (2015)
- [67] M. Jamil, F. Rahaman, R. Myrzakulov, P. K. F. Kuhfittig, N. Ahmed and U. F. Mondal, J. Korean Phys. Soc. **65**, no. 6, 917 (2014)
- [68] F. Rahaman, S. Islam, P. K. F. Kuhfittig and S. Ray, Phys. Rev. D **86**, 106010 (2012)
- [69] A. A. Starobinsky, Phys. Lett. B **91**: 99-102 (1980)
- [70] N. Godani and G. C. Samanta, “Traversable Wormholes in $R + \alpha R^n$ Gravity,” Eur. Phys. J. C **80** (2020) no.1, 30 doi:10.1140/epjc/s10052-019-7587-5 [arXiv:2001.00010 [gr-qc]].
- [71] M. Visser and C. Barcelo, [arXiv:gr-qc/0001099 [gr-qc]].
- [72] F. Zwicky, Gen Relativ Gravit **41**, 207–224 (2009).
- [73] V. C. Rubin, W. K. Ford, and N. Thonnard, Astrophys. J. **238**, 471 (1980).

- [74] M. Persic, P. Salucci, and F. Stel, *Mon. Not. R. astr. Soc.* **281**, 27 (1996).
- [75] A.G. Riess et al., *Astron. J.* **116**, 1009 (1998).
- [76] P. de Bernardis et al., *Nature* **404**, 995 (2000).
- [77] S. Hanany et al., *ApJ* **545**, L5 (2000).
- [78] N. A. Bahcall, J. P. Ostriker, S. Perlmutter and P. J. Steinhardt, *Science* **284**, 1481-1488 (1999) doi:10.1126/science.284.5419.1481 [arXiv:astro-ph/9906463 [astro-ph]].
- [79] V. Sahni and A. A. Starobinsky, *Int. J. Mod. Phys. D* **9**, 373-444 (2000) doi:10.1142/S0218271800000542 [arXiv:astro-ph/9904398 [astro-ph]].
- [80] P. J. E. Peebles and B. Ratra, *Rev. Mod. Phys.* **75**, 559-606 (2003) doi:10.1103/RevModPhys.75.559 [arXiv:astro-ph/0207347 [astro-ph]].
- [81] T. Padmanabhan, *Phys. Rept.* **380**, 235-320 (2003) doi:10.1016/S0370-1573(03)00120-0 [arXiv:hep-th/0212290 [hep-th]].
- [82] H. J. de Vega, P. Salucci, and N. G. Sanchez, *Mon. Not. R. Astron. Soc.* **442**, 2717 (2014).
- [83] P. H. Chavanis, M. Lemou, and F. Mehats, *Phys. Rev. D* **91**, 063531 (2015).
- [84] A. Suarez, V. H. Robles, and T. Matos, *Astrophys. Space Sci. Proc.* **38**, 107 (2014).
- [85] T. Rindler-Daller, and P.R. Shapiro, *Astrophys. Space Sci. Proc.* **38**, 163 (2014).

- [86] S. Weinberg, Rev. Mod. Phys. **61**, 1 (1989).
- [87] T. Padmanabhan, Phys. Rep. **380**, 235 (2003).
- [88] A. Kamenshchik, U. Moschella, and V. Pasquier, Phys. Lett. B **511**, 265 (2001).
- [89] S. Chaplygin, Sci. Mem. Moscow Univ. Math. Phys. **21**, 1 (1904).
- [90] H. S. Tsien, J. Aeron. Sci. **6**, 399 (1939).
- [91] T. von Karman, J. Aeron. Sci. **8**, 337 (1941).
- [92] V. Gorini, A. Kamenshchik, U. Moschella and V. Pasquier, doi: 10.1142/9789812704030_0050 [arXiv:gr-qc/0403062 [gr-qc]].
- [93] A. Y. Kamenshchik, U. Moschella and V. Pasquier, Phys. Lett. B **511** (2001), 265-268 doi:10.1016/S0370-2693(01)00571-8 [arXiv:gr-qc/0103004 [gr-qc]].
- [94] M. C. Bento, O. Bertolami and A. A. Sen, Phys. Rev. D **66** (2002), 043507 doi:10.1103/PhysRevD.66.043507 [arXiv:gr-qc/0202064 [gr-qc]].
- [95] V. M. C. Ferreira and P. P. Avelino, Phys. Rev. D **98** (2018) no.4, 043515 doi:10.1103/PhysRevD.98.043515 [arXiv:1807.04656 [gr-qc]].
- [96] P. H. Chavanis, Phys. Lett. B **758**, 59-66 (2016) doi:10.1016/j.physletb.2016.04.042 [arXiv:1505.00034 [astro-ph.CO]].
- [97] D. E. McLaughlin and R. E. Pudritz, Astrophys. J. **469**, 194 (1996) doi: 10.1086/177771 [arXiv:astro-ph/9605018 [astro-ph]].

- [98] P. H. Chavanis, and C. Sire, *Physica. A.* **375**, 140 (2007) no.1, 0378-4371 doi: 10.1016/j.physa.2006.08.076 [arXiv:cond-mat/0610410 [cond-mat]].
- [99] P. H. Chavanis, *Phys. Rev. D* **84**, 4 (2011) doi:10.1103/physrevd.84.04353.
- [100] S. Ponglertsakul, P. Burikham and T. Tangphati, *Phys. Rev. D* **99** (2019) no. 8, 084002 doi:10.1103/PhysRevD.99.084002 [arXiv:1812.09838 [hep-th]].
- [101] B. Gwak, *Eur. Phys. J. C* **79** (2019) no.12, 1004 doi:10.1140/epjc/s10052-019-7532-7 [arXiv:1903.11758 [gr-qc]].
- [102] S. Ponglertsakul and B. Gwak, [arXiv:2007.16108 [gr-qc]].
- [103] P. Wongjun, C. H. Chen and R. Nakarachinda, *Phys. Rev. D* **101** (2020) no. 12, 124033 doi:10.1103/PhysRevD.101.124033 [arXiv:1910.05908 [gr-qc]].
- [104] S. Kanzi, S. H. Mazharimousavi and İ. Sakallı, [arXiv:2007.05814 [hep-th]].





APPENDICES

จุฬาลงกรณ์มหาวิทยาลัย
CHULALONGKORN UNIVERSITY

APPENDIX A

The Vainshtein mechanism

To study the nonlinearity of massive gravity, we start with Einstein-Hilbert action representing the nonlinear kinetic term of graviton.

$$S_{\text{EH}} = \frac{1}{16\pi G} \int d^4x \sqrt{-g} R. \quad (\text{A.1})$$

This action is invariant under the diffeomorphisms of the form

$$x \rightarrow f(x), \quad g^{\mu\nu}(x) \rightarrow \frac{\partial f^\alpha}{\partial x^\mu} \frac{\partial f^\beta}{\partial x^\nu} g^{\mu\nu}(f(x)). \quad (\text{A.2})$$

According to the linear theory, we apply the linear expansion of the metric $g_{\mu\nu}$ around the flat spacetime $\eta_{\mu\nu}$ with the metric perturbation $h_{\mu\nu}$ as Eq. (2.3). In general, the metric $g_{\mu\nu}$ can be written as

$$g_{\mu\nu} = g_{\mu\nu}^{(0)} + h_{\mu\nu}, \quad (\text{A.3})$$

where $g^{(0)\mu\nu}$ is the absolute metric that the linear massive graviton propagates, $h_{\mu\nu} = g_{\mu\nu} - g_{\mu\nu}^{(0)}$ is the metric perturbation, and the indices on $h_{\mu\nu}$ are raised and lowered by the absolute metric. To construct the linear expansion of nonlinear theory, we cannot use only the full metric $g_{\mu\nu}$ since its trace provides a constant, $g^{\mu\alpha} g_{\alpha\mu} = \text{Tr}(\mathbb{I}_{4 \times 4}) = 4$ for four dimensions. The non-dynamical absolute metric

$g^{(0)\mu\nu}$ is needed for the traces and contractions. Thus, the most fundamental mass term for massive graviton is

$$S_{\text{mass}} = \frac{1}{16\pi G} \int d^4x \left[-\frac{\sqrt{-g^0}}{4} m^2 g^{(0)\mu\alpha} g^{(0)\nu\beta} (h_{\mu\nu} h_{\alpha\beta} - h_{\mu\alpha} h_{\nu\beta}) \right], \quad (\text{A.4})$$

where the mass term breaks the gauge transformation in Eq. (A.2) and reduces to the Fierz-Pauli mass term if $g^{(0)\mu\nu} = \eta^{\mu\nu}$ as shown in Eq. (2.20). The simplest nonlinear massive gravity becomes

$$\begin{aligned} S &= S_{\text{EH}} + S_{\text{mass}} \\ &= \frac{1}{16\pi G} \int d^4x \left[\sqrt{-g} R - \frac{\sqrt{-g^0}}{4} m^2 g^{(0)\mu\alpha} g^{(0)\nu\beta} (h_{\mu\nu} h_{\alpha\beta} - h_{\mu\alpha} h_{\nu\beta}) \right] \end{aligned} \quad (\text{A.5})$$

where this nonlinear action is still not the full nonlinear action since the more general form of mass term in nonlinear theory will be discussed further. Applying the Euler-Lagrange method gives the equation of motion

$$\sqrt{-g} \left(R^{\mu\nu} - \frac{1}{2} R g^{\mu\nu} \right) + \frac{\sqrt{-g^0} m^2}{2} (g^{(0)\mu\alpha} g^{(0)\nu\beta} h_{\alpha\beta} - g^{(0)\alpha\beta} h_{\alpha\beta} g^{(0)\mu\nu}) = 0. \quad (\text{A.6})$$

Now we will solve the static spherical solution and determine the Vainstein radius. The ansatz for the absolute metric is the four-dimensional flat spacetime

$$g^{(0)}_{\mu\nu} dx^\mu dx^\nu = -dt^2 + dr^2 + r^2 d\Omega^2, \quad (\text{A.7})$$

and the general form of the full metric solution is given by

$$g_{\mu\nu} dx^\mu dx^\nu = (g^{(0)}_{\mu\nu} + h_{\mu\nu}) dx^\mu dx^\nu = -B(r) dt^2 + C(r) dr^2 + A(r) r^2 d\Omega^2. \quad (\text{A.8})$$

The functions $A(r)$, $B(r)$, and $C(r)$ can be expanded for higher orders as follows

$$A(r) = 1 + \epsilon A_1(r) + \epsilon^2 A_2(r) + \dots \quad (\text{A.9})$$

$$B(r) = 1 + \epsilon B_1(r) + \epsilon^2 B_2(r) + \dots \quad (\text{A.10})$$

$$C(r) = 1 + \epsilon C_1(r) + \epsilon^2 C_2(r) + \dots \quad (\text{A.11})$$

We apply the expansion of functions A , B , and C and the ansatz of the full metric Eq. (A.8) into the equation of motion Eq. (A.6).

We find the solutions for $mr \ll 1$,

$$\begin{aligned} B(r) &= 1 - \frac{\epsilon M \kappa}{6\pi r} \left(1 - \frac{\epsilon M \kappa}{96\pi m^4 r^5} + \dots \right) \\ C(r) &= 1 - \frac{\epsilon M \kappa}{6\pi m^2 r^3} \left(1 - \frac{7\epsilon M \kappa}{8\pi m^4 r^5} + \dots \right) \\ A(r) &= 1 + \frac{\epsilon M \kappa}{12\pi m^2 r^3} \left(1 - \frac{\epsilon M \kappa}{4m^4 r^5} + \dots \right), \end{aligned} \quad (\text{A.12})$$

where $\kappa = 16\pi G$. We show the results up to the second order of nonlinearity. The criteria for considering the domination of nonlinearity is the parameter

$$r_V \equiv \left(\frac{GM}{m^4} \right)^{1/5}, \quad (\text{A.13})$$

where a novel length scale r_V is called Vainshtein radius. It is defined as the upper limit of the nonlinear effect [15]. The approximation of the linear GR works well for the distance $r > r_V$. On the other hand, the linear theory cannot be trusted at the distance $r < r_V$ which the nonlinear massive gravity dominates. Moreover, the Vainshtein radius increases to infinity as graviton mass $m \rightarrow 0$.

Note that we obtain $B_1(r) = -M\kappa/6\pi r$, $C_1(r) = -M\kappa/6\pi m^2 r^3$, and $A_1(r) = M\kappa/12\pi m^2 r^3$ when considering the first order $\mathcal{O}(\epsilon)$ and $mr \ll 1$. These results agree with the solution from FP massive gravity in Eq. (2.28).

APPENDIX B

The higher order derivatives of the scalar field from BD ghost

Let us consider the degree of freedom in non-linear massive gravity with FP mass term. Its action is given in Eq. (2.56) as

$$S = \frac{1}{16\pi G} \int d^4x \left[\sqrt{-g} R - \frac{1}{2} m^2 \eta^{\mu\alpha} \eta^{\nu\beta} (h_{\mu\nu} h_{\alpha\beta} - h_{\mu\alpha} h_{\nu\beta}) \right].$$

Since theory has neither constraints nor gauge symmetries, then there are 6 real degrees of freedom instead of 5. The extra degree of freedom is called Boulware Deser (BD) ghost. In this chapter, we will show that the higher order derivatives from BD ghost lead to the wrong sign of the kinetic terms and also cause the unbounded Hamiltonian.

B.1 The wrong sign of the kinetic terms from the scalar field

According to the Stueckelberg trick revealing the BD ghost in subsection 2.5.2, we obtain the mass term of the nonlinear massive gravity as shown in Eq. (2.83). We omit the tensor ($h_{\mu\nu}$) and vector (A_μ) modes since they are not responsible for the extra degree of freedom. The Lagrangian of the mass term from Eq. (2.83) reads

$$L_{\text{mass}} = -\frac{2}{m^2} ([\Pi^2] - [\Pi]^2) + \frac{2}{m^4} ([\Pi^3] - [\Pi][\Pi]^2) + \frac{1}{2m^6} ([\Pi^4] - [\Pi^2]^2) + \dots$$

To show the wrong sign of the kinetic term, we consider the lowest order of the higher order derivatives of the scalar field

$$\begin{aligned} L_{\text{mass}}^{2\text{nd}} &= [\Pi^2] = \partial_\mu \partial_\nu \pi \partial^\mu \partial^\nu \pi \\ &= \pi \square^2 \pi, \end{aligned} \tag{B.1}$$

where π is the helicity-0 mode, $\Pi_{\mu\nu} \equiv \partial_\mu \partial_\nu \pi$ and $\square \equiv \partial_\mu \partial^\mu$. The second line of Eq. (B.1) is obtained from the integration by part where the total derivative is neglected. By this expression, the propagator for Eq. (B.1) is \square^{-2} which can be written in the sum of two propagators with opposite signs

$$\frac{1}{\square^2} = \lim_{m \rightarrow 0} \frac{1}{2m^2} \left(\frac{1}{\square - m^2} - \frac{1}{\square + m^2} \right), \tag{B.2}$$

where this hints a problem with the wrong sign coupling to the external sources. One could see the appearance of the BD ghost by introducing a Lagrange multiplier

$\tilde{\pi}$, then the Lagrangian in Eq. (B.1) is equivalent to

$$\tilde{L}_{\text{mass}}^{2\text{nd}} = \tilde{\pi} \square \pi - \frac{1}{4} \tilde{\pi}^2, \quad (\text{B.3})$$

After integrating out the Lagrange multiplier, we obtain

$$\tilde{\pi} = 2 \square \pi. \quad (\text{B.4})$$

We introduce new fields $\phi_1 = (\pi + \tilde{\pi})/2$ and $\phi_2 = (\pi - \tilde{\pi})/2$. The Lagrangian in Eq. (B.3) becomes

$$\tilde{L}_{\text{mass}}^{2\text{nd}} = \phi_1 \square \phi_1 - \phi_2 \square \phi_2 - \frac{1}{4} (\phi_1 - \phi_2)^2. \quad (\text{B.5})$$

Finally, the signs of the kinetic terms of the scalar fields (ϕ_1 and ϕ_2) are opposite. This shows that one of them is BD ghost. Fortunately, the second order derivative terms can be written in the total derivatives as shown in Eq. (2.84),

$$[\Pi^2] - [\Pi]^2 = \partial_\rho (\partial^\mu \pi \partial^\rho \partial_\mu \pi) - \partial_\rho (\partial^\rho \pi \partial^\mu \partial_\mu \pi).$$

However, one could straightforwardly show that the other higher derivatives of the scalar fields, i.e. $[\Pi^3] - [\Pi][\Pi]^2$ and $[\Pi^4] - [\Pi^2]^2$ cannot be written in the total derivatives at all. They will lead to the wrong signs of kinetic terms and are responsible for the extra degree of freedom from ghost since there are no constraints or gauge symmetries in the nonlinear massive gravity.

B.2 The instability from BD ghost

The nonlinear massive gravity with FP mass terms suffers from the extra degree of freedom or the BD ghost since the higher order derivatives are not eliminated.

Here in this section, we will demonstrate how the BD ghost make the Hamiltonian unbounded leading to the instability of the system.

B.2.1 A bounded Hamiltonian

To study the instability from BD ghost, we consider a simple case of non-higher derivatives. In this case of $L = L(x, \dot{x})$ where x is a coordinate, the Euler-Lagrange equation is

$$\frac{\partial L}{\partial x} - \frac{\partial}{\partial t} \left(\frac{\partial L}{\partial \dot{x}} \right) = 0. \quad (\text{B.6})$$

If the Lagrangian is nondegeneracy ($\frac{\partial^2 L}{\partial \dot{x}^2} \neq 0$), the solutions must be written as follow

$$x = x(x_0, \dot{x}_0), \quad (\text{B.7})$$

where x_0 and \dot{x}_0 are the initial value data of coordinate. Then there must be two canonical variables of the solutions. Traditionally, the choices are the canonical coordinate x and its canonical momentum $P \equiv \frac{\partial L}{\partial \dot{x}}$.

The canonical Hamiltonian H is obtained by the Legendre transformation on \dot{x}

$$H(x, P) \equiv P\dot{x} - L(x, \dot{x}). \quad (\text{B.8})$$

The canonical evolution equations are

$$\dot{x} = \frac{\partial H}{\partial P}, \quad (\text{B.9})$$

$$\dot{P} = -\frac{\partial H}{\partial x} = \frac{\partial L}{\partial x}. \quad (\text{B.10})$$

A well-known problem is the linear free scalar field theory whose Lagrangian is

$$L = \frac{1}{2}(\dot{\pi})^2 - V(\pi), \quad (\text{B.11})$$

where $V(\pi)$ is the potential of the scalar field π . Then the Hamiltonian from Eq. (B.8) is given by

$$H = \frac{1}{2}(\dot{\pi})^2 + V(\pi), \quad (\text{B.12})$$

where, in this case, the Hamiltonian has a lower bound at zero.

B.2.2 An unbounded Hamiltonian from the higher order derivative

Now we consider the higher order derivative in the Lagrangian $L(x, \dot{x}, \ddot{x})$. The Euler-Lagrange equation for this case is

$$\frac{\partial L}{\partial x} - \frac{\partial}{\partial t} \left(\frac{\partial L}{\partial \dot{x}} \right) + \frac{\partial^2}{\partial t^2} \left(\frac{\partial L}{\partial \ddot{x}} \right) = 0. \quad (\text{B.13})$$

If the Lagrangian is nondegeneracy ($\frac{\partial^2 L}{\partial \ddot{x}^2} \neq 0$), the solution can be written as

$$x = x(x_0, \dot{x}_0, \ddot{x}_0, \ddot{\ddot{x}}_0). \quad (\text{B.14})$$

Since the solution depends on four initial value data, there must be four canonical variables. In this case, the canonical coordinates are

$$x \text{ and } \dot{x}, \quad (\text{B.15})$$

and their canonical momenta are

$$P_1 \equiv \frac{\partial L}{\partial \dot{x}} - \frac{d}{dt} \frac{\partial L}{\partial \ddot{x}}, \quad (\text{B.16})$$

$$P_2 \equiv \frac{\partial L}{\partial \ddot{x}}. \quad (\text{B.17})$$

The canonical Hamiltonian by the Legendre transformation reads

$$H(x, \dot{x}, P_1, P_2) = P_1 \dot{x} + P_2 \ddot{x} - L(x, \dot{x}, \ddot{x}). \quad (\text{B.18})$$

One could show that the time evolution equations are

$$\dot{x} = \frac{\partial H}{\partial P_1} \quad (\text{B.19})$$

$$\ddot{x} = \frac{\partial H}{\partial P_2} \quad (\text{B.20})$$

$$\dot{P}_1 = -\frac{\partial H}{\partial x} = \frac{\partial L}{\partial x} \quad (\text{B.21})$$

$$\dot{P}_2 = -\frac{\partial H}{\partial \dot{x}} = -P_1 + \frac{\partial L}{\partial \dot{x}}. \quad (\text{B.22})$$

Let consider the higher order derivative Lagrangian

$$L = -\frac{\epsilon m}{2\omega^2} \ddot{x}^2 + \frac{m}{2} \dot{x}^2 - \frac{m\omega^2}{2} x^2, \quad (\text{B.23})$$

where ϵ is a dimensionless constant. For this problem, the canonical momenta are

$$P_1 = m\dot{x} + \frac{\epsilon m}{\omega^2} \ddot{x}, \quad (\text{B.24})$$

$$P_2 = -\frac{\epsilon m}{\omega^2} \ddot{x}. \quad (\text{B.25})$$

The Hamiltonian can be expressed in terms of canonical variables

$$\begin{aligned} H(x, \dot{x}, P_1, P_2) &= P_1 \dot{x} + P_2 \ddot{x} - L(x, \dot{x}, \ddot{x}) \\ &= \frac{\epsilon m}{\omega^2} \dot{x} \ddot{x} - \frac{\epsilon m}{2\omega^2} \ddot{x}^2 + \frac{m}{2} \dot{x}^2 + \frac{m\omega^2}{2} x^2, \end{aligned} \quad (\text{B.26})$$

where there is no lower bound for this case since $P_1 \neq m\dot{x}$. The energy of the system that has the higher order derivatives is unbounded from below. When the unbounded Hamiltonian interacts with external source (which has the lower bound of energy), it is possible that the unbounded Hamiltonian would lose energy since

there is no lower bound and the external source would gain the infinite amount of energy which is called instability.

In the nonlinear massive gravity with FP mass term, the higher order derivatives play a major of the extra degree of freedom. The additional degree of freedom does not only allow the recovery to GR but also causes the negative kinetic terms leading to the instability.



Vitae

Mr. Takol Tangphati was born on 3 December 1990, graduating Bachelor's degree in physics from Prince of Songkhla University in 2012. His research covers the theoretical non-linear physics and condensed matter.

Publication

1. T. Tangphati, A. Chatrabhuti, D. Samart, and P. Channuie, "Thin-shell wormholes in de Rham-Gabadadze-Tolley massive gravity," *Eur. Phys. J. C* **80** (2020) no.8, 722 doi:10.1140/epjc/s10052-020-8294-y, [arXiv: 1912.12208[gr-qc]].
2. T. Tangphati, A. Chatrabhuti, D. Samart, and P. Channuie, "Traversable wormholes in $f(R)$ -massive gravity," *Phys. Rev.* **102** (2020) no.8, 084026 doi:10.1103/PhysRevD.102.084026 [arXiv: 2003.01544 [gr-qc]].

Other contributions

1. C. Pongkitivanichkul, D. Samart, T. Tangphati, P. Koomhin, P. Pimton, P. Dam-O, A. Payaka, and P. Channuie, "Estimating the size of COVID-19 epidemic outbreak," *Phys. Scr.* **95** (2020) no. 8, doi: 10.1088/1402-4896/ab9bdf.
2. A. Banerjee, T. Tangphati, and P. Channuie, "Strange Quark Stars in 4D Einstein-Gauss-Bonnet Gravity," *Astrophys. J.* **909** (2021) 1, 14, doi: 10.3847/1538-4357/abd094 [arXiv: 2006.00479[gr-qc]].

3. A. Banerjee, T. Tangphati, D. Samart and P. Channuie, “Quark Stars in 4D Einstein-Gauss-Bonnet gravity with an Interacting Quark Equation of State,” *Astrophys. J.* **906** (2021) 2, 114, doi: 10.3847/1538-4357/abc87f [arXiv: 2007.04121[gr-qc]].
4. G. Panotopoulos, T. Tangphati, A. Banerjee and M. K. Jasim, “Anisotropic quark stars in R^2 gravity,” *Phys. Lett. B* **817** 136330 (2021), doi: 10.1016/j.physletb.2021.136330 [arXiv: 2104.00590[gr-qc]].
5. G. Panotopoulos, T. Tangphati and A. Banerjee, “Electrically charged compact stars with an interacting quark equation of state,” [arXiv:2105.10638 [gr-qc]].
6. T. Tangphati, A. Pradhan, A. Errehymy and A. Banerjee, “Quark stars in the Einstein-Gauss-Bonnet theory: A new branch of stellar configurations,” *Annals Phys.* **430**, 168498 (2021), doi:10.1016/j.aop.2021.168498.
7. T. Tangphati, A. Pradhan, A. Errehymy and A. Banerjee, “Anisotropic quark stars in Einstein-Gauss-Bonnet theory,” *Phys. Lett. B* **819**, 136423 (2021), doi:10.1016/j.physletb.2021.136423.